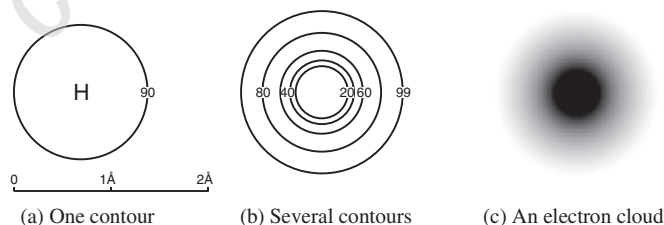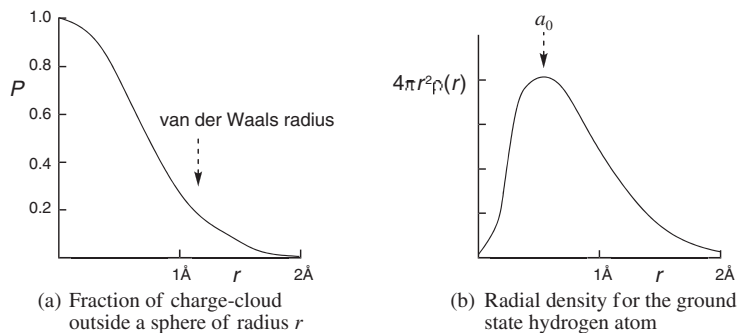# 1 Molecular Orbital Theory

## 1.1 The Atomic Orbitals of a Hydrogen Atom

To understand the nature of the simplest chemical bond, that between two hydrogen atoms, we look at the effect on the electron distribution when two atoms are held within bonding distance, but first we need a picture of the hydrogen atoms themselves. Since a hydrogen atom consists of a proton and a single electron, we only need a description of the spatial distribution of that electron. This is usually expressed as a *wave function* $\phi$, where $\phi^2 d\tau$ is the probability of finding the electron in the volume $d\tau$, and the integral of $\phi^2 d\tau$ over the whole of space is 1. The wave function is the underlying mathematical description, and it may be positive or negative; it can even be complex with a real and an imaginary part, but this will not be needed in any of the discussion in this book. Only when squared does it correspond to anything with physical reality—the probability of finding an electron in any given space. Quantum theory[12] gives us a number of permitted wave equations, but the only one that matters here is the lowest in energy, in which the distribution of the electron is described as being in a 1s orbital. This is spherically symmetrical about the nucleus, with a maximum at the centre, and falling off rapidly, so that the probability of finding the electron within a sphere of radius 1.4 Å is 90 % and within 2 Å better than 99%. This orbital is calculated to be 13.60 eV lower in energy than a completely separated electron and proton.

We need pictures to illustrate the electron distribution, and the most common is simply to draw a circle, Fig. 1.1a, which can be thought of as a section through a spherical contour, within which the electron would be found, say, 90 % of the time. This picture will suffice for most of what we need in this book, but it might be worth looking at some others, because the circle alone disguises some features that are worth appreciating. Thus a section showing more contours, Fig. 1.1b, has more detail. Another picture, even less amenable to a quick drawing, is to plot the electron distribution as a section through a cloud, Fig. 1.1c, where one imagines blinking one's eyes a very large number of times, and plotting the points at which the electron was at each blink. This picture contributes to the language often used, in which the electron population in a given volume of space is referred to as the electron density.



(a) One contour    (b) Several contours    (c) An electron cloud

**Fig. 1.1**   The 1s atomic orbital of a hydrogen atom

(a) Fraction of charge-cloud
outside a sphere of radius $r$

(b) Radial density for the ground
state hydrogen atom

**Fig. 1.2**    Radial probability plots for the 1s orbital of a hydrogen atom

Taking advantage of the spherical symmetry, we can also plot the fraction of the electron population outside a radius $r$ against $r$, as in Fig. 1.2a, showing the rapid fall off of electron population with distance. The van der Waals radius at 1.2 Å has no theoretical significance—it is an empirical measurement from solid-state structures, being one-half of the distance apart of the hydrogen atom in a C—H bond and the hydrogen atom in the C—H bond of an adjacent molecule.[13] It does not even have a fixed value, but is an average of several measurements. Yet another way to appreciate the electron distribution is to look at the radial density, where we plot the probability of finding the electron between one sphere of radius $r$ and another of radius $r + dr$. This has a revealing form, Fig. 1.2b, with a maximum 0.529 Å from the nucleus, showing that, in spite of the wave function being at a maximum at the nucleus, the chance of finding an electron precisely there is very small. The distance 0.529 Å proves to be the same as the radius calculated for the orbit of an electron in the early but untenable planetary model of a hydrogen atom. It is called the Bohr radius $a_0$, and is often used as a unit of length in molecular orbital calculations.

## 1.2    Molecules Made from Hydrogen Atoms

### 1.2.1 *The $H_2$ Molecule*

To understand the bonding in a hydrogen molecule, we have to see what happens when two hydrogen atoms are close enough for their atomic orbitals to interact. We now have two protons and two nuclei, and even with this small a molecule we cannot expect theory to give us complete solutions. We need a description of the electron distribution over the whole molecule—a molecular orbital. The way the problem is handled is to accept that a first approximation has the two atoms remaining more or less unchanged, so that the description of the molecule will resemble the sum of the two isolated atoms. Thus we combine the two atomic orbitals in a linear combination expressed in Equation 1.1, where the function which describes the new electron distribution, the *molecular orbital*, is called $\sigma$ and $\phi_1$ and $\phi_2$ are the atomic 1s wave functions on atoms 1 and 2.

$$\sigma = c_1\phi_1 + c_2\phi_2 \qquad\qquad 1.1$$

The coefficients, $c_1$ and $c_2$, are a measure of the contribution which the atomic orbital is making to the molecular orbital. They are of course equal in magnitude in this case, since the two atoms are the same, but they may be positive or negative. To obtain the electron distribution, we square the function in Equation 1.1, which is written in two ways in Equation 1.2.

$$\sigma^2 = (c_1\phi_1 + c_2\phi_2)^2 = (c_1\phi_1)^2 + (c_2\phi_2)^2 + 2c_1\phi_1 c_2\phi_2 \qquad\qquad 1.2$$

Taking the expanded version, we can see that the molecular orbital $\sigma^2$ differs from the superposition of the two atomic orbitals $(c_1\phi_1)^2+(c_2\phi_2)^2$ by the term $2c_1\phi_1c_2\phi_2$. Thus we have two solutions (Fig. 1.3). In the first, both $c_1$ and $c_2$ are positive, with orbitals of the same sign placed next to each other; the electron population *between* the two atoms is increased (shaded area), and hence the negative charge which these electrons carry *attracts* the two positively charged nuclei. This results in a lowering in energy and is illustrated in Fig. 1.3, where the horizontal line next to the drawing of this orbital is placed low on the diagram. In the second way in which the orbitals can combine, $c_1$ and $c_2$ are of opposite sign, and, if there were any electrons in this orbital, there would be a low electron population in the space between the nuclei, since the function is changing sign. We represent the sign change by shading one of the orbitals, and we call the plane which divides the function at the sign change a node. If there were any electrons in this orbital, the reduced electron population between the nuclei would lead to repulsion between them; thus, if we wanted to have electrons in this orbital and still keep the nuclei reasonably close, energy would have to be put into the system. In summary, by making a bond between two hydrogen atoms, we create two new orbitals, $\sigma$ and $\sigma^*$, which we call the molecular orbitals; the former is *bonding* and the latter *antibonding* (an asterisk generally signifies an antibonding orbital). In the ground state of the molecule, the two electrons will be in the orbital labelled $\sigma$. There is, therefore, when we make a bond, a lowering of energy equal to twice the value of $E_\sigma$ in Fig. 1.3 (*twice* the value, because there are two electrons in the bonding orbital).
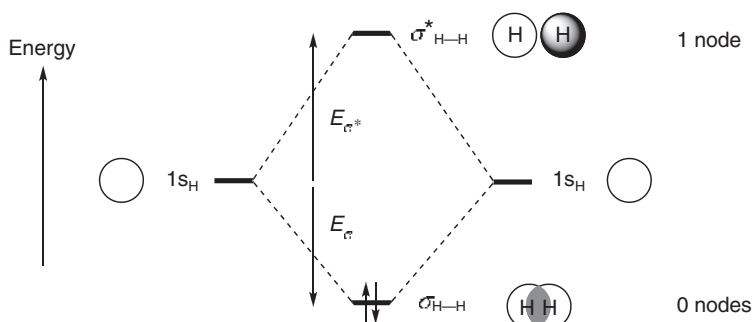


**Fig. 1.3** The molecular orbitals of hydrogen

The force holding the two atoms together is obviously dependent upon the extent of the overlap in the bonding orbital. If we bring the two 1s orbitals from a position where there is essentially no overlap at 3 Å through the bonding arrangement to superimposition, the extent of overlap steadily increases. The mathematical description of the overlap is an integral $S_{12}$ (Equation 1.3) called the *overlap integral*, which, for a pair of 1s orbitals, rises from 0 at infinite separation to 1 at superimposition (Fig. 1.4).

$$S_{12} = \int \phi_1\phi_2 d\tau \qquad 1.3$$

The mathematical description of the effect of overlap on the electronic energy is complex, but some of the terminology is worth recognising, and will be used from time to time in the rest of this book. The energy $E$ of
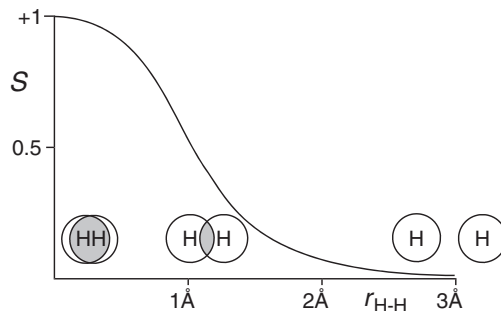
**Fig. 1.4**    The overlap integral $S$ for two $1s_H$ orbitals as a function of internuclear distance

an electron in a bonding molecular orbital is given by Equation 1.4 and for the antibonding molecular orbital is given by Equation 1.5:

$$E = \frac{\alpha + \beta}{1 + S} \qquad\qquad 1.4$$

$$E = \frac{\alpha - \beta}{1 - S} \qquad\qquad 1.5$$

in which the symbol $\alpha$ represents the energy of an electron in an isolated atomic orbital, and is called a *Coulomb integral*. The function represented by the symbol $\beta$ contributes to the energy of an electron in the field of both nuclei, and is called the *resonance* integral. It is roughly proportional to $S$, and so the overlap integral appears in the equations twice. It is important to realise that the use of the word resonance does not imply an oscillation, nor is it exactly the same as the 'resonance' of valence bond theory. In both cases the word is used because the mathematical form of the function is similar to that for the mechanical coupling of oscillators. We also use the words *delocalised* and *delocalisation* to describe the electron distribution enshrined in the $\beta$ function—unlike the words resonating and resonance, these are not misleading, and are the better words to use.

The function $\beta$ is a negative number, lowering the value of $E$ in Equation 1.4 and raising it in Equation 1.5. In this book, $\beta$ will not be given a sign on the diagrams on which it is used, because the sign can be misleading. The symbol $\beta$ should be interpreted as $|\beta|$, the positive absolute value of $\beta$. Since the diagrams are always plotted with energy upwards and almost always with the $\alpha$ value visible, it should be obvious which $\beta$ values refer to a lowering of the energy below the $\alpha$ level, and which to raising the energy above it.

The overall effect on the energy of the hydrogen molecule relative to that of two separate hydrogen atoms as a function of the internuclear distance is given in Fig. 1.5. If the bonding orbital is filled (Fig. 1.5a), the energy derived from the electronic contribution (Equation 1.4) steadily falls as the two hydrogen atoms are moved from infinity towards one another (curve A). At the same time the nuclei repel each other ever more strongly, and the nuclear contribution to the energy goes steadily up (curve B). The sum of these two is the familiar Morse plot (curve C) for the relationship between internuclear distance and energy, with a minimum at the bond length. If we had filled the antibonding orbital instead (Fig. 1.5b), there would have been no change to curve B. The electronic energy would be given by Equation 1.5 which provides only a little shielding between the separated nuclei giving at first a small curve down for curve A, and even that would change to a repulsion earlier than in the Morse curve. The resultant curve, C, is a steady increase in energy as the nuclei are pushed together. The characteristic of a bonding orbital is that the nuclei are held together, whereas the characteristic of an antibonding orbital, if it were to be filled, is that the nuclei would fly apart unless there are enough compensating filled bonding orbitals. In hydrogen, having both orbitals occupied is overall antibonding, and there is no possibility of compensating for a filled antibonding orbital.
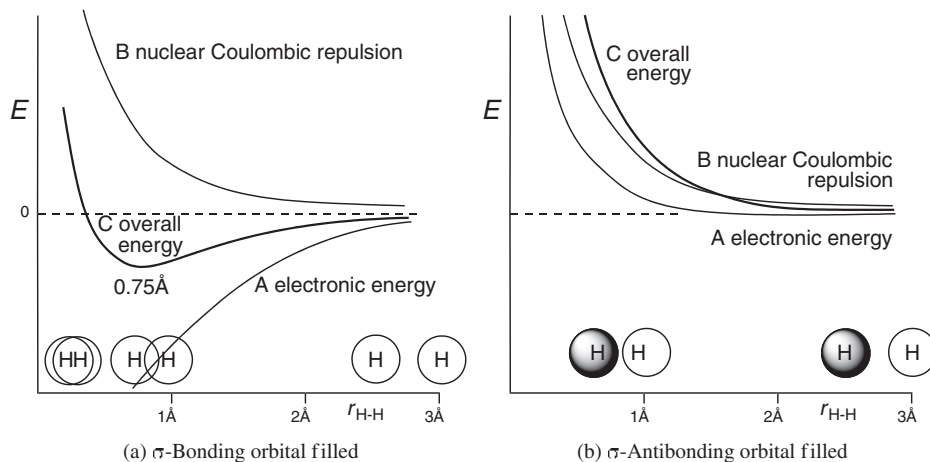
**Fig. 1.5** Electronic attraction, nuclear repulsion and the overall effect as a function of internuclear distance for two $1s_H$ atoms

We can see from the form of Equations 1.4 and 1.5 that the term $\alpha$ relates to the energy levels of the isolated atoms labelled $1s_H$ in Fig. 1.3, and the term $\beta$ to the drop in energy labelled $E_\sigma$ (and the rise labelled $E_{\sigma*}$). Equations 1.4 and 1.5 show that, since the denominator in the bonding combination is $1 + S$ and the denominator in the antibonding combination is $1 - S$, the bonding orbital is not as much lowered in energy as the antibonding is raised. In addition, putting *two* electrons into a bonding orbital does not achieve exactly twice the energy-lowering of putting *one* electron into it. We are *allowed* to put two electrons into the one orbital if they have opposite spins, but they still repel each other, because they have to share the same space; consequently, in forcing a second electron into the $\sigma$ orbital, we lose some of the bonding we might otherwise have gained. For this reason too, the value of $E_\sigma$ in Fig. 1.3 is smaller than that of $E_{\sigma*}$. This is why two helium atoms do not combine to form an $He_2$ molecule. There are four electrons in two helium atoms, two of which would go into the $\sigma$-bonding orbital in an $He_2$ molecule and two into the $\sigma$*-antibonding orbital. Since $2E_{\sigma*}$ is greater than $2E_\sigma$, we would need extra energy to keep the two helium atoms together.

Two electrons in the same orbital can keep out of each other's way, with one electron on one side of the orbital, while the other is on the other side most of the time, and so the energetic penalty for having a second electron in the orbital is not large. This synchronisation of the electrons' movements is referred to as *electron correlation*. The energy-raising effect of the repulsion of one electron by the other is automatically included in calculations based on Equations 1.4 and 1.5, but each electron is treated as having an average distribution with respect to the other. The effect of electron correlation is often not included, without much penalty in accuracy, but when it is included the calculation is described as being with *configuration interaction*, a bit of fine tuning sometimes added to a careful calculation.

The detailed form that $\alpha$ and $\beta$ take is where the mathematical complexity appears. They come from the Schrödinger equation, and they are integrals over all coordinates, represented here simply by $d\tau$, in the form of Equations 1.6 and 1.7:

$$\alpha = \int \phi_1 H \phi_1 d\tau \qquad\qquad 1.6$$

$$\beta = \int \phi_1 H \phi_2 d\tau \qquad\qquad 1.7$$

where $H$ is the energy operator known as a Hamiltonian. Even without going into this in more detail, it is clear how the term $\alpha$ relates to the atom, and the term $\beta$ to the interaction of one atom with another.

As with atomic orbitals, we need pictures to illustrate the electron distribution in the molecular orbitals. For most purposes, the conventional drawings of the bonding and antibonding orbitals in Fig. 1.3 are clear enough—we simply make mental reservations about what they represent. In order to be sure that we do understand enough detail, we can look at a slice through the two atoms showing the contours (Fig. 1.6). Here we see in the bonding orbital that the electron population close in to the nucleus is pulled in to the midpoint between the nuclei (Fig. 1.6a), but that further out the contours are an elliptical envelope with the nuclei as the foci. The antibonding orbital, however, still has some dense contours between the nuclei, but further out the electron population is pushed out on the back side of each nucleus. The node is half way between the nuclei, with the change of sign in the wave function symbolised by the shaded contours on the one side. If there were electrons in this orbital, their distribution on the outside would pull the nuclei apart—the closer the atoms get, the more the electrons are pushed to the outside, explaining the rise in energy of curve A in Fig. 1.5b.



(a) The σ-bonding orbital                    (b) The σ*-antibonding orbital
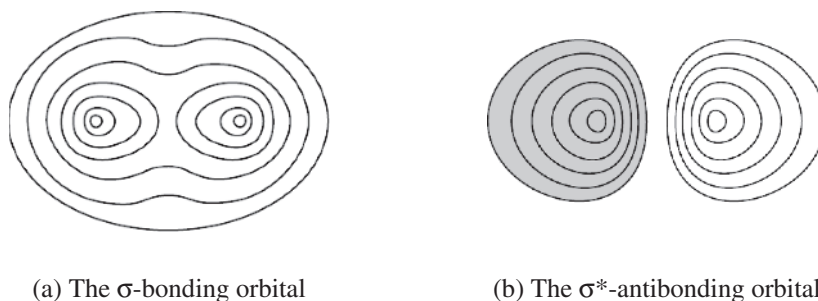
**Fig. 1.6**   Contours of the wave function of the molecular orbitals of $H_2$

We can take away the sign changes in the wave function by plotting $\sigma^2$ along the internuclear axis, as in Fig. 1.7. The solid lines are the plots for the molecular orbitals, and the dashed lines are plots, for comparison, of the undisturbed atomic orbitals $\phi^2$. The electron population in the bonding orbital (Fig. 1.7a) can be seen to be slightly contracted relative to the sum of the squares of the atomic orbitals, and the electron population



(a)  σ bonding                                        (b) σ* antibonding
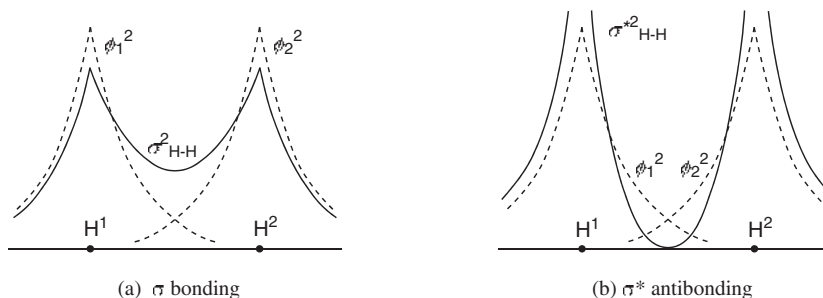
**Fig. 1.7**   Plots of the square of the wave function for the molecular orbitals of $H_2$ (solid lines) and its component atomic orbitals (dashed lines). [The atomic orbital plot is scaled down by a factor of 2 to allow us to compare $\sigma^2$ with the sum of the atomic densities $(\phi_1{}^2+\phi_2{}^2)/2$]

between the nuclei is increased relative to that sum, as we saw when we considered Equation 1.2. In the antibonding orbital (Fig. 1.7b) it is the other way round, if there were electrons in the molecular orbital, the electron population would be slightly expanded relative to a simple addition of the squares of the atomic orbitals, and the electron population between the nuclei is correspondingly decreased.

Let us return to the coefficients $c_1$ and $c_2$ of Equation 1.1, which are a measure of the contribution which each atomic orbital is making to the molecular orbital (equal in this case). When there are electrons in the orbital, the squares of the $c$-values are a measure of the electron population in the neighbourhood of the atom in question. Thus *in each orbital* the sum of the squares of all the $c$-values must equal one, since only one electron in each spin state can be in the orbital. Since $|c_1|$ must equal $|c_2|$ in a homonuclear diatomic like $H_2$, we have defined what the values of $c_1$ and $c_2$ in the bonding orbital must be, namely $1/\sqrt{2} = 0.707$:



If all molecular orbitals were filled, then there would have to be one electron in each spin state on each atom, and this gives rise to a second criterion for $c$-values, namely that the sum of the squares of all the $c$-values *on any one atom* in *all* the molecular orbitals must also equal one. Thus the $\sigma^*$-antibonding orbital of hydrogen will have $c$-values of 0.707 and –0.707, because these values make the whole set fit both criteria. Of course, we could have taken $c_1$ and $c_2$ in the antibonding orbital the other way round, giving $c_1$ the negative sign and $c_2$ the positive.

This derivation of the coefficients is not strictly accurate—a proper normalisation involves the overlap integral $S$, which is present with opposite sign in the bonding and the antibonding orbitals (see Equations 1.4 and 1.5). As a result the coefficients in the antibonding orbitals are actually slightly larger than those in the bonding orbital. This subtlety need not exercise us at the level of molecular orbital theory used in this book, and it is not a problem at all in Hückel theory, which is what we shall be using for $\pi$ systems. We can, however, recognise its importance when we see that it is another way of explaining that the degree of antibonding from the antibonding orbital ($E_{\sigma^*}$ in Fig. 1.3) is greater than the degree of bonding from the bonding orbital ($E_\sigma$).

### 1.2.2 The H₃ Molecule

We might ask whether we can join more than two hydrogen atoms together. We shall consider first the possibility of joining three atoms together in a triangular arrangement. It presents us for the first time with the problem of how to account for three atoms forming bonds to each other. With three atomic orbitals to combine, we can no longer simply draw an interaction diagram as we did in Fig. 1.3, where there were only two atomic orbitals. One way of dealing with the problem is first to take two of them together. In this case, we take two of the hydrogen atoms, and allow them to interact to form a hydrogen molecule, and then we combine the $\sigma$ and $\sigma^*$ orbitals, on the right of Fig. 1.8, with the 1s orbital of the third hydrogen atom on the left.

We now meet an important rule: we are only allowed to combine those orbitals that have the same symmetry with respect to all the symmetry elements present in the structure of the product and in the orbitals of the components we are combining. This problem did not arise in forming a bond between two identical hydrogen atoms, because they have inherently the same symmetry, but now we are combining different sets
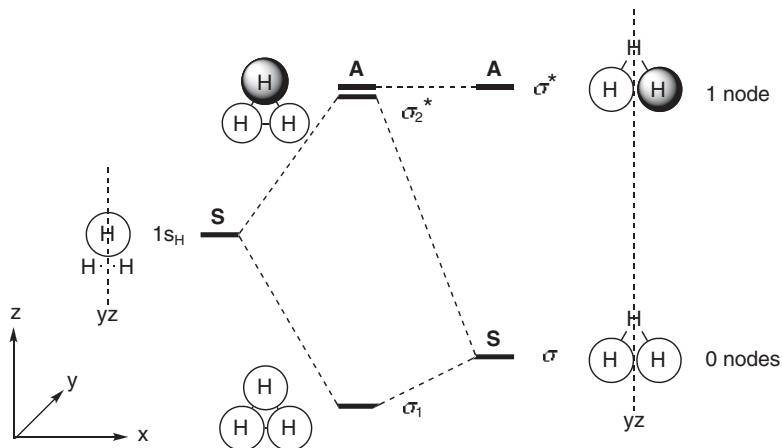
**Fig. 1.8** Interacting orbitals for $H_3$

of orbitals with each other. The need to match, and to maintain, symmetry will become a constant refrain as the molecules get more complex. The first task is to identify the symmetry elements, and to classify the orbitals with respect to them. Because all the orbitals are s orbitals, there is a trivial symmetry plane in the plane of the page, which we shall label throughout this book as the xz plane. We can ignore it, and other similar symmetry elements, in this case. The only symmetry element that is not trivial is the plane in what we shall call the yz plane, running from top to bottom of the page and rising vertically from it. The $\sigma$ orbital and the 1s orbital are symmetric with respect to this plane, but the $\sigma^*$ orbital is antisymmetric, because the component atomic orbitals are out of phase. We therefore label the orbitals as S (symmetric) or A (antisymmetric).

The $\sigma$ orbital and the 1s orbital are both S and they can interact in the same way as we saw in Fig. 1.3, to create a new pair of molecular orbitals labelled $\sigma_1$ and $\sigma_2^*$. The former is lowered in energy, because all the s orbitals are of the same sign, and the latter is raised in energy, because there is a node between the top hydrogen atom and the two bottom ones. The latter orbital is antibonding overall, because there are two antibonding interactions between hydrogen atoms and only one bonding interaction. As it happens, its energy is the same as that of the $\sigma^*$ orbital, but we cannot justify that fully now. In any case, the other orbital $\sigma^*$ remains unchanged in the $H_3$ molecule, because there is no orbital of the correct symmetry to interact with it.

Thus we have three molecular orbitals, just as we had three atomic orbitals to make them from. Whether we have a stable 'molecule' now depends upon how many electrons we have. If we have two in $H_3^+$, in other words a protonated hydrogen molecule, they would both go into the $\sigma_1$ orbital, and the molecule would have a lower electronic energy than the separate proton and $H_2$ molecule. If we had three electrons $H_3\bullet$ from combining three hydrogen atoms, we would also have a stable 'molecule', with *two* electrons in $\sigma_1$ and only *one* in $\sigma_2^*$, making the combination overall more bonding than antibonding. Only with four electrons in $H_3^-$ is the overall result of the interaction antibonding, because the energy-raising interaction is, as usual, greater than the energy-lowering interaction. This device of building up the orbitals and only then feeding the electrons in is known as the *aufbau* method.

We could have combined the three atoms in a straight line, pulling the two lower hydrogen atoms in Fig. 1.8 out to lay one on each side of the upper atom. Since the symmetries do not change, the result would have been similar (Fig. 1.9). There would be less bonding in $\sigma_1$ and $\sigma_2^*$, because the overlap between the two lower hydrogen atoms would be removed. There would also be less antibonding from the $\sigma^*$ orbital, since it would revert to having the same energy as the two more or less independent 1s orbitals.
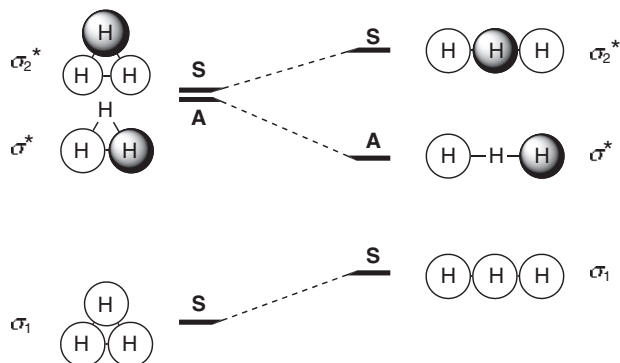
**Fig. 1.9** Relative energies for the orbitals of triangular and linear $H_3$

### 1.2.3 The $H_4$ 'Molecule'

There are even more possible ways of arranging four hydrogen atoms, but we shall limit ourselves to tetrahedral, since we shall be using these orbitals later. This time, we combine them in pairs, as in Fig. 1.3, to create two hydrogen molecules, and then we ask ourselves what happens to the energy when the two hydrogen molecules are held within bonding distance, one at right angles to the other.

   We can keep one pair of hydrogen atoms aligned along the x axis, on the right in Fig. 1.10, and orient the other along the y axis, on the left of Fig. 1.10. The symmetry elements present are then the xz and yz planes. The bonding orbital $\sigma_x$ on the right is symmetric with respect to both planes, and is labelled SS. The antibonding orbital $\sigma_x^*$ is symmetric with respect to the xz plane but antisymmetric with respect to the yz plane, and is accordingly labelled SA. The bonding orbital $\sigma_y$ on the left is symmetric with respect to both planes, and is also labelled SS. The antibonding orbital $\sigma_y^*$ is antisymmetric with respect to the xz plane but symmetric with respect to the yz plane, and is labelled AS. The only orbitals with the same symmetry are therefore the two bonding orbitals, and they can interact to give a bonding combination $\sigma_1$ and an antibonding combination $\sigma_2^*$. As it happens, the latter has the same energy as the unchanged orbitals $\sigma_x^*$ and $\sigma_y^*$. This is not too difficult to understand: in the new orbitals $\sigma_1$ and $\sigma_2^*$, the coefficients $c$, will be (ignoring the full
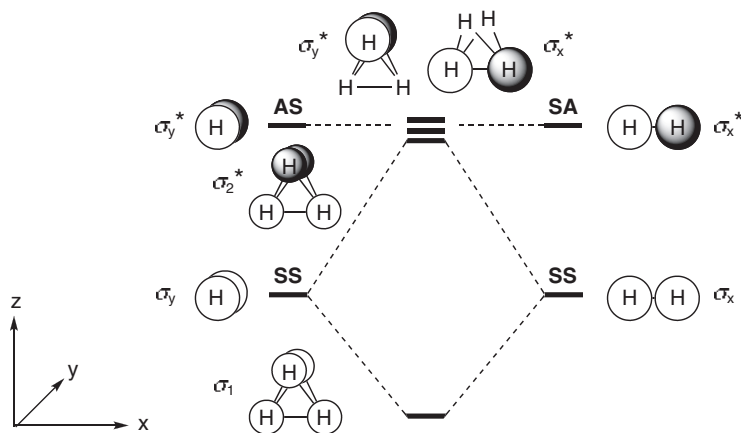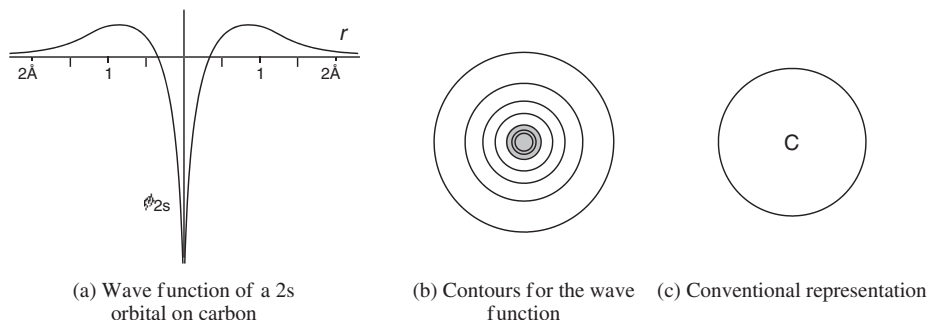


**Fig. 1.10** The orbitals of tetrahedral $H_4$

treatment of normalisation) 0.5 instead of 0.707, in order that the sum of their squares shall be 1. In the antibonding combination $\sigma_2$*, there are two bonding relationships between hydrogen atoms, and four antibonding relationships, giving a net value of two antibonding combinations, compared with the one in each of the orbitals $\sigma_x$* and $\sigma_y$*. However the antibonding in the orbital $\sigma_2$* is between s orbitals with coefficients of $1/\sqrt{4}$, and two such interactions is the same as one between orbitals with coefficients of $1/\sqrt{2}$ (see Equation 1.3, and remember that the change in electronic energy is roughly proportional to the overlap integral $S$).

We now have four molecular orbitals, $\sigma_1$, $\sigma_2$*, $\sigma_x$* and $\sigma_y$*, one lowered in energy and one raised relative to the energy of the orbitals of the pair of hydrogen molecules. If we have four electrons in the system, the net result is repulsion, as usual when two filled orbitals combine with each other. Thus two $H_2$ molecules do not combine to form an $H_4$ molecule. This is an important conclusion, and is true no matter what geometry we use in the combination. It is important, because it shows us in the simplest possible case why molecules exist, and why they largely retain their identity—when two molecules approach each other, the interaction of their molecular orbitals usually leads to this repulsion. Overcoming the repulsion is a prerequisite for chemical reaction and the energy needed is a major part of the activation energy.

## 1.3   C—H and C—C Bonds

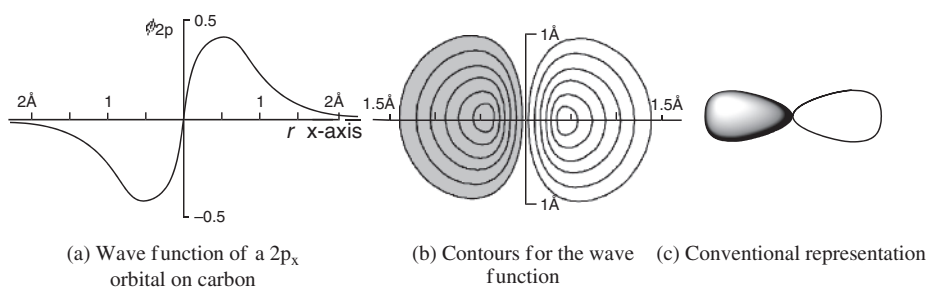### 1.3.1  The Atomic Orbitals of a Carbon Atom

Carbon has s and p orbitals, but we can immediately discount the 1s orbital as contributing to bonding, because the two electrons in it are held so tightly in to the nucleus that there is no possibility of significant overlap with this orbital—the electrons simply shield the nucleus, effectively giving it less of a positive charge. We are left with four electrons in 2s and 2p orbitals to use for bonding. The 2s orbital is like the 1s orbital in being spherically symmetrical, but it has a spherical node, with a wave function like that shown in Fig. 1.11a, and a contour plot like that in Fig. 1.11b. The node is close to the nucleus, and overlap with the inner sphere is never important, making the 2s orbital effectively similar to a 1s orbital. Accordingly, a 2s orbital is usually drawn simply as a circle, as in Fig. 1.11c. The overlap integral $S$ of a 1s orbital on hydrogen with the outer part of the 2s orbital on carbon has a similar form to the overlap integral for two 1s orbitals in Fig. 1.4 (except that it does not rise as high, is at a maximum at greater atomic separation, and would not reach unity at superimposition). The 2s orbital on carbon, at –19.5 eV, is 5.9 eV lower in energy than the 1s orbital in hydrogen. The attractive force on the 2s electrons is high because the nucleus has six protons, even though this is offset by the greater average distance of the electrons from the nucleus and by the shielding from the other electrons. Slater's rules suggest that the two 1s electrons reduce the nuclear charge by 0.85 atomic charges each, and the other 2s and the two 2p electrons reduce it by $3 \times 0.35$ atomic charges, giving the nucleus an effective charge of 3.25.
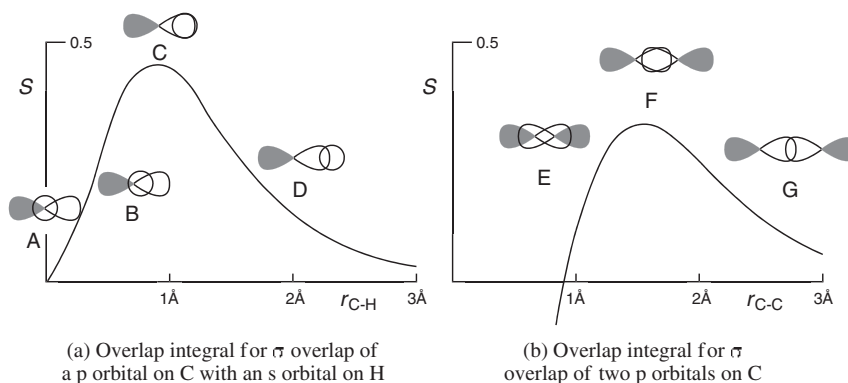


| (a) Wave function of a 2s orbital on carbon | (b) Contours for the wave function | (c) Conventional representation |

**Fig. 1.11**   The 2s atomic orbital on carbon

The 2p orbitals on carbon also have one node each, but they have a completely different shape. They point mutually at right angles, one each along the three axes, x, y and z. A plot of the wave function for the $2p_x$ orbital along the x axis is shown in Fig. 1.12a, and a contour plot of a slice through the orbital is shown in Fig. 1.12b. Scale drawings of p orbitals based on the shapes defined by these functions would clutter up any attempt to analyse their contribution to bonding, and so it is conventional to draw much narrower lobes, as in Fig. 1.12c, and we make a mental reservation about their true size and shape. The 2p orbitals, at $-10.7$ eV, are higher in energy than the 2s, because they are held on average further from the nucleus. When wave functions for all three p orbitals, $p_x$, $p_y$ and $p_z$, are squared and added together, the overall electron probability has spherical symmetry, just like that in the corresponding s orbital, but concentrated further from the nucleus.

Bonds to carbon will be made by overlap of s orbitals with each other, as they are in the hydrogen molecule, of s orbitals with p orbitals, and of p orbitals with each other. The overlap integrals $S$ between a p orbital and an s or p orbital are dependent upon the angles at which they approach each other. The overlap integral for a head on approach of an s orbital on hydrogen along the axis of a p orbital on carbon with a lobe of the same sign in the wave function (Fig. 1.13a), leading to a $\sigma$ bond, grows as the orbitals begin to overlap (D), goes through a maximum when the nuclei are a little over 0.9 Å apart (C), falls fast as some of the s orbital overlaps with the back lobe of the p orbital (B), and goes to zero when the s orbital is centred on the carbon atom (A). In the last configuration, whatever bonding there would be from the overlap with the lobe of the same sign (unshaded lobes are conventionally used to represent a positive sign in the wave function) is exactly cancelled by overlap with the lobe (shaded) of opposite sign in the wave function. Of course this



(a) Wave function of a $2p_x$          (b) Contours for the wave   (c) Conventional representation
      orbital on carbon                      function

**Fig. 1.12**   A $2p_x$ atomic orbital on carbon



(a) Overlap integral for $\sigma$ overlap of        (b) Overlap integral for $\sigma$
   a p orbital on C with an s orbital on H          overlap of two p orbitals on C

**Fig. 1.13**   Overlap integrals for $\sigma$ overlap with a p orbital on carbon

configuration is never reached, in chemistry at least, since the nuclei cannot coincide. The overlap integral for two p orbitals approaching head-on in the bonding mode with matching signs (Fig. 1.13b) begins to grow when the nuclei approach (G), rises to a maximum when they are about 1.5 Å apart (F), falls to zero as overlap of the front lobes with each other is cancelled by overlap of the front lobes with the back lobes (E), and would fall eventually to –1 at superimposition. The signs of the wave functions for the individual s and p atomic orbitals can get confusing, which is why we adopt the convention of shaded and unshaded. The signs will not be used in this book, except in Figs. 1.17 and 1.18, where they are effectively in equations.

In both cases, s overlapping with p and p overlapping with p, the overlap need not be perfectly head-on for some contribution to bonding to be still possible. For imperfectly aligned orbitals, the integral is inevitably less, because the build up of electron population between the nuclei, which is responsible for holding the nuclei together, is correspondingly less; furthermore, since the overlapping region will also be off centre, the nuclei are less shielded from each other. The overlap integral for a 1s orbital on hydrogen and a 2p orbital on carbon is actually proportional to the cosine of the angle of approach $\theta$, where $\theta$ is 0° for head-on approach and 90° if the hydrogen atom is in the nodal plane of the p orbital.

### 1.3.2 Methane

In methane, there are eight valence electrons, four from the carbon and one each from the hydrogen atoms, for which we need four molecular orbitals. We can begin by combining two hydrogen molecules into a composite $H_4$ unit, and then combine the orbitals of that species (Fig. 1.10) with the orbitals of the carbon atom. It is not perhaps obvious where in space to put the four hydrogen atoms. They will repel each other, and the furthest apart they can get is a tetrahedral arrangement. In this arrangement, it is still possible to retain bonding interactions between the hydrogen atoms and the carbon atoms in all four orbitals, as we shall see, and the maximum amount of total bonding is obtained with this arrangement.

We begin by classifying the orbitals with respect to the two symmetry elements, the xz plane and the yz plane. The symmetries of the molecular orbitals of the $H_4$ 'molecule' taken from Fig. 1.10 are placed on the left in Fig. 1.14, but the energies of each are now close to the energy of an isolated 1s orbital on hydrogen, because the four hydrogen atoms are now further apart than we imagined them to be in Fig. 1.10. The s and p
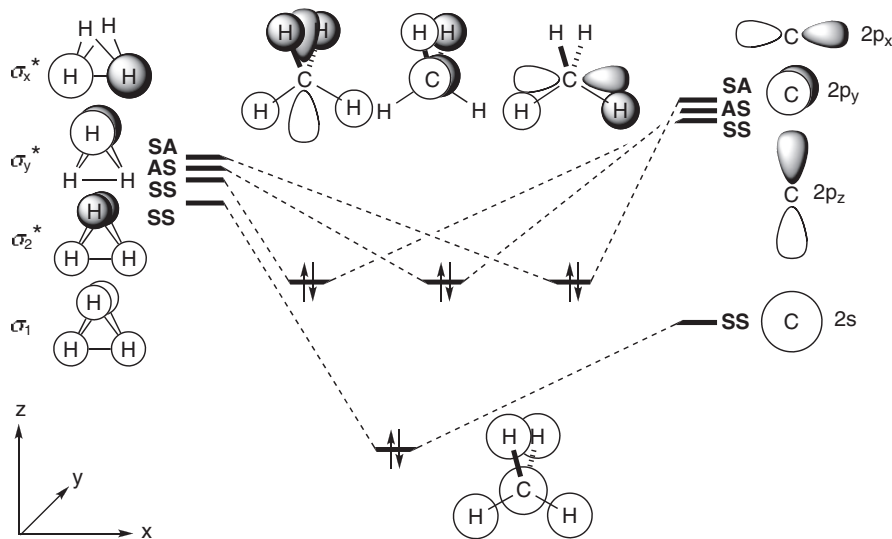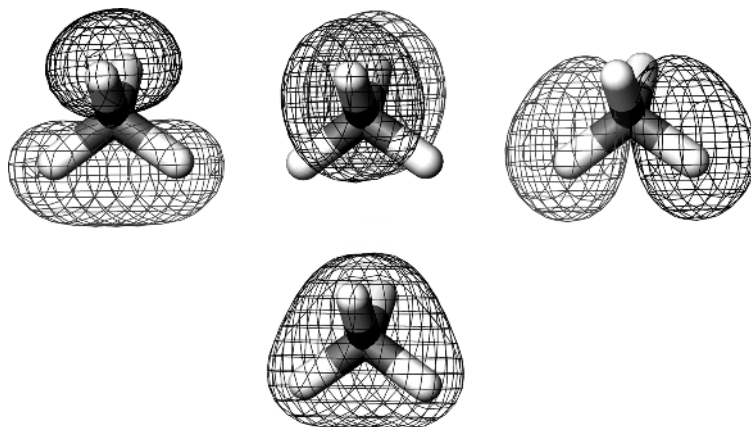


**Fig. 1.14**   The molecular orbitals of methane constructed from the interaction of the orbitals of tetrahedral $H_4$ and a carbon atom

orbitals on the single carbon atom are shown on the right. There are two SS orbitals on each side, but the overlap integral for the interaction of the 2s orbital on carbon with the $\sigma_2^*$ orbital is zero—there is as much bonding with the lower lobes as there is antibonding with the upper lobes. This interaction leads nowhere. We therefore have four interactions, leading to four bonding molecular orbitals (shown in Fig. 1.14) and four antibonding (not shown). One is lower in energy than the others, because it uses overlap from the 2s orbital on carbon, which is lower in energy than the 2p orbitals. The other three orbitals are actually equal in energy, just like the component orbitals on each side, and the four orbitals are all we need to accommodate the eight valence electrons. There will be, higher in energy, a corresponding set of antibonding orbitals, which we shall not be concerned with for now.

In this picture, the force holding any one of the hydrogen atoms bonded to the carbon is derived from more than one molecular orbital. The two hydrogen atoms drawn below the carbon atom in Fig. 1.14 have bonding from the low energy orbital made up of the overlap of all the s orbitals, and further bonding from the orbitals, drawn on the upper left and upper right, made up from overlap of the 1s orbital on the hydrogen with the $2p_z$ and $2p_x$ orbitals on carbon. These two hydrogen atoms are in the node of the $2p_y$ orbital, and there is no bonding to them from the molecular orbital in the centre of the top row. However, the hydrogens drawn above the carbon atom, one in front of the plane of the page and one behind, are bonded by contributions from the overlap of their 1s orbitals with the 2s, $2p_y$ and $2p_z$ orbitals of the carbon atom, but not with the $2p_x$ orbital.

Fig. 1.14 uses the conventional representations of the atomic orbitals, revealing which atomic orbitals contribute to each of the molecular orbitals, but they do not give an accurate picture of the resulting electron distribution. A better picture can be found in Jorgensen's and Salem's pioneering book, *The Organic Chemist's Book of Orbitals*,[14] which is also available as a CD.[15] There are also several computer programs which allow you easily to construct more realistic pictures. The pictures in Fig. 1.15 come from one of these, Jaguar, and show the four filled orbitals of methane. The wire mesh drawn to represent the outline of each molecular orbital shows one of the contours of the wave function, with the signs symbolised by light and heavier shading. It is easy to see what the component s and p orbitals must have been, and for comparison the four orbitals are laid out here in the same way as those in Fig. 1.14.



**Fig. 1.15**   One contour of the wave function for the four filled molecular orbitals of methane

### 1.3.3 Methylene

Methylene, $CH_2$, is not a molecule that we can isolate, but it is a well known reactive intermediate with a bent H—C—H structure, and in that sense is a 'stable' molecule. Although more simple than methane, it brings us for the first time to another feature of orbital interactions which we need to understand. We take the orbitals

of a hydrogen molecule from Fig. 1.3 and place them on the left of Fig. 1.16, except that again the atoms are further apart, so that the bonding and antibonding combination have relatively little difference in energy. On the right are the atomic orbitals of carbon. In this case we have three symmetry elements: (i) the xz plane, bisecting all three atoms; (ii) the yz plane, bisecting the carbon atom, and through which the hydrogen atoms reflect each other; and (iii) a two-fold rotation axis along the z coordinate, bisecting the H—C—H angle. The two orbitals, $\sigma_{HH}$ and $\sigma^*_{HH}$ in Fig. 1.16, are SSS and SAA with respect to these symmetry elements, and the atomic orbitals of carbon are SSS, SSS, ASA and SAA. Thus there are two orbitals on the right and one on the left with SSS symmetry, and the overlap integral is positive for the interactions of the $\sigma_{HH}$ and both the 2s and $2p_z$ orbitals, so that we cannot have as simple a way of creating a picture as we did with methane, where one of the possible interactions had a zero overlap integral.

In more detail, we have three molecular orbitals to create from three atomic orbitals, and the linear combination is Equation 1.8, like Equation 1.1 but with three terms:

$$\sigma = c_1\phi_1 + c_2\phi_2 + c_3\phi_3 \qquad\qquad 1.8$$

Because of symmetry, $|c_1|$ must equal $|c_3|$, but $|c_2|$ can be different. On account of the energy difference, it only makes a small contribution to the lowest-energy orbital, as shown in Fig. 1.17, where there is a small p lobe, in phase, buried inside the s orbital $\sigma_s$. It would show in a full contour diagram, but does not intrude in a simple picture like that in Fig. 1.16. The second molecular orbital up in energy created from this interaction, the $\sigma_z$ orbital, is a mix of the $\sigma_{HH}$ orbital, the 2s orbital on carbon, out of phase, and the $2p_z$ orbital, in phase, which has the effect of boosting the upper lobe, and reducing the lower lobe. There is then a third orbital higher in energy, shown in Fig. 1.17 but not in Fig. 1.16, antibonding overall, with both the 2s and $2p_z$ orbitals out of phase with the $\sigma_{HH}$ orbital. Thus, we have created three molecular orbitals from three atomic orbitals.

Returning to Fig. 1.16, the other interaction, between the $\sigma^*_{HH}$ orbital and its SAA counterpart, the $2p_x$ orbital, gives a bonding combination $\sigma_x$ and an antibonding combination (not shown). Finally, the remaining p orbital, $2p_y$ with no orbital of matching symmetry to interact with, remains unchanged, and, as it happens, unoccupied.

If we had used the linear arrangement H—C—H, the $\sigma_x$ orbital would have had a lower energy, because the overlap integral, with perfect head-on overlap ($\theta = 0°$), would be larger, but the $\sigma_z$ orbital would have made no contribution to bonding, since the H atoms would have been in the node of the p orbital. This orbital would
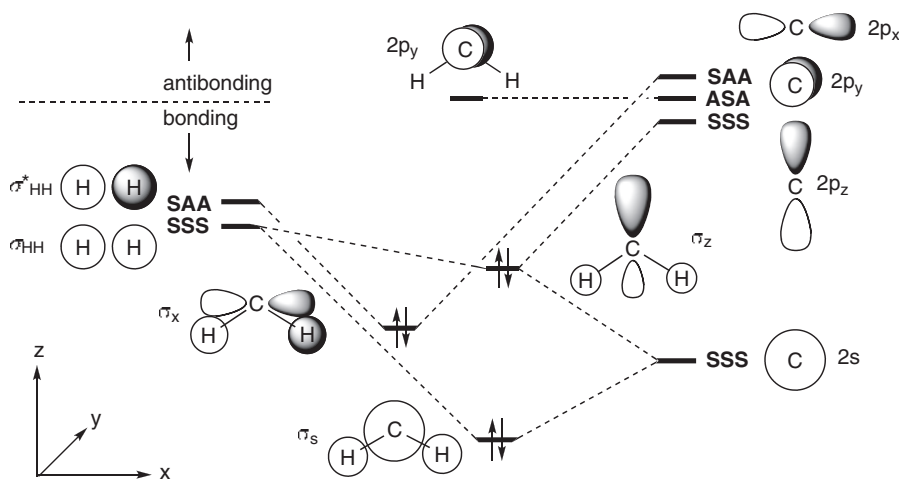


**Fig. 1.16**   The molecular orbitals of methylene constructed from the interaction of the orbitals of $H_2$ and a carbon atom
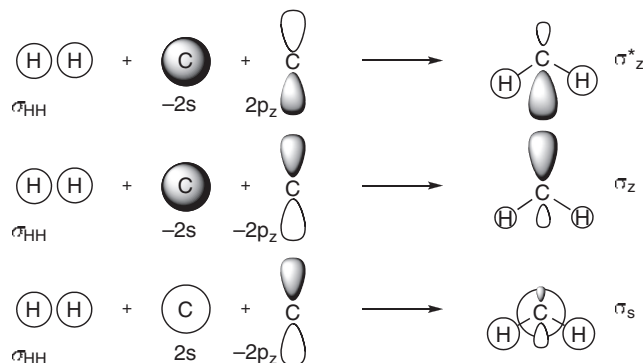
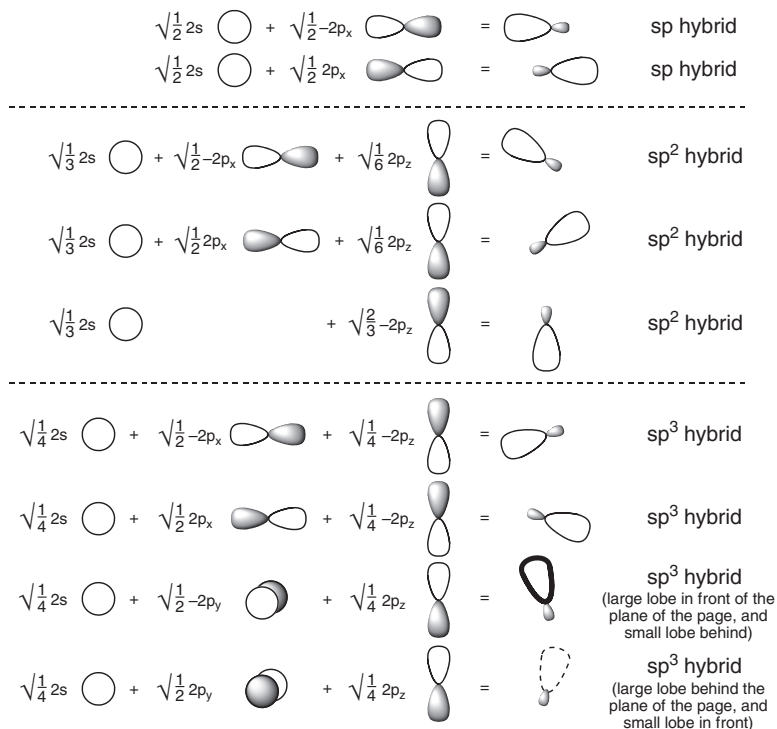**Fig. 1.17**   Interactions of a 2s and $2p_z$ orbital on carbon with the $\sigma_{HH}$ orbital with the same symmetry

simply have been a new orbital on carbon, half way between the s and p orbitals, making no contribution to bonding, and the overall lowering in energy would be less than for the bent structure.

   We do not actually need to combine the orbitals of the two hydrogen atoms before we start. All we need to see is that the combinations of all the available s and p orbitals leading to the picture in Fig. 1.16 will account for the bent configuration which has the lowest energy. Needless to say, a full calculation, optimising the bonding, comes to the same conclusion. Methylene is a bent molecule, with a filled orbital of p character, labelled $\sigma_z$, bulging out in the same plane as the three atoms. The orbital $\sigma_s$ made up largely from the s orbitals is lowest in energy, both because the component atomic orbitals start off with lower energy, and because their combination is inherently head-on. An empty $p_y$ orbital is left unused, and this will be the lowest in energy of the unfilled orbitals—it is nonbonding and therefore lower in energy than the various antibonding orbitals created, but not illustrated, by the orbital interactions shown in Fig. 1.16.

### 1.3.4 Hybridisation

One difficulty with these pictures, explaining the bonding in methane and in methylene, is that there is no single orbital which we can associate with the C—H bond. To avoid this inconvenience, chemists often use Pauling's idea of hybridisation; that is, they mix together the atomic orbitals of the carbon atom, adding the s and p orbitals together in various proportions, to produce a set of hybrids, *before* using them to make the molecular orbitals. We began to do this in the account of the orbitals of methylene, but the difference now is that we do all the mixing of the carbon-based orbitals first, before combining them with anything else.

   Thus one-half of the 2s orbital on carbon can be mixed with one-half of the $2p_x$ orbital on carbon, with its wave function in each of the two possible orientations, to create a degenerate pair of hybrid orbitals, called sp hybrids, leaving the $2p_y$ and $2p_z$ orbitals unused (Fig. 1.18, top). The 2s orbital on carbon can also be mixed with the $2p_x$ and $2p_z$ orbitals, taking one-third of the 2s orbital in each case successively with one-half of the $2p_x$ and one-sixth of the $2p_z$ in two combinations to create two hybrids, and with the remaining two-thirds of the $2p_z$ orbital to make the third hybrid. This set is called $sp^2$ (Fig. 1.18, centre); it leaves the $2p_y$ orbital unused at right angles to the plane of the page. The three hybrid orbitals lie in the plane of the page at angles of 120° to each other, and are used to describe the bonding in trigonal carbon compounds. For tetrahedral carbon, the mixing is one-quarter of the 2s orbital with one-half of the $2p_x$ and one-quarter of the $2p_z$ orbital, in two combinations, to make one pair of hybrids, and one quarter of the 2s orbital with one-half of the $2p_y$ and one-quarter of the $2p_z$ orbital, also in two combinations, to make the other pair of hybrids, with the set of four called $sp^3$ hybrids (Fig. 1.18, bottom).

$\sqrt{\frac{1}{2}}\,2s$ ◯ $+ \sqrt{\frac{1}{2}}\,-2p_x$ ◌◉ $=$ ◌●     sp hybrid

$\sqrt{\frac{1}{2}}\,2s$ ◯ $+ \sqrt{\frac{1}{2}}\,2p_x$ ◉◌ $=$ ●◌     sp hybrid

$\sqrt{\frac{1}{3}}\,2s$ ◯ $+ \sqrt{\frac{1}{2}}\,-2p_x$ ◌◉ $+ \sqrt{\frac{1}{6}}\,2p_z$   $=$   $sp^2$ hybrid

$\sqrt{\frac{1}{3}}\,2s$ ◯ $+ \sqrt{\frac{1}{2}}\,2p_x$ ◉◌ $+ \sqrt{\frac{1}{6}}\,2p_z$   $=$   $sp^2$ hybrid

$\sqrt{\frac{1}{3}}\,2s$ ◯ $+ \sqrt{\frac{2}{3}}\,-2p_z$   $=$   $sp^2$ hybrid

$\sqrt{\frac{1}{4}}\,2s$ ◯ $+ \sqrt{\frac{1}{2}}\,-2p_x$ ◌◉ $+ \sqrt{\frac{1}{4}}\,-2p_z$   $=$   $sp^3$ hybrid

$\sqrt{\frac{1}{4}}\,2s$ ◯ $+ \sqrt{\frac{1}{2}}\,2p_x$ ◉◌ $+ \sqrt{\frac{1}{4}}\,-2p_z$   $=$   $sp^3$ hybrid

$\sqrt{\frac{1}{4}}\,2s$ ◯ $+ \sqrt{\frac{1}{2}}\,-2p_y$ ◯ $+ \sqrt{\frac{1}{4}}\,2p_z$   $=$   $sp^3$ hybrid
(large lobe in front of the plane of the page, and small lobe behind)

$\sqrt{\frac{1}{4}}\,2s$ ◯ $+ \sqrt{\frac{1}{2}}\,2p_y$ ● $+ \sqrt{\frac{1}{4}}\,2p_z$   $=$   $sp^3$ hybrid
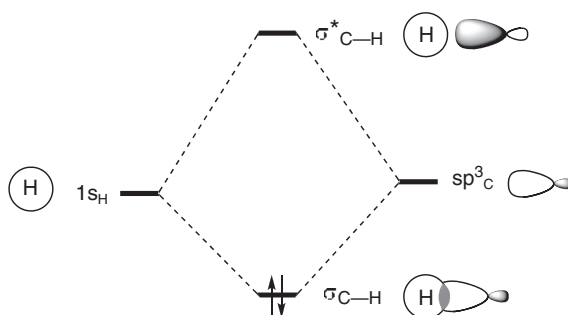(large lobe behind the plane of the page, and small lobe in front)

**Fig. 1.18**  Hybrid orbitals

The conventional representations of hybrid orbitals used in Fig. 1.18 are just as misleading as the conventional representations of the p orbitals from which they are derived. A more accurate picture of the $sp^3$ hybrid is given by the contours of the wave function in Fig. 1.19. Because of the presence of the inner sphere in the 2s orbital (Fig. 1.11a), the nucleus is actually inside the back lobe, and a small proportion of the front lobe reaches behind the nucleus. This follows from the way a hybrid is constructed by adding one-quarter of the wave function of the s orbital (Fig. 1.11a) and three-quarters in total of the wave functions of the p orbitals (Fig. 1.12a). As usual, we draw the conventional hybrids relatively thin, and make the mental reservation that they are fatter than they are usually drawn.
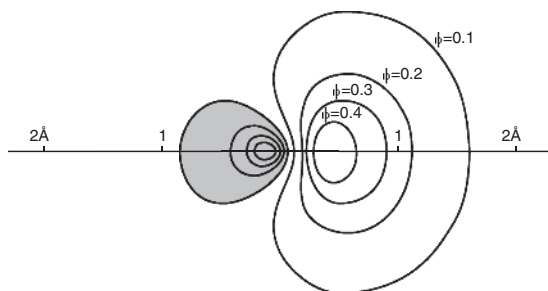


**Fig. 1.19**  A section through an $sp^3$ hybrid on carbon

The interaction of the 1s orbital of a hydrogen atom with an sp$^3$ hybrid on carbon can be used in the usual way to create a $\sigma_{CH}$ bonding orbital and a $\sigma^*_{CH}$ antibonding orbital (Fig. 1.20). Four of the bonding orbitals, each with two electrons in it, one from each of the four hybrids, point towards the corners of a regular tetrahedron, and give rise to the familiar picture for the bonds in methane shown in Fig. 1.21a.



**Fig. 1.20**  Bonding and antibonding orbitals of a C—H bond



(a) The sp$^3$ hybrids on carbon overlapping with the s orbitals of hydrogen

(b) Conventional bonds
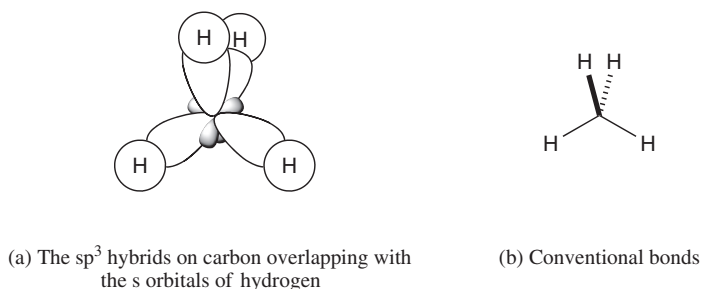
**Fig. 1.21**  Methane built up using sp$^3$ hybridised orbitals

This picture has the advantage over that in Fig. 1.14 that the C—H bonds do have a direct relationship with the lines drawn on the conventional structure (Fig. 1.21b). The bonds drawn in Fig. 1.14 do not represent anything material but without them the picture would be hard to interpret. The two descriptions of the overall wave function for methane are in fact identical; hybridisation involves the same approximations, and the taking of s and p orbitals in various proportions and various combinations, as those used to arrive at the picture in Fig. 1.14. For many purposes it is wise to avoid localising the electrons in the bonds, and to use pictures like Fig. 1.14. This is what most theoreticians do when they deal with organic molecules, and it is what the computer programs will produce. It is also, in most respects, a more realistic model. Measurements of ionisation potentials, for example, show that there are two energy levels from which electrons may be removed; this is immediately easy to understand in Fig. 1.14, where there are filled orbitals of different energy, but the picture of four identical bonds from Fig. 1.20 hides this information.

For other purposes, however, it is undoubtedly helpful to take advantage of the simple picture provided by the hybridisation model, even though hybridisation is an extra concept to learn. It immediately reveals, for example, that all four bonds are equal. It can be used whenever it offers a simplification to an argument as we shall find later in this book, but it is good practice to avoid it wherever possible. In particular, the common

practice of referring to a molecule or an atom as 'rehybridising' is not good usage—the rehybridisation in question is in *our* picture, not in the molecule. It is likewise poor (but unfortunately common) practice to refer to atoms as being $sp^3$, $sp^2$ or sp hybridised. Again the atoms themselves are not, in a sense, hybridised, it is *we who have chosen to picture them that way*. It is better in such circumstances to refer to the atoms as being tetrahedral, trigonal, or digonal, as appropriate, and allow for the fact that the bonds around carbon (and other) atoms may not have exactly any of those geometries.

### 1.3.5  C—C σ Bonds and π Bonds: Ethane

With a total of fourteen valence electrons to accommodate in molecular orbitals, ethane presents a more complicated picture, and we now meet a C—C bond. We will not go into the full picture—finding the symmetry elements and identifying which atomic orbitals mix to set up the molecular orbitals. It is easy enough to see the various combinations of the 1s orbitals on the hydrogen atoms and the 2s, $2p_x$, $2p_y$ and $2p_z$ orbitals on the two carbon atoms giving the set of seven bonding molecular orbitals in Fig. 1.22.
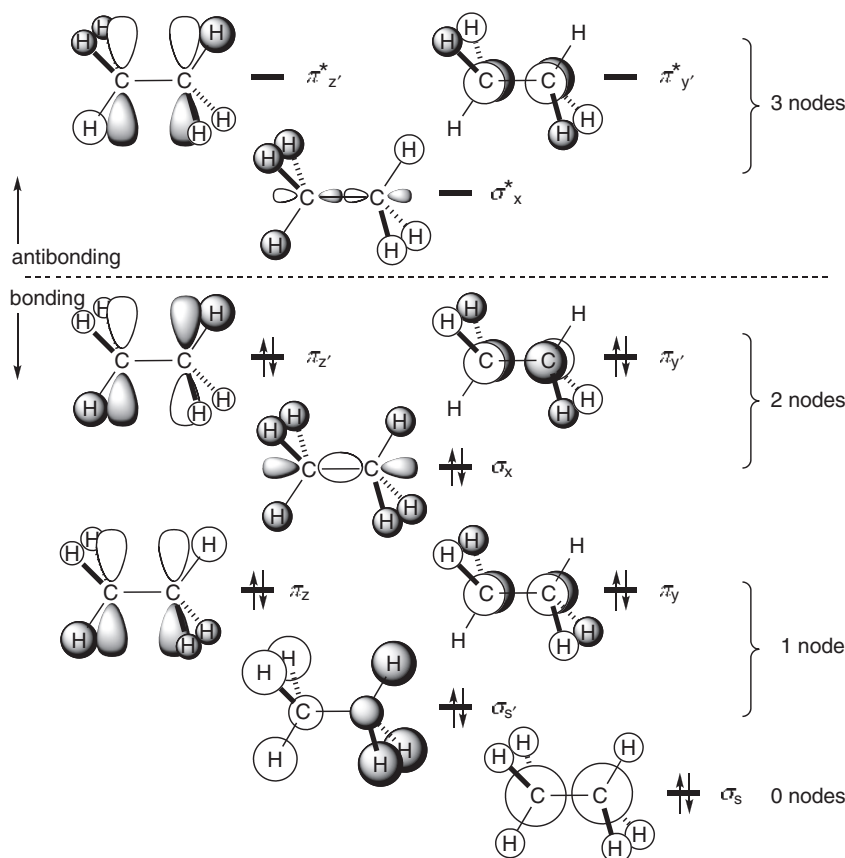


Fig. 1.22   The bonding orbitals and three antibonding orbitals of ethane

There is of course a corresponding picture using $sp^3$ hybrids, but the following account shows how easy it is to avoid them. We shall concentrate for the moment on those orbitals which give rise to the force holding the two carbon atoms together; between them they make up the C—C bond. The molecular orbitals ($\sigma_s$ and $\sigma_{s'}$), made up

largely from 2s orbitals on carbon, are very like the orbitals in hydrogen, in that the region of overlap is directly on a line between the carbon nuclei; as before, they are called $\sigma$ orbitals. The bonding in the lower one is very strong, but it is somewhat offset by the antibonding (as far as the C—C bond is concerned) in the upper one. They are both strongly bonding with respect to the C—H bonds. There is actually a little of the $2p_x$ orbital mixed in with this orbital, just as we saw in Fig. 1.17 with a $2p_z$ orbital, but most of the $2p_x$ orbital contributes to the molecular orbital $\sigma_x$, which is also $\sigma$ in character, and very strong as far as the C—C bond is concerned. This orbital has a little of the 2s orbital mixed in, resulting in the asymmetric extension of the lobes between the two carbon nuclei and a reduction in size of the outer lobes. This time, its antibonding counterpart ($\sigma^*_x$) is not involved in the total bonding of ethane, nor is it bonding overall. It is in fact the lowest-energy antibonding orbital.

In the molecular orbitals using the $2p_y$ and $2p_z$ orbitals of carbon, the lobes of the atomic orbitals overlap sideways on. This is the distinctive feature of what is called $\pi$ bonding, although it may be unfamiliar to meet this type of bonding in ethane. Nevertheless, let us see where it takes us. The conventional way of drawing a p orbital (Fig. 1.12c) is designed to give elegant and uncluttered drawings, like those in Fig. 1.22, and is used throughout this book for that reason. A better picture as we have already seen, and which we keep as a mental reservation when confronted with the conventional drawings, is the contour diagram (Fig. 1.12b). With these pictures in mind, the overlap sideways-on can be seen to lead to an enhanced electron population between the nuclei. However, since it is no longer directly on a line between the nuclei, it does not hold the carbon nuclei together as strongly as a $\sigma$-bonding orbital. The overlap integral $S$ for two p orbitals with a dihedral angle of zero has the form shown in Fig. 1.23, where it can be compared with the corresponding $\sigma$ overlap integral taken from Fig. 1.13b. Whereas the $\sigma$ overlap integral goes through a maximum at about 1.5 Å and then falls rapidly to a value of –1, the $\pi$ overlap integral rises more slowly but reaches unity at superimposition. Since C—C single bonds are typically about 1.54 Å long, the overlap integral at this distance for $\pi$ bonding is a little less than half that for $\sigma$ bonding. $\pi$ Bonds are therefore much weaker.
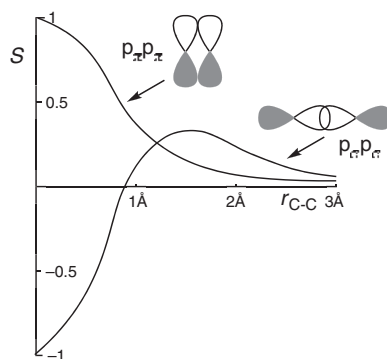


**Fig. 1.23**   Comparison of overlap integrals for $\pi$ and $\sigma$ bonding of p orbitals on C

Returning to the molecular orbitals in ethane made from the $2p_y$ and $2p_z$ orbitals, we see that they again fall in pairs, a bonding pair ($\pi_y$ and $\pi_z$) and (as far as C—C bonding is concerned, but not overall) an antibonding pair ($\pi_{y'}$ and $\pi_{z'}$). These orbitals have the wrong symmetry to have any of the 2s orbital mixed in with them. The electron population in the four orbitals ($p_y$, $p_z$, $p_{y'}$ and $p_{z'}$) is higher in the vicinity of the hydrogen atoms than in the vicinity of the carbon atoms, and these orbitals mainly contribute to the strength of the C—H bonds, towards which all four orbitals are bonding. The amount both of bonding and antibonding that they contribute to the C—C bond is small, with the bonding and antibonding combinations more or less cancelling each other out.

Thus the orbital ($\sigma_x$) is the most important single orbital making up the C—C bond. We can construct for it an interaction diagram (Fig. 1.24), just as we did for the H—H bond in Fig. 1.3. The other major contribution to C—C bonding comes from the fact that $\sigma_s$ is more C—C bonding than $\sigma_{s'}$ is C—C antibonding, as already mentioned.
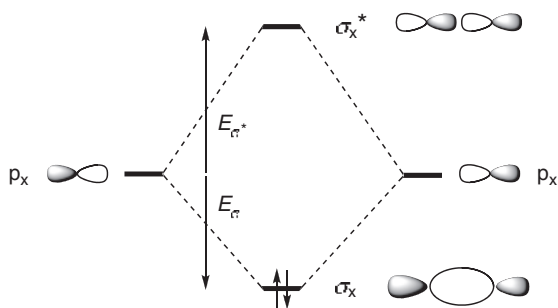
**Fig. 1.24** A major part of the C—C $\sigma$ bond of ethane

Had we used the concept of hybridisation, the C—C bond would, of course, simply have been seen as coming from the bonding overlap of sp³ hybridised orbitals on carbon with each other, and the overall picture for the C—C bond would have looked very similar to $\sigma_x$ in Fig. 1.24, except that it would have used different proportions of s and p orbitals, and would have been labelled sp³. For simplicity, we shall often discuss the orbitals of $\sigma$ bonds as though they could be localised into bonding and antibonding orbitals like $\sigma_x$ and $\sigma_x$*. We shall not often need to refer to the full set of orbitals, except when they become important for one reason or another. Any property we may in future attribute to the bonding and antibonding orbitals of a $\sigma$ bond, as though there were just one such pair, can always be found in the full set of all the bonding orbitals, or they can be found in the interaction of appropriately hybridised orbitals.

### 1.3.6 C=C $\pi$ Bonds: Ethylene

The orbitals of ethylene are made up from the 1s orbitals of the four hydrogen atoms and the 2s, $2p_x$, $2p_y$ and $2p_z$ orbitals of the two carbon atoms (Fig. 1.25). One group, made up from the 1s orbitals on hydrogen and the 2s, $2p_x$ and $2p_y$ orbitals on carbon, is substantially $\sigma$ bonding, which causes the orbitals to be relatively low in energy. These five orbitals with ten of the electrons make up what we call the $\sigma$ *framework*. Standing out, higher in energy than the $\sigma$-framework orbitals, is a filled orbital made up entirely from the $2p_z$ orbitals of the carbon atom overlapping in a $\pi$ bond. This time, the $\pi$ orbital is localised on the carbon atoms with no mixing in of the 1s orbitals on the hydrogen atoms, which all sit in the nodal plane of the $\pi_z$ orbital. The bonding in this orbital gives greater strength to the C—C bonding in ethylene than the $\pi$ orbitals give to the C—C bonding in ethane, which is one reason why we talk of ethylene as having a *double* bond. Nevertheless, the C—C $\sigma$ bonding in the $\sigma$ framework is greater than the $\pi$ bonding from overlap of the two $p_z$ orbitals. This is because, other things being equal, $\pi$ overlap is inherently less effective in lowering the energy than $\sigma$ overlap. Thus in the interaction diagram for a $\pi$ bond (Fig. 1.26), the drop in energy $E_\pi$ from $\pi$ bonding is less than $E_\sigma$ in Fig. 1.24 for comparable $\sigma$ bonding, and this follows from the larger overlap integral for $\sigma$ approach than for $\pi$ approach (Fig. 1.23).

Similarly, $E_{\pi*}$ in Fig. 1.26 is less than $E_{\sigma*}$ in Fig. 1.24. Another consequence of having an orbital localised on two atoms is that the equation for the linear combination of atomic orbitals contains only two terms (Equation 1.1), and the $c$-values are again 0.707 in the bonding orbital and 0.707 and –0.707 in the antibonding orbital. In simple Hückel theory, the energy of the p orbital on carbon is given the value $\alpha$, which is used as a reference point from which to measure rises and drops in energy, and will be especially useful when we come to deal with other elements. The value of $E_\pi$ in Fig. 1.26 is given the symbol $\beta$, and is also used as a reference with which to compare the degree of bonding in other $\pi$-bonding systems. To give a sense of scale, its value for ethylene is approximately 140 kJ mol$^{-1}$ (= 1.45 eV = 33 kcal mol$^{-1}$). In other words the total $\pi$ bonding in ethylene is 280 kJ mol$^{-1}$, since there are two electrons in the bonding orbital.
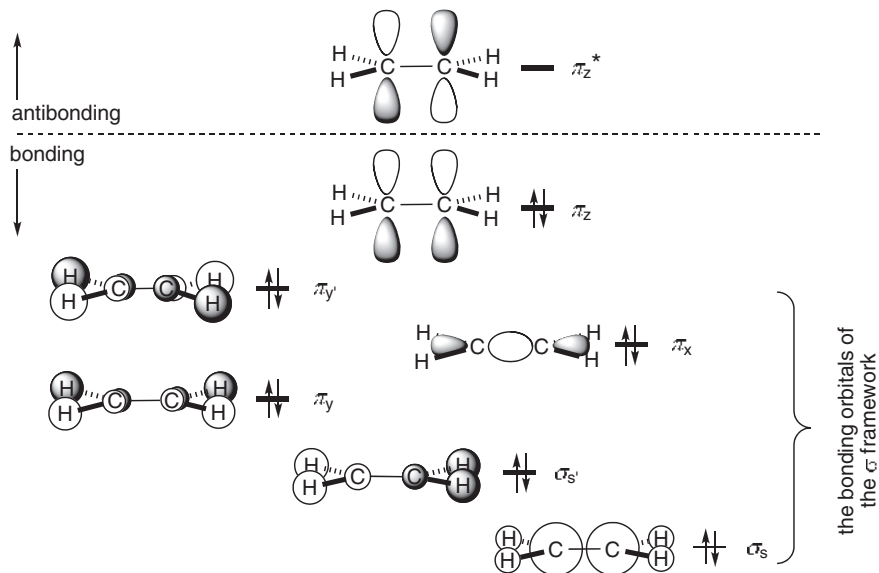
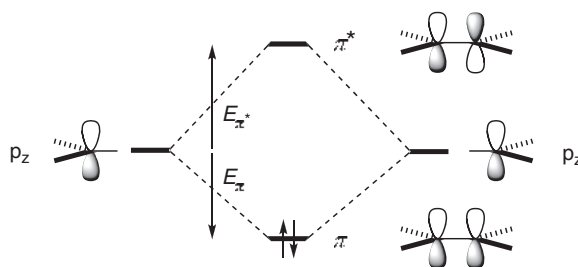**Fig. 1.25** The bonding orbitals and one antibonding orbital of ethylene



**Fig. 1.26** A C=C $\pi$ bond

This separation of the $\sigma$ framework and the $\pi$ bond is the essence of Hückel theory. Because the $\pi$ bond in ethylene in this treatment is self-contained, free of any complications from involvement with the hydrogen atoms, we may treat the electrons in it in the same way as we do for the fundamental quantum mechanical picture of an electron in a box. We look at each molecular wave function as one of a series of sine waves. In these simple molecules we only have the two energy levels, and so we only need to draw an analogy between them and the two lowest levels for the electron in the box. The convention is to draw the limits of the box *one bond length* out from the atoms at the end of the conjugated system, and then inscribe sine waves so that a node always comes at the edge of the box. With two orbitals to consider for the $\pi$ bond of ethylene, we only need the 180° sine curve for $\pi$ and the 360° sine curve for $\pi^*$. These curves can be inscribed over the orbitals as they are on the left of Fig. 1.27, and we can see on the right how the vertical lines above and below the atoms duplicate the pattern of the coefficients, with both $c_1$ and $c_2$ positive in the $\pi$ orbital, and $c_1$ positive and $c_2$ negative in $\pi^*$.

The drawings of the p orbitals in Figs. 1.26 and 1.27 have the usual problem of being schematic. A better picture as we have already seen, and which we keep as a mental reservation when confronted with the
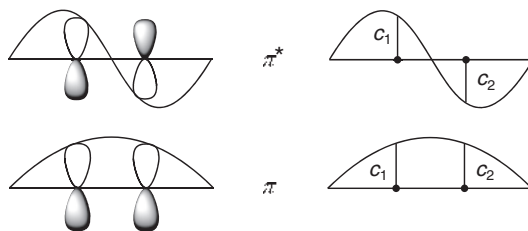
**Fig. 1.27**    The $\pi$ orbitals of ethylene and the electron in the box

conventional drawings, is the contour diagram (Fig. 1.12b). A better sense of the overlap from two side-by-side p orbitals is given in Fig. 1.28, where we see more clearly that in the bonding combination, even sideways-on, there is enhanced electron population between the nuclei, but that it is no longer directly on a line between the nuclei. The wire-mesh diagrams in Fig. 1.29, illustrate the shapes of the $\pi$ and $\pi^*$ orbitals even better, with some sense of their 3D character.
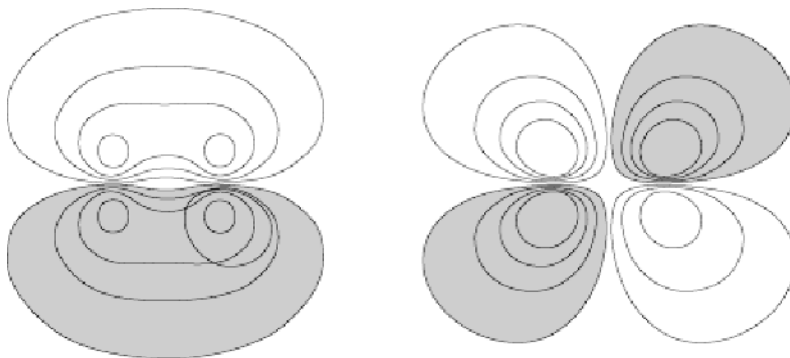


**Fig. 1.28**    A section through the contours of the $\pi$ and $\pi^*$ wave functions of ethylene
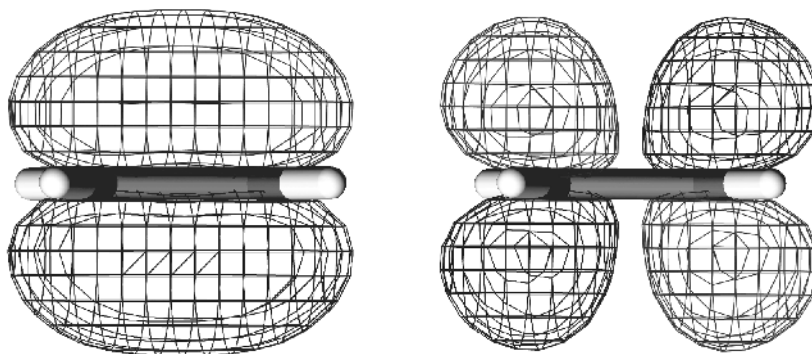


**Fig. 1.29**    Wire-mesh outlines of one contour of the $\pi$ and $\pi^*$ wave functions of ethylene

## 1.4   Conjugation—Hückel Theory[16,17]

The interaction of atomic orbitals giving rise to molecular orbitals is the simplest type of conjugation. Thus in ethylene the two p orbitals can be described as being conjugated with each other to make the $\pi$ bond. The simplest extension to make longer conjugated systems is to add one p orbital at a time to the $\pi$ bond to make successively the $\pi$ components of the allyl system with three carbon atoms, of butadiene with four, of the pentadienyl system with five, and so on. Hückel theory applies, because in each case we separate completely the $\pi$ system from the $\sigma$ framework, and we can continue to use the electron-in-the-box model.

### 1.4.1  The Allyl System

The members of the allyl system are reactive intermediates rather than stable molecules, and there are three of them: the allyl cation **1.1**, the allyl radical **1.2** and the allyl anion **1.3**. They have the same $\sigma$ framework and the same $\pi$ orbitals, but different numbers of electrons in the $\pi$ system.
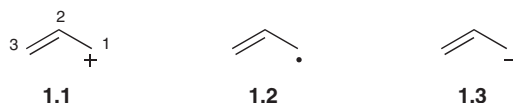


It is necessary to make a mental reservation about the diagrams **1.1–1.3**, so commonly used by organic chemists. These diagrams are localised structures that seem to imply that C-1 has the positive charge (an empty p orbital), the odd electron (a half-filled p orbital) or the negative charge (a filled p orbital), respectively, and that C-2 and C-3 are in a double bond in each case. However, we could have drawn the cation **1.1**, redrawn as **1.4a**, equally well the other way round as **1.4b**, and the curly arrow symbolism shows how the two *drawings* are interconvertible. This device is at the heart of valence bond theory. For now we need only to recognise that these two drawings are representations of the *same* species—there is no reaction connecting them, although many people sooner or later fall into the trap of thinking that 'resonance' like **1.4a** → **1.4b** is a step in a reaction sequence. The double-headed arrow interconnecting them is a useful signal; this symbol should be used only for interconnecting 'resonance structures' and never to represent an equilibrium There are corresponding pairs of drawings for the radical **1.5a** and **1.5b** and for the anion **1.6a** and **1.6b**.
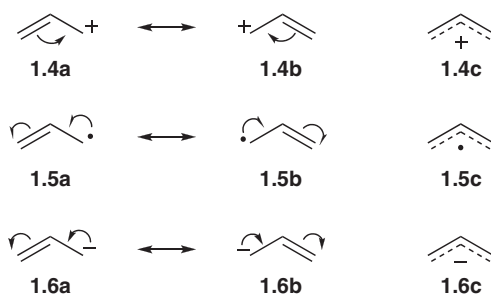


One way of avoiding these misleading structures is to draw the allyl cation, radical or anion as in **1.4c**, **1.5c** and **1.6c**, respectively, illustrating the delocalisation of the p orbitals with a dashed line, and placing the positive or negative charge in the middle. The trouble with these drawings is that they are hard to use clearly with curly arrows in mechanistic schemes, and they do not show that the positive charge in the cation, the odd electron in the radical or the negative charge in the anion are largely concentrated on C-1 and C-3, the very feature that the drawings **1.4a** and **1.4b**, **1.5a** and **1.5b** and **1.6a** and **1.6b** illustrate so well. We shall see that the drawings with

apparently localised charges **1.4a**, **1.4b**, **1.5a** and **1.5b** and **1.6a** and **1.6b** illustrate not only the overall $\pi$ electron distribution but also the important frontier orbital. It is probably better in most situations to use one of the localised drawings rather than any of the 'molecular orbital' versions **1.4c**, **1.5c** or **1.6c**, and then make the necessary mental reservation that each of the localised drawings implies the other.



**1.7**
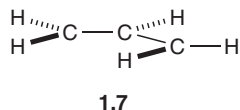
The allyl cation, radical and anion have the same $\sigma$ framework **1.7**, with 14 bonding molecular orbitals filled with 28 electrons made by mixing the 1s orbitals of the five hydrogen atoms either with the $sp^2$ hybrids or with the 2s, $2p_x$ and $2p_y$ orbitals of the three carbon atoms. The allyl systems are bent not linear, but we shall treat them as linear to simplify the discussion. The x, y and z coordinates have to be redefined as local x, y and z coordinates, different at each atom, in order to make this simplification, but this leads to no complications in the general story.

As with ethylene, we keep the $\sigma$ framework separate from the $\pi$ system, which is made up from the three $p_z$ orbitals on the carbon atoms that were not used in making the $\sigma$ framework. The linear combination of these orbitals takes the form of Equation 1.9, with three terms, creating a pattern of three molecular orbitals, $\psi_1$, $\psi_2$ and $\psi_3*$, that bear some resemblance to the set we saw in Section 1.3.3 for methylene. In the allyl cation there are two electrons left to go into the $\pi$ system after filling the $\sigma$ framework (and in the radical, three, and in the anion, four).

$$\psi = c_1\phi_1 + c_2\phi_2 + c_3\phi_3 \qquad\qquad 1.9$$

We can derive a picture of these orbitals using the electron in the box, recognising that we now have three orbitals and therefore three energy levels. If the lowest energy orbital is, as usual, to have no nodes (except the inevitable one in the plane of the molecule), and the next one up one node, we now need an orbital with two nodes. We therefore construct a diagram like that of Fig. 1.27, but with one more turn of the sine curve, to include that for 540°, the next one up in energy that fulfils the criterion that there are nodes at the edges of the box, one bond length out, as well as the two inside (Fig. 1.30).

The lowest-energy orbital, $\psi_1$, has bonding across the whole conjugated system, with the electrons concentrated in the middle. Because of the bonding, this orbital will be lower in energy than an isolated p
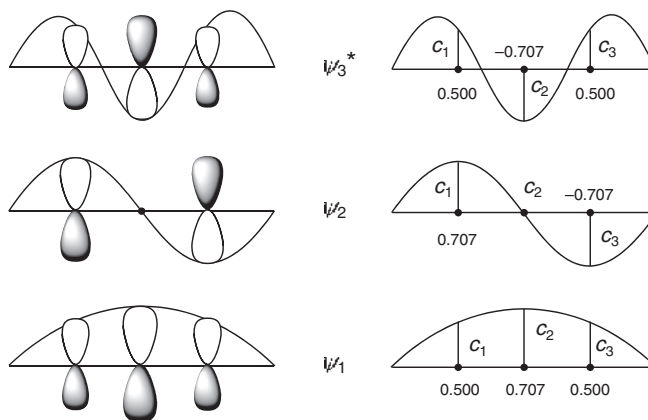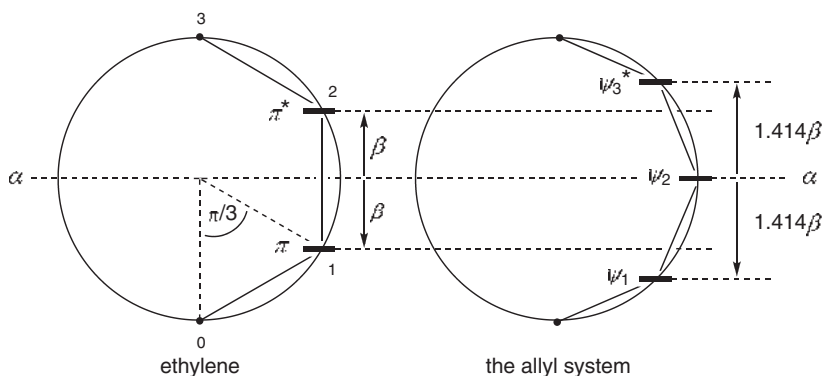


**Fig. 1.30**  The $\pi$ orbitals of the allyl system

orbital. The next orbital up in energy $\psi_2$, is different from those we have met so far. Its symmetry demands that the node be in the middle; but this time the centre of the conjugated system is occupied by an *atom* and not by a *bond*. Having a node in the middle means having a zero coefficient $c_2$ on C-2, and hence the coefficients on C-l and C-3 in this orbital must be $\pm 1/\sqrt{2}$, if, squared and summed, they are to equal one. The atomic orbitals in $\psi_2$ are so far apart in space that their repulsive interaction does not, to a first approximation, raise the energy of this molecular orbital relative to that of an isolated p orbital. In consequence, whether filled or not, it does not contribute to the overall bonding. If the sum of the squares of the three orbitals on C-2 is also to equal one, then the coefficients on C-2 in $\psi_1$ and $\psi_3$* must also be $\pm 1/\sqrt{2}$. Finally, since symmetry requires that the coefficients on C-1 and C-3 in $\psi_1$ and $\psi_3$* have the same absolute magnitude, and the sum of their squares must equal $1-(1/\sqrt{2})^2$, we can deduce the unique set of *c*-values shown in Fig. 1.30. A pattern present in the allyl system because of its symmetry is seen with other symmetrical conjugated systems: the |*c*| values are reflected across a mirror plane placed horizontally, half way up the set of orbitals, between $\psi_1$ and $\psi_3$*, and also across a mirror plane placed vertically, through C-2. It is only necessary therefore to calculate four of the nine numbers in Fig. 1.30, and deduce the rest from the symmetry.

   In this picture of the bonding, we get no immediate appreciation of the energies of these orbitals relative to those of ethylene. The nonbonding orbital $\psi_2$ is clearly on the $\alpha$ level, that of a p orbital on carbon, and $\psi_1$ is lowered by the extra $\pi$ bonding and $\psi_3$* is raised. To assess the energies, there is a simple geometrical device that works for linear conjugated systems. The conjugated system, *including the dummy atoms at the ends of the sine curves*, is inscribed vertically inside a circle of radius $2\beta$, following the convention that one $\pi$ bond in ethylene defines $\beta$. This is shown for ethylene and the allyl system in Fig. 1.31, where the dummy atoms are marked as dots at the top and bottom of the circle. The energies $E$ of the $\pi$ orbitals can then be calculated using Equation 1.10:

$$E = 2\beta \cos \frac{k\pi}{n+1} \qquad\qquad 1.10$$

where $k$ is the number of the atom along the sequence of $n$ atoms. This is simply an expression based on the trigonometry of Fig. 1.31, where, for example, the $\pi$ orbital of ethylene is placed on the first atom ($k=1$) of the sequence of two ($n=2$) reading anticlockwise from the bottom. Thus the energies of the $\pi$ orbitals in the allyl system are $1.414\beta$ below the $\alpha$ level and $1.414\beta$ above the $\alpha$ level.



**Fig. 1.31**   Energies of $\pi$ molecular orbitals in ethylene and the allyl system

We can gain further insight by building the picture of the $\pi$ orbitals of the allyl system in another way. Instead of mixing together three p orbitals on carbon, we can combine two of them in a $\pi$ bond first, as in Fig. 1.26, and then work out the consequences of having a third p orbital held within bonding distance of

the C=C $\pi$ bond. Although Fig. 1.26, and all the interaction diagrams for single bonds, illustrated the bonding orbital as less bonding than the antibonding orbital is antibonding, this detail confuses the simple picture for conjugated systems that we want to build up here, and is left out of the discussion. We have to consider the effect of the p orbital, on the right of Fig. 1.32 on both the $\pi$ and $\pi^*$ orbitals of ethylene on the left. If we look *only* at the interaction with the $\pi$ orbital, we can expect to create two new orbitals in much the same way as we saw when the two $2p_z$ orbitals of carbon were allowed to interact in the formation of the $\pi$ bond of Fig. 1.26. One orbital $\psi_1$ will be lowered in energy and the other $\psi_x$ raised. Similarly if we look *only* at its interaction with the $\pi^*$ orbital, we can expect to create two new orbitals, one lowered in energy $\psi_y$ and one raised $\psi_3^*$. We cannot create four orbitals from three, because we cannot use the p orbital separately twice.
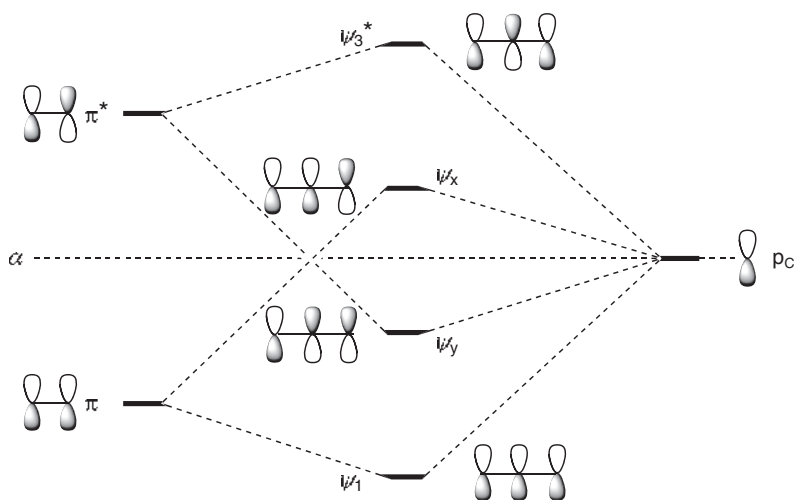


**Fig. 1.32**   A p orbital interacting independently with $\pi$ and $\pi^*$ orbitals. (No attempt is made to represent the relative sizes of the atomic orbitals)

We can see in Fig. 1.32 that the orbital $\psi_1$ has been created by mixing the p orbital with the $\pi$ orbital in a *bonding* sense, with the signs of the wave function of the two adjacent atomic orbitals matching. We can also see that the orbital $\psi_3^*$ has been created by mixing the p orbital with the $\pi^*$ orbital in an *antibonding* sense, with the signs of the wave functions unmatched. The third orbital that we are seeking, $\psi_2$ in Fig. 1.33, is a combination created by mixing the p orbital with the $\pi$ orbital in an *antibonding* sense *and* with the $\pi^*$ orbital in a *bonding* sense. We do not get the two orbitals, $\psi_x$ and $\psi_y$ in Fig. 1.32, but something half way between, namely $\psi_2$ in Fig. 1.33. By adding $\psi_x$ and $\psi_y$ in this way, the atomic orbitals drawn to the left of the energy levels labelled $\psi_x$ and $\psi_y$ in Fig. 1.32 cancel each other out on C-2 and reinforce each other on C-1 and C-3, thereby creating the molecular orbital $\psi_2$ in Fig. 1.33.

   We have of course arrived at the same picture for the molecular orbitals as that created from mixing the three separate p orbitals in Fig. 1.30. As before, the atomic orbitals in $\psi_2$ are far enough apart in space for the molecular orbital $\psi_2$ to have the same energy as the isolated p orbital in Fig. 1.33. It is a nonbonding molecular orbital (NBMO), as distinct from a bonding ($\psi_1$) or an antibonding ($\psi_3^*$) orbital. Again we see for the allyl cation, radical and anion, that, as a result of the overlap in $\psi_1$, the overall $\pi$ energy of the allyl system has dropped relative to the sum of the energies of an isolated p orbital and of ethylene by $2E$, which we know from Fig. 1.31 is $2 \times 0.414\beta$ or something of the order of 116 kJ mol$^{-1}$ of extra $\pi$ bonding relative to that in
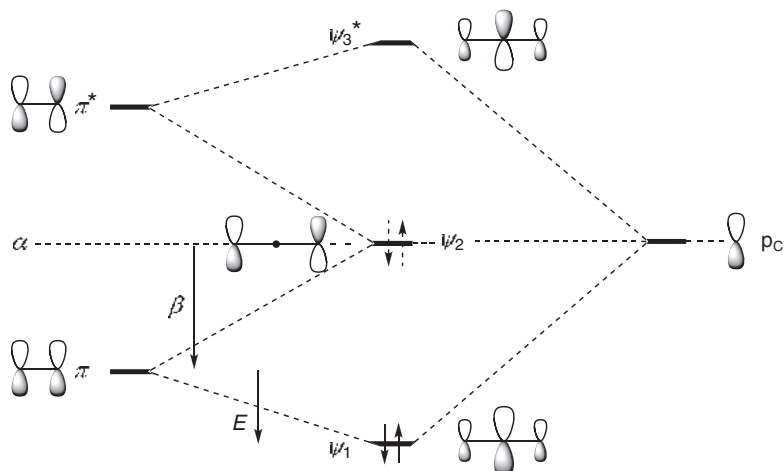
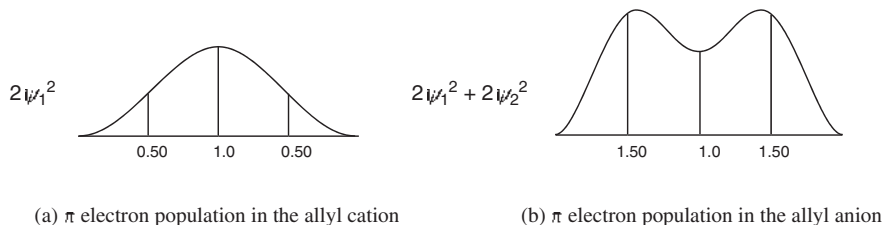**Fig. 1.33** The allyl system by interaction of a p orbital with $\pi$ and $\pi^*$ orbitals

ethylene. In the radical and anion, where $\psi_2$ has either one or two electrons, and $\psi_3^*$ is still empty, the energy drop is still $2E$, because p and $\psi_2$ are essentially on the same level. (It is not uncommon to express these drops in energy as a 'gain' in energy—in this sense, the gain is understood to be to us, or to the outside world, and hence means a loss of energy in the system and stronger bonding.)

It is worth considering at this stage what the overall $\pi$ electron distribution will be in this conjugated system. The electron population in any molecular orbital is derived from the square of the atomic orbital functions, so that the sine waves describing the coefficients in Fig. 1.34a are squared to describe the electron distribution in Fig. 1.34b. The $\pi$ electron population in the molecule as a whole is then obtained by adding up the electron populations, allowing for the number of electrons in each orbital, for all the *filled* $\pi$ molecular orbitals. Looking only at the $\pi$ system, we can see that the overall $\pi$ electron distribution for the cation is



(a) Wave functions  (b) Electron populations for one electron
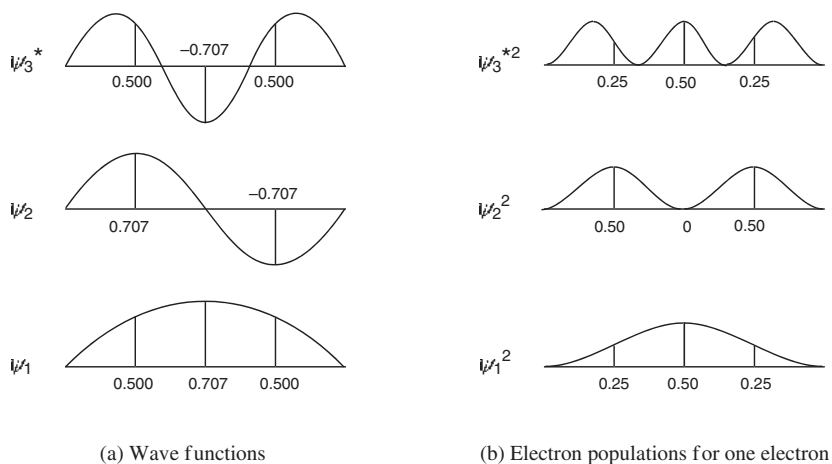
**Fig. 1.34** Wave functions and electron population for the allyl orbitals

derived from the squares of the coefficients in $\psi_1$ alone, since this is the only populated $\pi$ orbital. Roughly speaking, there is half an electron ($2 \times 0.5^2$) on each of C-1 and C-3, and one electron ($2 \times 0.707^2$) on C-2. This is illustrated graphically in Fig. 1.35a. Since the nucleus has a charge of $+1$, the excess charge on C-1 and C-3 is $+0.5$, in other words the electron deficiency in the cation is concentrated at the two ends.



$2\psi_1^2$                     $2\psi_1^2 + 2\psi_2^2$

0.50    1.0    0.50              1.50    1.0    1.50

(a) $\pi$ electron population in the allyl cation        (b) $\pi$ electron population in the allyl anion

**Fig. 1.35**    Total $\pi$ electron populations in the allyl cation and anion

For the anion, the $\pi$ electron population is derived by adding up the squares of the coefficients in both $\psi_1$ and $\psi_2$. Since there are two electrons in both orbitals, there are 1.5 electrons ($2 \times 0.5^2 + 2 \times 0.707^2$) roughly centred on each of C-1 and each of C-3, and one electron ($2 \times 0.707^2$) centred on C-2. This is illustrated graphically in Fig. 1.35b. Subtracting the charge of the nucleus then gives the excess charge as $-0.5$ on C-1 and C-3, in other words the electron excess in the anion is concentrated at the two ends. Thus the drawings of the allyl cation **1.4a** and **1.4b** illustrate the overall $\pi$ electron population, and the corresponding drawings for the anion **1.6a** and **1.6b** do the same for that species.

As we shall see later, the most important orbitals with respect to reactivity are the highest occupied molecular orbital (HOMO) and the lowest unoccupied molecular orbital (LUMO). These are the *frontier orbitals*. For the allyl cation, the HOMO is $\psi_1$, and the LUMO is $\psi_2$. For the allyl anion, the HOMO is $\psi_2$, and the LUMO is $\psi_3^*$. The drawings of the allyl cation **1.4a** and **1.4b** emphasise not only the overall $\pi$ electron population but even better emphasise the electron distribution in the LUMO. Similarly, the drawings of the allyl anion **1.6a** and **1.6b** emphasise the HOMO for that species. It is significant that it is the LUMO of the cation and the HOMO of the anion that will prove to be the more important frontier orbital in each case. In radicals, the most important orbital is the singly occupied molecular orbital (SOMO). For the allyl radical this is the half-filled orbital $\psi_2$. Once again, the drawings **1.5a** and **1.5b** emphasise the distribution of the odd electron in this orbital.

One final detail with respect to this, the most important orbital, is that it is not quite perfectly nonbonding. Although C-1 and C-3 are separated in space, they do interact slightly in $\psi_2$, as can be seen in the wire-mesh drawing of the nonlinear allyl system in Fig. 1.36, where the perspective allows one to see that the right hand



$\psi_1$                     $\psi_2$                     $\psi_3^*$
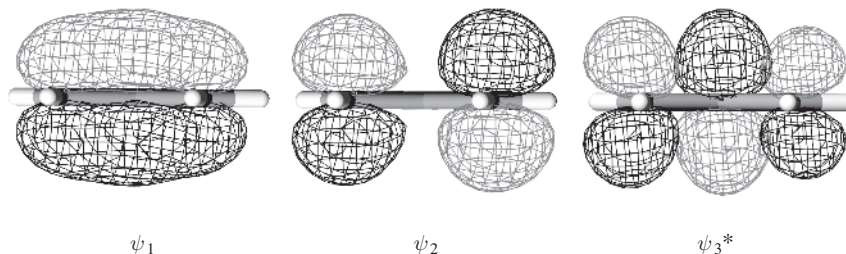
**Fig. 1.36**    The $\pi$ molecular orbitals of the allyl system

lobes, which are somewhat closer to the viewer, are just perceptibly repelled by the left hand lobes, and that neither of the atomic orbitals on C-1 and C-3 in $\psi_2$ is a straightforwardly symmetrical p orbital. This orbital does not therefore have exactly the same energy as an isolated p orbital—it is slightly higher in energy.
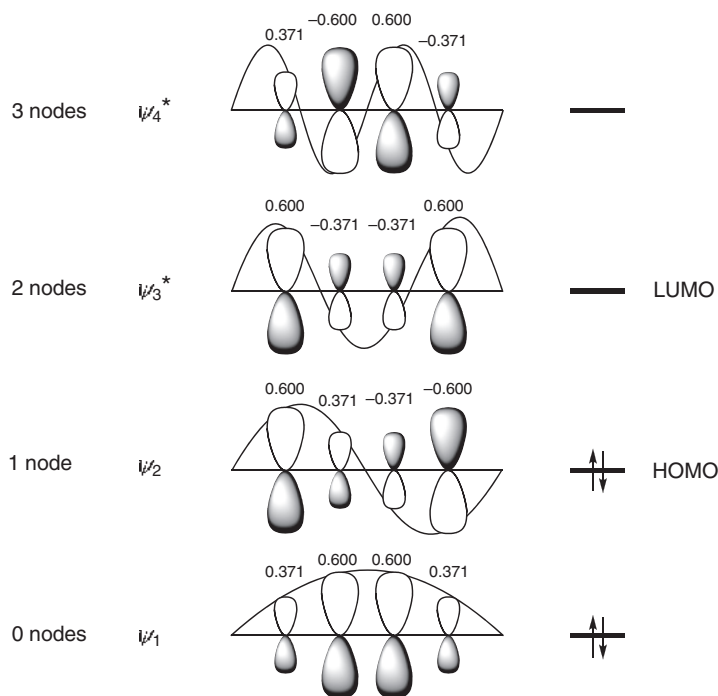
### 1.4.2 Butadiene

The next step up in complexity comes with four p orbitals conjugated together, with butadiene **1.8** as the parent member. As usual there is a $\sigma$ framework **1.9**, which can be constructed from the 1s orbitals of the six hydrogen atoms and either the sp$^2$ hybrids of the four carbon atoms or the separate 2s, 2p$_x$ and 2p$_y$ orbitals. The $\sigma$ framework has 18 bonding molecular orbitals filled with 36 electrons. Again we have two ways by which we may deduce the electron distribution in the $\pi$ system, made up from the four p$_z$ orbitals and holding the remaining four electrons. Starting with the electron in the box with four p orbitals, we can construct Fig. 1.37, which shows the four wave functions, inside which the p orbitals are placed at the appropriate regular intervals.
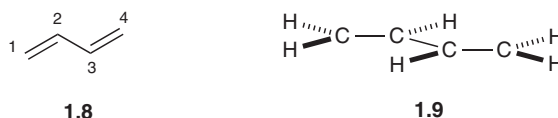


We get a new set of orbitals, $\psi_1$, $\psi_2$, $\psi_3$*, and $\psi_4$*, each described by Equation 1.11 with four terms:

$$\psi = c_1\phi_1 + c_2\phi_2 + c_3\phi_3 + c_4\phi_4 \qquad\qquad 1.11$$



**Fig. 1.37** $\pi$ Molecular orbitals of butadiene

The lowest-energy orbital $\psi_1$ has all the $c$-values positive, and hence bonding is at its best. The next-highest energy level has one node, between C-2 and C-3; in other words, $c_1$ and $c_2$ are positive and $c_3$ and $c_4$ are negative. There is therefore bonding between C-l and C-2 and between C-3 and C-4, but not between C-2 and C-3. With two bonding and one antibonding interaction, this orbital is also overall bonding. Thus the lowest-energy orbital of butadiene, $\psi_1$, reasonably enough, has a high population of electrons in the middle, but in the next orbital up, $\psi_2$, because of the repulsion between the wave functions of opposite sign on C-2 and C-3, the electron population is concentrated at the ends of the conjugated system. Overall, summing the squares of the coefficients of the filled orbitals, $\psi_1$ and $\psi_2$, the $\pi$ electrons are, at this level of approximation, evenly spread over all four carbon atoms of the conjugated system.

We can easily give numerical values to these coefficients, using the convention that the edge of the box is drawn one bond length out from the terminal carbon atoms. Treating the conjugated system as being linear, the coefficients are proportional to the sine of the angle, as defined by the position of the atom within the sine curve. The algebraic expression for this idea in the general case, and illustrated in Fig. 1.37 for the specific case of butadiene, with the atomic orbitals inscribed within the sine curves, is Equation 1.12:

$$c_{jr} = \sqrt{\frac{2}{n+1}} \, sin \frac{rj\pi}{n+1} \qquad\qquad 1.12$$

giving the coefficient $c_{jr}$ for atom $j$ in molecular orbital $r$ of a conjugated system of $n$ atoms (so that $j$ and $r = 1, 2, 3, \ldots, n$). The expression in front of the sine function is the normalisation factor to make the squares of the coefficients add up to one. Thus, taking $\psi_2$ for butadiene ($r = 2$, $n = 4$ and the sine curve is a full $2\pi$): the normalisation factor for $n = 4$ is 0.632, the angle for the first atom ($j = 1$) is $2\pi/5$, the sine of which is 0.951, and the coefficient $c_1$ is the product $0.632 \times 0.951 = 0.600$. Similarly, $c_2$ is 0.371, $c_3$ is –0.371 and $c_4$ is –0.600.

Large lists of coefficients for conjugated systems, some as easily calculated as butadiene above, some more complicated, have been published.[18] As with the allyl system, other patterns are also present because of the symmetry of the molecule: for alternant conjugated systems (those having no odd-membered rings), the $|c|$ values are reflected across a mirror plane placed horizontally, half way between $\psi_2$ and $\psi_3^*$, and also across a mirror plane placed vertically, half way between C-2 and C-3. It is only necessary therefore to calculate four of the 16 numbers in Fig. 1.37, and deduce the rest from the symmetry.

Alternatively, we can set up the conjugated system of butadiene by looking at the consequences of allowing two isolated $\pi$ bonds to interact, as they will if they are held within bonding distance. It is perhaps a little easier to see on this diagram the pattern of raised and lowered energy levels relative to those of the $\pi$ bonds from which they are derived. Let us first look at the consequence of allowing the orbitals close in energy to interact, which they will do strongly (Fig. 1.38). (For a brief account of how the energy difference between interacting orbitals affects the extent of their interaction, see the discussion of Equations 1.13 and 1.14 on p. 54.) The interactions of $\pi$ with $\pi$ and of $\pi^*$ with $\pi^*$ on the left create a new set of orbitals, $\psi_a$-$\psi_d^*$. This is not the whole story, because we must also allow for the weaker interaction, shown on the right, of the orbitals further apart in energy, $\pi$ with $\pi^*$, which on their own would create another set of orbitals, $\psi_w$-$\psi_z^*$.

Mixing these two sets together, and allowing for the greater contribution from the stronger interactions, we get the set of orbitals (Fig. 1.39), matching those we saw in Fig. 1.37. Thus, to take just the filled orbitals, we see that $\psi_1$ is derived by the interaction of $\pi$ with $\pi$ in a bonding sense ($\psi_a$), lowering the energy of $\psi_1$ below that of the $\pi$ orbital, and by the interaction of $\pi$ with $\pi^*$ in a bonding sense ($\psi_w$), also lowering the energy below that of the $\pi$ orbital. Since the former is a strong interaction and the latter weak, the net effect is to lower the energy of $\psi_1$ below the $\pi$ level, but by a little more than the amount ($\beta$ in simple Hückel theory, illustrated as $E_\pi$ in Fig. 1.26) that a $\pi$ orbital is lowered below the p level (the dashed line $\alpha$ in Figs. 1.31, 1.32 and 1.33, called $\alpha$ in simple Hückel theory) in making the $\pi$ bond of ethylene. However, $\psi_2$ is derived from the interaction of $\pi$ with $\pi$ in an antibonding sense ($\psi_b$), raising the energy above that of the $\pi$ orbital, and by the interaction of $\pi^*$ with $\pi$ in a bonding sense ($\psi_x$), lowering it again. Since the former is a strong interaction
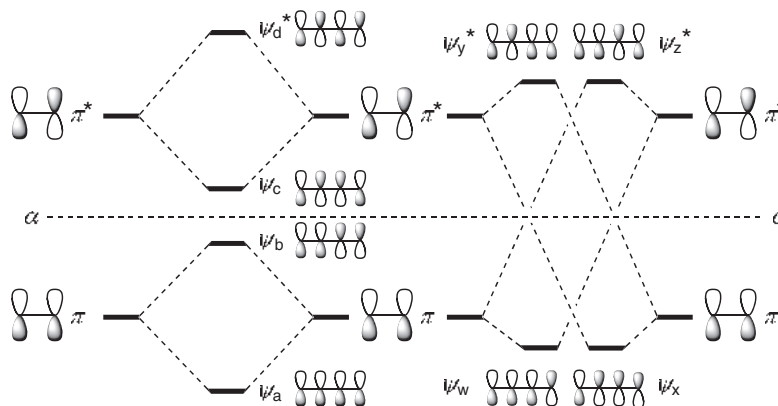
**Fig. 1.38**  Primary interactions of the $\pi$ molecular orbitals of two molecules of ethylene. (No attempt is made to represent the relative sizes of the atomic orbitals)

and the latter weak, the net effect is to raise the energy of $\psi_2$ above the $\pi$ level, but not by as much as a $\pi^*$ orbital is raised above the p level in making the $\pi$ bond of ethylene. Yet another way of looking at this system is to say that the orbitals $\psi_1$ and $\psi_2$ and the orbitals $\psi_3^*$ and $\psi_4^*$ mutually repel each other.

We are now in a position to explain the well-known property that conjugated systems are often, but not always, lower in energy than unconjugated systems. It comes about because $\psi_1$ is lowered in energy more than $\psi_2$ is raised ($E_1$ in Fig. 1.39 is larger than $E_2$). The energy ($E_1$) given out in forming $\psi_1$ comes from the
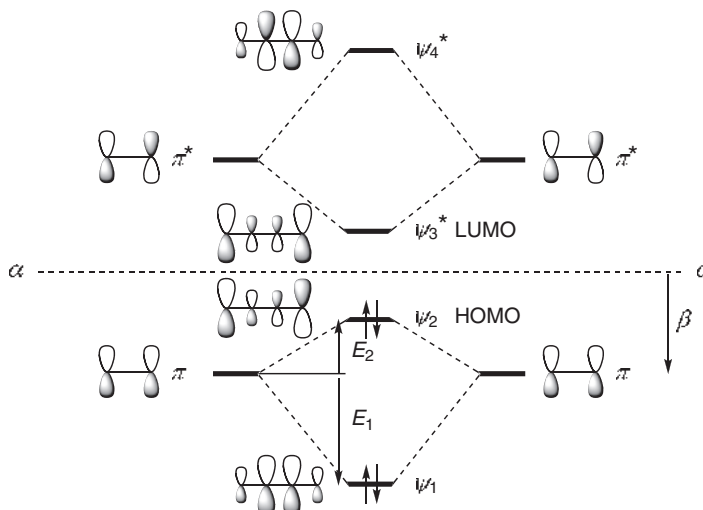


**Fig. 1.39**  Energies of the $\pi$ molecular orbitals of ethylene and butadiene by orbital interaction

overlap between the atomic orbitals on C-2 and C-3; this overlap did not exist in the isolated $\pi$ bonds. It is particularly effective in lowering the energy of $\psi_1$, because the coefficients on C-2 and C-3 are large. By contrast, the increase in energy of $\psi_2$, caused by the repulsion between the orbitals on C-2 and C-3, is not as great, because the coefficients on these atoms are smaller in $\psi_2$. Thus the energy lost from the system in forming $\psi_1$ is greater than the energy needed to form $\psi_2$, and the overall $\pi$ energy of the ground state of the system ($\psi_1{}^2\psi_2{}^2$) is lower. We can of course see the same pattern, and attach some very approximate numbers, using the geometrical analogy. This is illustrated in Fig. 1.40, which shows that $\psi_2$ is raised above $\pi$ by $0.382\beta$ and $\psi_1$ is lowered below $\pi$ by $0.618\beta$. The overall lowering in energy for the extra conjugation is therefore $(2 \times 0.618 + 2 \times 1.618) - 4 = 0.472\beta$ or about 66 kJ mol$^{-1}$.
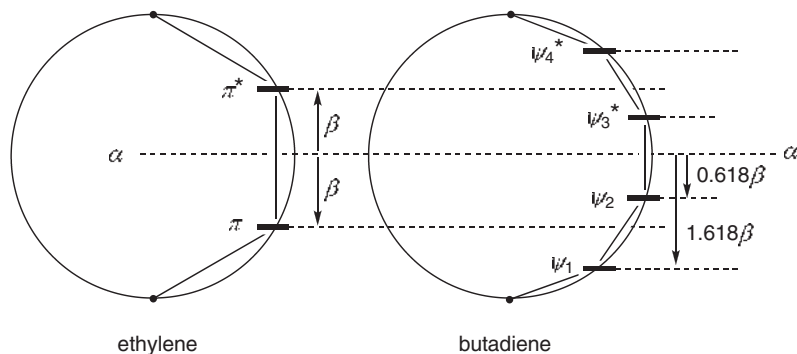


**Fig. 1.40**    Energies of the $\pi$ molecular orbitals of ethylene and butadiene by geometry

Before we leave butadiene, it is instructive to look at the same $\pi$ orbitals in wire-mesh diagrams (Fig. 1.41) to reveal more accurately what the electron distribution in the $\pi$ molecular orbitals looks like. In the allyl system and in butadiene, we have seen more than one filled and more than one empty orbital in the same molecule. The $\sigma$ framework, of course, with its strong $\sigma$ bonds, has several other filled orbitals lying lower in energy than either $\psi_1$ or $\psi_2$, but we do not usually pay much attention to them when we are thinking of reactivity, simply because they lie so much lower in energy. In fact, we shall be paying special attention to the filled molecular orbital which is highest in energy ($\psi_2$, the HOMO) and to the unoccupied orbital of lowest energy ($\psi_3{}^*$, the LUMO).
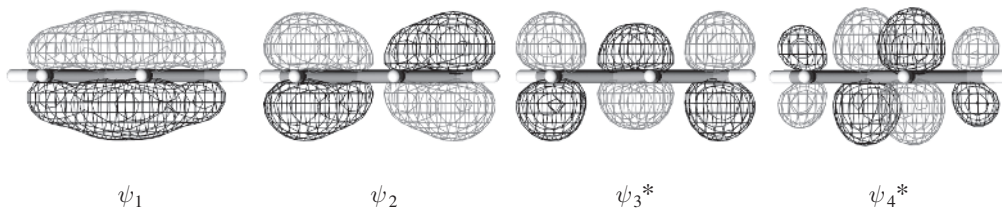


**Fig. 1.41**    The $\pi$ molecular orbitals of butadiene in the s-*trans* conformation

### 1.4.3 Longer Conjugated Systems

In extending our understanding to the longer linear conjugated systems, we need not go through all the arguments again. The methods are essentially the same. The energies and coefficients of the $\pi$ molecular orbitals for all six systems from an isolated p orbital up to hexatriene are summarised in Fig. 1.42. The viewpoint in this drawing is directly above the p orbitals, which appear therefore to be circular. This is a common simplification, rarely likely to lead to confusion between a p orbital and an s orbital, and we shall use it through much of this book.
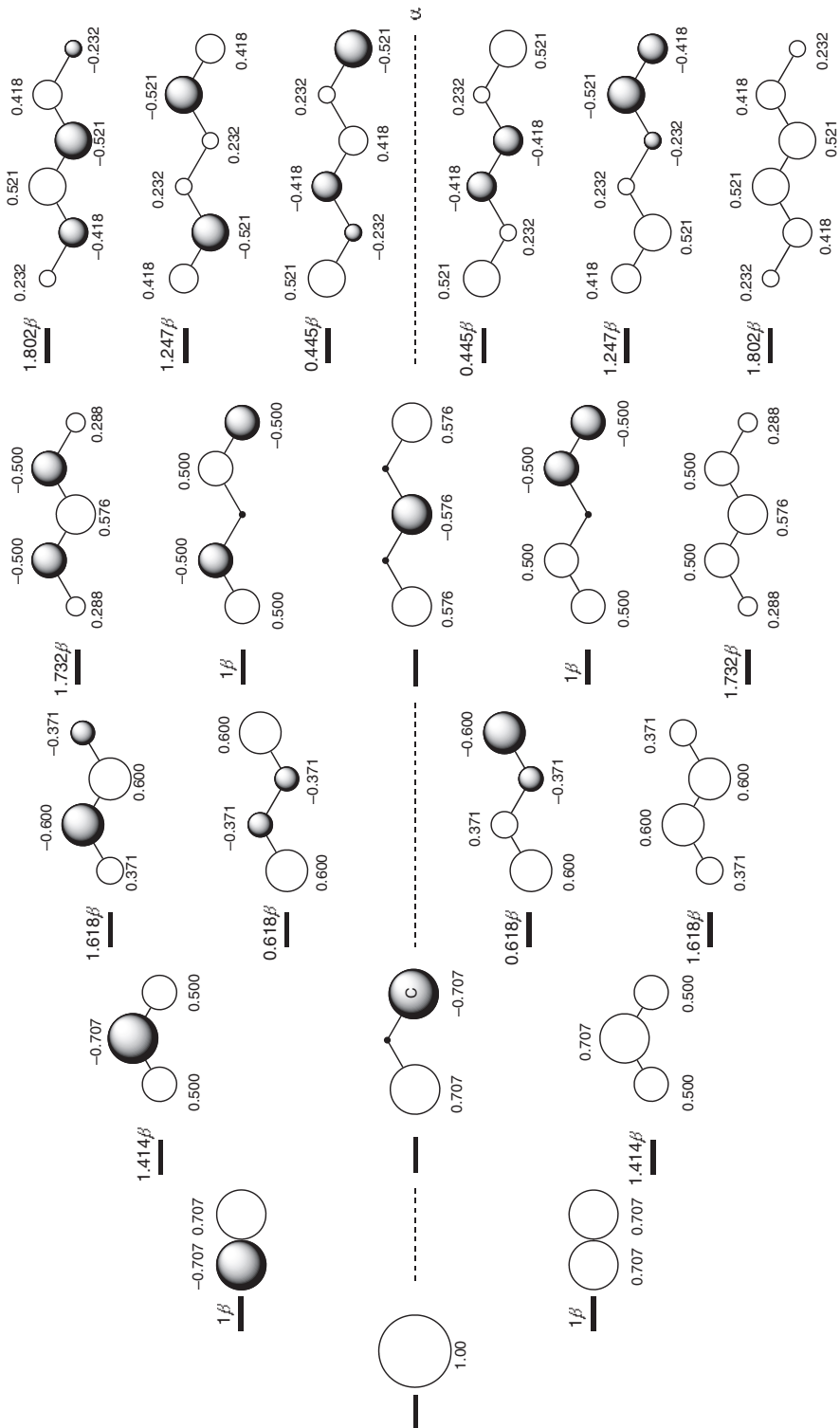
**Fig. 1.42** The energies and coefficients of the π molecular orbitals of the smaller conjugated systems

The longer the conjugated system, the lower the energy of $\psi_1$, but each successive drop in energy is less than it was for the system with one fewer atoms, with a limit at infinite length of $2\beta$. Among the even-atom species, the longer the conjugated system, the higher the energy of the HOMO, and the lower the energy of the LUMO, with the energy gap becoming ever smaller. With a narrow HOMO—LUMO gap, polyenes allow the easy promotion of an electron from the HOMO to the LUMO, and the longer the conjugated system, the easier it is, making the absorption of UV and visible light ever less energetic. Most organic chemists will be happy with this picture, and most of the consequences in organic chemistry can be left at this level of understanding.

At the extreme of an infinite polyene, however, simple Hückel theory reduces the HOMO—LUMO gap to zero, since the secants in diagrams like Fig. 1.40, would become infinitely small as they moved to the perimeter of the circle. Such a polyene would have equal bond lengths between each pair of carbon atoms, there would be no gap between the HOMO and the LUMO, and it would be a metallic conductor. This is not what happens— long polyenes, like polyacetylene, have alternating double (or triple) and single bonds, and their interconversion, which is the equivalent of the movement of current along the chain, requires energy. The theoretical description of this modification to simple Hückel theory is known by physicists as a Peierls distortion. It has its counterpart for chemists in the Jahn-Teller distortion seen, for example, in cyclobutadiene, which distorts to have alternating double and single bonds, avoiding the degenerate orbitals and equal bond lengths of square cyclobutadiene (see Section 1.5.2). The simple Hückel picture is evidently wrong at this extreme of very long conjugated systems. One way of appreciating what is happening is to think of the HOMO and the LUMO interacting more strongly when they are close in energy, just as the filled and unfilled orbitals of butadiene repel each other (Fig. 1.39), but more so. The residual gap, corresponding approximately to what is called by physicists the 'band-gap energy', is amenable to tuning, by attaching suitable substituents, just like any other HOMO—LUMO gap. Tailoring it has proved to be a basis for tuning the properties of optical devices.[19]

The process by which alternating double and single bonds might exchange places is strictly forbidden by symmetry, but occurs in practice, because the mismatch in symmetry of adjacent elements is disrupted by having an atom lacking an electron or carrying an extra electron in the chain.[20] Thus an 'infinite' polyene can have long stretches of alternating single and double bonds interrupted by a length of conjugated p orbitals resembling a conjugated cation, radical or anion. Such 'defects' are chains of conjugated atoms, but like the chain of the polyene itself, the feature of equal bond lengths does not stretch infinitely along the whole 'molecule', as simple Hückel theory would suggest. It is limited in what physicists call 'solitons'. In the soliton, there is no bond alternation at its centre, but bond alternation appears at greater distances out from its centre. Solitons provide a mechanism for electrical conduction along the chain, which is described as being 'doped'. Unfortunately, the physicists' nomenclature in the polymer area departs from that of the organic chemist, with expressions like 'tight binding model' meaning much the same as the LCAO approximation, 'band structure' for the stack of orbitals, 'band gap' for the HOMO—LUMO gap, 'valence band' for the HOMO, 'Fermi energy' meaning roughly the same as the energy of the HOMO, and the 'conduction band' meaning roughly the same as the LUMO. The physical events are of course similar, and the comparisons have been elegantly discussed.[21] Such a breakdown in Hückel theory is not normally encountered in organic chemistry, where delocalisation can be expected to stretch undeterred by the length of the conjugated systems in what we might call ordinary molecules.

# 1.5  Aromaticity[22]

## 1.5.1  Aromatic Systems

One of the most striking properties of conjugated organic molecules is the special stability found in the group of molecules called aromatic, with benzene **1.10** as the parent member and the longest established example. Hückel predicted that benzene was by no means alone, and that cyclic conjugated polyenes would have exceptionally low energy if the total number of $\pi$ electrons could be described as a number of the form $(4n + 2)$, where $n$ is an integer. Other $6\pi$-electron cyclic systems such as the cyclopentadienyl anion **1.11** and the cycloheptatrienyl cation **1.12** belong in this category. The cyclopropenyl cation **1.13** ($n = 0$),

[14]annulene **1.14** ($n = 3$), [18]annulene **1.15** ($n = 4$) and many other systems have been added over the years.[23] Where does this special stability come from?



**1.10**      **1.11**      **1.12**      **1.13**

**1.14**          **1.15**
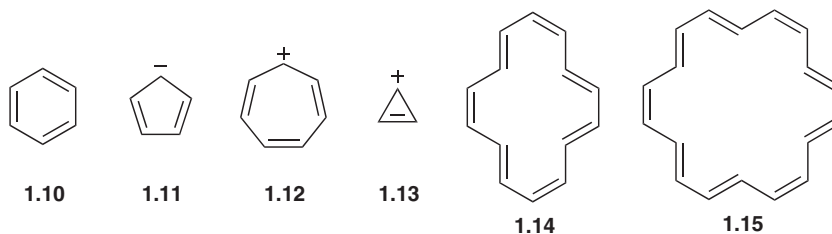
We can approach this question in much the same way as we approached the derivation of the molecular orbitals of conjugated systems. We begin with a $\sigma$ framework containing the C—C and C—H $\sigma$ bonds. We must then deduce the nodal properties of the $\pi$ molecular orbitals created from six p orbitals in a ring. They are all shown both in elevation and in plan in Fig. 1.43. The lowest-energy orbital $\psi_1$ has no node as usual, but because the conjugated system goes round the ring instead of spilling out at the ends of the molecule, as it did
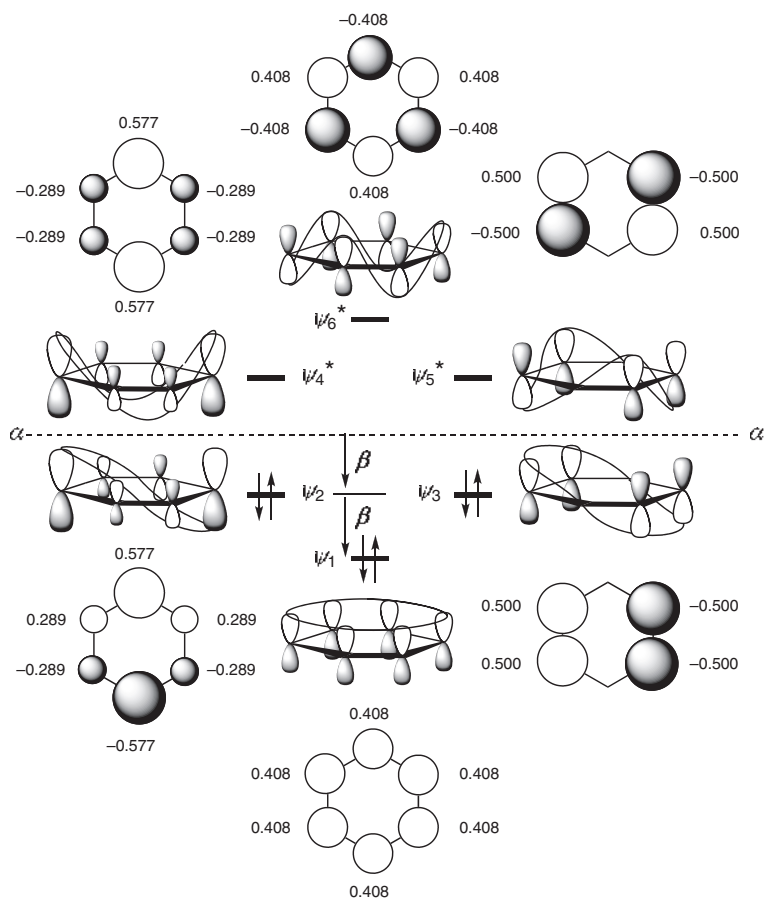


**Fig. 1.43**    The $\pi$ molecular orbitals of benzene

with the linear conjugated systems, the coefficients on all six atoms are equal. The other special feature is that there are two orbitals having the same energy with one node $\psi_2$ and $\psi_3$, because they can be created in two symmetrical ways, one with the node horizontal $\psi_2$ and one with it vertical $\psi_3$. Similarly, there are two orbitals, $\psi_4^*$ and $\psi_5^*$, with the same energy having two nodes. Finally there is the one orbital, $\psi_6^*$, with three nodes.

The size of the coefficients can be deduced from the position of the atoms within the sine curves, in the usual way. They support the assumption from symmetry that the amount of bonding in $\psi_2$ equals that in $\psi_3$. Thus the allyl-like overlap in the two halves of $\psi_2$ has bonding between a large ($\pm 0.577$) and two small ($\pm 0.289$) lobes, whereas the antibonding interaction is between the two small lobes. The result is actually a lowering of energy for this orbital equal to that of the $\pi$ bond in ethylene ($\beta$). In $\psi_3$ there is bonding between lobes of intermediate size ($\pm 0.500$) and the interaction across the ring between the lobes of opposite sign is, like $\psi_2$ in the allyl system, nonbonding rather than antibonding. Overlap between the p orbitals in ethylene ($c = 0.707$) gives rise to a lowering of energy ($\beta$) worth one full $\pi$ bond. Overlap between two lobes of the same sign in $\psi_3$ with coefficients of $\pm 0.50$ gives rise to half a $\pi$ bond ($0.707^2 = 0.500$), and two such interactions comes again to one full $\pi$ bond. The fully bonding overlap of the six orbitals ($c = 0.408$) in $\psi_1$ gives rise to two $\pi$ bond's worth of bonding. The total of $\pi$ bonding is thus $2 \times 4\beta$, which is two more $\beta$ units than three *isolated* $\pi$ bonds. Benzene is also lowered in $\pi$ energy by more than the amount for three *linearly conjugated* $\pi$ bonds: taking the numbers for hexatriene from Fig. 1.40, the total of $\pi$ bonding is $2 \times (1.802 + 1.247 + 0.445)\beta = 7\beta$. The extra $\pi$ bonding is the special feature of aromatic systems.

The energies of the molecular orbitals can also be deduced by the same device, used for linear conjugated systems, of inscribing the conjugated system inside a circle of radius $2\beta$. There is no need for dummy atoms, since the sine curves go right round the ring, and the picture is therefore that shown in Fig. 1.44.
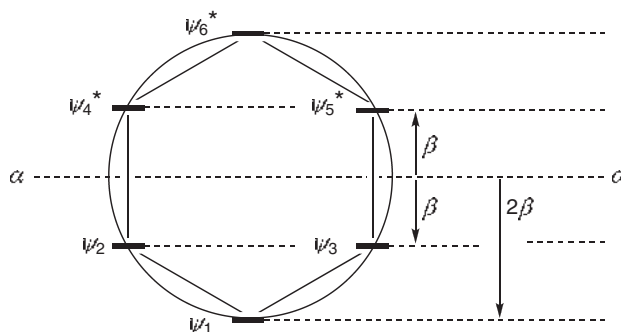


**Fig. 1.44**   The energies of the $\pi$ molecular orbitals of benzene

It is also possible to find the source of aromatic stabilisation by looking at an interaction diagram. For benzene **1.10**, one way is to start with hexatriene **1.16**, and examine the effect of bringing the ends of the conjugated system, C-1 and C-6, within bonding distance (Fig. 1.45). Since we are only looking at the $\pi$ energy, we ignore the C—H bonds, and the fact that to carry out this 'reaction' we would have to break two of them and make a C—C $\sigma$ bond in their place. In $\psi_1$ and $\psi_3$ the atomic orbitals on C-1 and C-6 have the same sign on the top surface. Bringing them within bonding distance will increase the amount of $\pi$ bonding, and lower the energy of $\psi_1$ and $\psi_3$ in going from hexatriene to benzene. In $\psi_2$ however, the signs of the atomic orbitals on C-1 and C-6 are opposite to each other on the top surface, and bringing them within bonding distance will be antibonding, raising the energy of $\psi_2$ in going from hexatriene to benzene. The overall result is two drops in energy to one rise, and hence a lowering of $\pi$ energy overall.
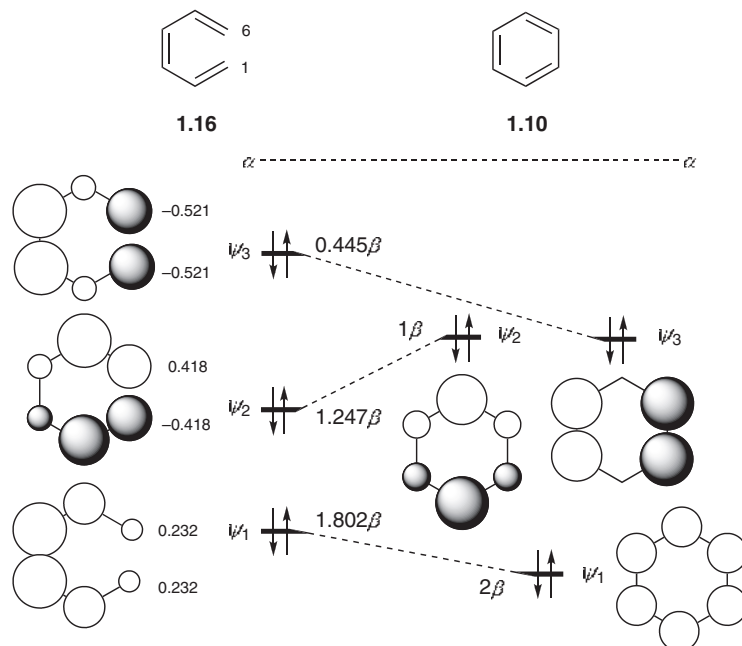
**Fig. 1.45** The drop in $\pi$ energy in going from hexatriene to benzene

However, the ups and downs are not all equal as Fig. 1.45, which is drawn to scale, shows. The net lowering in $\pi$ energy, relative to hexatriene, is actually only one $\beta$ value, as we deduced above, not two. It is barely legitimate, but there is some accounting for this difference—the overlap raising the energy of $\psi_2$ and lowering the energy of $\psi_3$ is between orbitals with large coefficients, more or less cancelling one another out; however, the overlap between C-1 and C-6 in $\psi_1$ is between orbitals with a small coefficient, making that drop close to $0.5\beta$ as shown in Fig. 1.45.

One of the most striking artifacts of aromaticity, in addition to the lowering in energy, is the diamagnetic anisotropy, which is characteristic of these rings. Although known long before NMR spectroscopy was introduced into organic chemistry, its most obvious manifestation is in the downfield shift experienced by protons on aromatic rings, and perhaps even more vividly by the upfield shift of protons on the inside of the large aromatic annulenes. The theory[24,25] is beyond the scope of this book, but it is associated with the system of $\pi$ molecular orbitals, and can perhaps be most simply appreciated from the idea that the movement of electrons round aromatic rings is free, like that in a conducting wire, as epitomised by the equal C—C bond lengths.

Like the conjugation in polyenes that we saw earlier, aromaticity does not stretch to infinitely conjugated cyclic systems, even when they do have $(4n+2)$ electrons. Just as long polyenes do not approach a state with equal bond lengths as the number of conjugated double bonds increases, the $(4n+2)$ rule of aromaticity breaks down, with bond alternation setting in when $n$ reaches a large number. It is not yet clear what that number is with neither theory nor experiment having proved decisive. Early predictions[26] that the largest possible aromatic system would be [22] or [26]annulene were too pessimistic, and aromaticity, using the ring-current criterion, probably peters out between [34] and [38]annulene.[27]

### 1.5.2 Antiaromatic Systems

A molecule with $4n$ $\pi$ electrons in the ring, with the molecular orbitals made up from $4n$ p orbitals, does not show this extra stabilisation. Molecules in this class that have been studied include cyclobutadiene **1.17**

($n = 1$), the cyclopentadienyl cation **1.18**, the cycloheptrienyl anion **1.19**, cyclooctatetraene **1.20** and pentalene **1.21** ($n = 2$), [12]annulene **1.22** ($n = 3$) and [16]annulene **1.23** ($n = 4$).

We can see this most easily by looking at the molecular orbitals of square cyclobutadiene in Fig. 1.46. As usual, the lowest energy orbital $\psi_1$ has no nodes, and, as with benzene and because of the symmetry, there are two exactly equivalent orbitals, $\psi_2$ and $\psi_3$, with one node. The bonding in $\psi_1$ is between atomic orbitals with coefficients of 0.500, not only between C-1 and C-2, but also between C-2 and C-3, between C-3 and C-4 and between C-4 and C-1. If the overlap in $\psi_3$ of benzene, which also has coefficients of 0.500, gives an energy-lowering of $1\beta$, then the overlap in $\psi_3$ of cyclobutadiene should give twice as much energy-lowering, since there are twice as many bonding interactions (this makes an assumption that the p orbitals are held at the same distance by the $\sigma$ framework in both cases). In contrast, the bonding interactions both in $\psi_2$ and $\psi_3$ are exactly matched by the antibonding interactions, and there is no lowering of the energy below the line ($\alpha$) representing the energy of a p atomic orbital on carbon. The molecular orbitals $\psi_2$ and $\psi_3$ are therefore nonbonding orbitals, and the net lowering in energy for the $\pi$ bonding in cyclobutadiene is only $2 \times 2\beta$. The energies of the four $\pi$ orbitals are again those we could have deduced from the model inscribing the conjugated system in a circle, with the point of the square at the bottom. The total $\pi$ stabilisation of $2 \times 2\beta$ is no better than having two isolated $\pi$ bonds—there is therefore no special extra stabilisation from the cyclic conjugation relative to two isolated $\pi$ bonds. There is however less stabilisation than that found in a pair of *conjugated* double bonds—the overall $\pi$ bonding in butadiene, taking values from Fig. 1.40, is $2 \times (1.618 + 0.618)\beta = 4.472\beta$ and the overall $\pi$ bonding in cyclobutadiene is only $2 \times 2\beta$ making it less stable by $0.472\beta$.
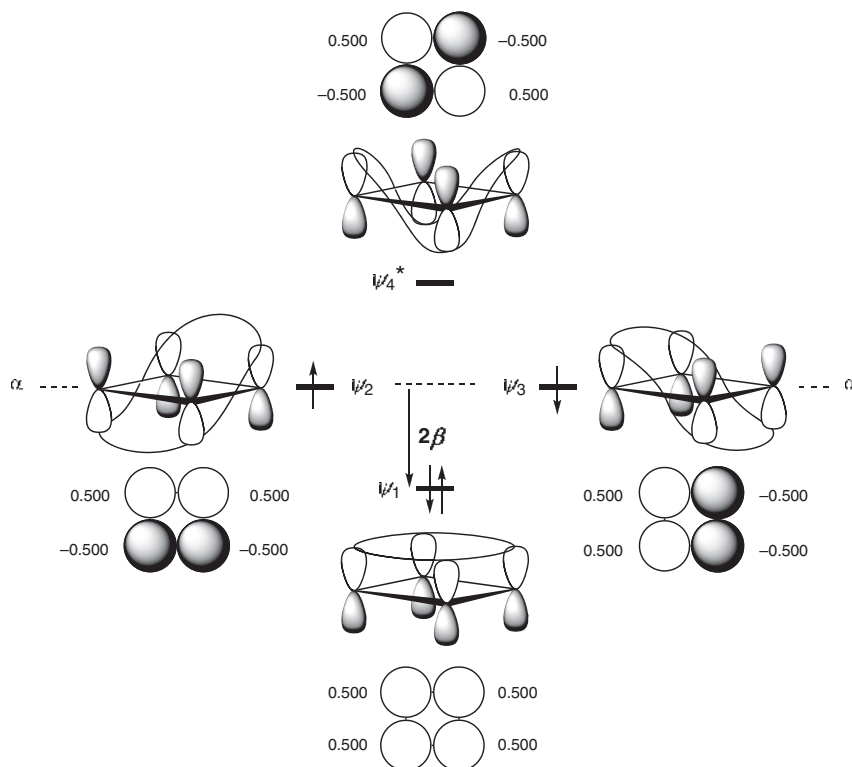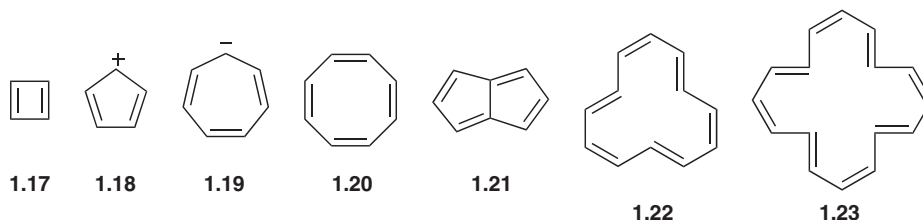


**Fig. 1.46**   The $\pi$ molecular orbitals of cyclobutadiene

We can reach a similar conclusion from an interaction diagram, by looking at the effect of changing butadiene **1.24** into cyclobutadiene **1.25** (Fig. 1.47). This time there is one drop in $\pi$ energy and one rise, and no net stabilisation from the cyclic conjugation. As with benzene, we can see that the drop is actually less (from overlap of orbitals with a small coefficient) than the rise (from overlap of orbitals with a large coefficient). Thus cyclobutadiene is less stabilised than butadiene.
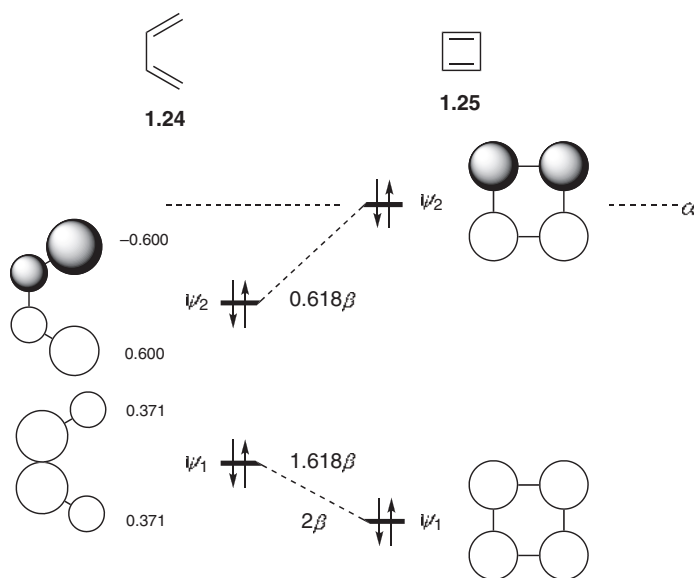


**Fig. 1.47**   No change in $\pi$ energy in going from butadiene to cyclobutadiene

There is much evidence that cyclic conjugated systems of $4n$ electrons show no special stability. Cyclobutadiene dimerises at extraordinarily low temperatures (>35K).[28] Cyclooctatetraene is not planar, and behaves like an alkene and not at all like benzene.[29] When it is forced to be planar, as in pentalene, it becomes unstable to dimerisation even at 0 °C.[30] [12]Annulene and [16]annulene are unstable with respect to electrocyclic reactions, which take place below 0 °C.[31] In fact, all these systems appear on the whole to be significantly higher in energy and more reactive than might be expected, and there has been much speculation that they are not only lacking in extra stabilisation, but are actually destabilised. They have been called 'antiaromatic'[32] as distinct from nonaromatic. The problem with this concept is what to make the comparisons with. We can see from the arguments above that we can account for the destabilisation

relative to conjugated $\pi$ bonds—linear conjugation is more energy-lowering than the cyclic conjugation of $4n$ electrons, which goes some way to setting the concept of antiaromaticity on a physical basis. This argument applies to the thermodynamics of the system, which indirectly affects the reactivity. That $4n$ systems are unusually reactive is also explicable with an argument based on the frontier orbitals, as we shall see later—the HOMO is unusually high in energy for a neutral molecule, at the nonbonding $\alpha$ level for cyclobutadiene and the other uncharged cyclic hydrocarbons **1.18–1.23**, significantly above the level of the HOMO of the linear conjugated hydrocarbons, and at the same time the LUMO is correspondingly low in energy.

The prediction from the argument in Fig. 1.46 is that square cyclobutadiene ought to be a diradical with one electron in each of $\psi_2$ and $\psi_3$, on the grounds that putting a second electron into an occupied orbital is not as energy-lowering as putting the first electron into that orbital (see Section 1.2). This is not borne out by experiment, which has shown that cyclobutadiene is rectangular with alternating double and single bonds and shows no electron spin resonance (ESR) signal.[33]

We can easily explain why the rectangular structure is lower in energy than the square. So far, we have made all $\pi$ bonds contribute equally one $\beta$-value to every $\pi$ bond. The difference in $\beta$-values, and hence in the strengths of $\pi$ bonds, as a function of how closely the p orbitals are held, can be dealt with by defining a standard $\beta_0$ value for a C=C double bond and applying a correction parameter $k$, just as we shall in Equation 1.16 for the effect of changing from a C=C double bond to a C=X double bond. Some values of $k$ for different distances $r$ can be seen in Table 1.1,[34] which was calculated with $\beta_0$ based on an aromatic double bond, rather than the double bond of ethylene, and by assuming that $\beta$ is proportional to the overlap integral $S$.

**Table 1.1**   Variation of the correction factor $k$ with distance $r$

| $r$ (Å) | $k$ | $r$ (Å) | $k$ |
|---------|------|---------|------|
| 1.20 | 1.38 | 1.45 | 0.91 |
| 1.33 | 1.11 | 1.48 | 0.87 |
| 1.35 | 1.09 | 1.54 | 0.78 |
| 1.397 | 1.00 | | |

In the rectangular structure of cyclobutadiene, the symmetry is lowered, and the molecular orbitals corresponding to $\psi_2$ and $\psi_3$ are no longer equal in energy (Fig. 1.48). The overall bonding in $\psi_1$ is more or less the same as in the square structure—C-1 and C-2 (and C-3 and C-4) move closer together in $\psi_1$, and the level of bonding is actually increased by about as much as the level of bonding is decreased in moving the
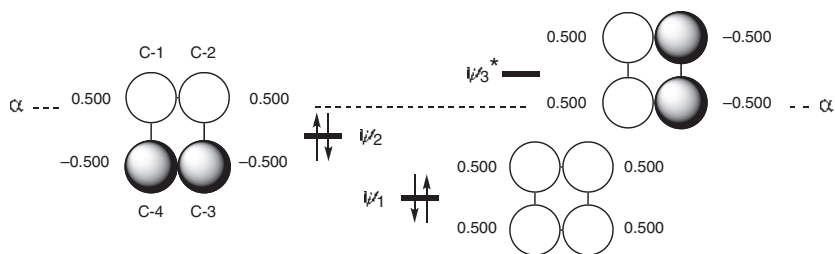


**Fig. 1.48**   The three lowest-energy $\pi$ molecular orbitals of rectangular cyclobutadiene

other pairs apart. In the other filled orbital, $\psi_2$, the same distortion, separating the pair (C-1 from C-4 and C-2 from C-3) will reduce the amount of $\pi$ *antibonding* between them, and hence lower the energy. The corresponding argument on $\psi_3$ will lead to its being raised in energy, and becoming an antibonding orbital. With one $\pi$ orbital raised in energy and the other lowered, the overall $\pi$ energy will be much the same, and the four electrons then go into the two bonding orbitals. This is known as a Jahn-Teller distortion, and can be expected to be a factor whenever a HOMO and a LUMO are very close in energy,[35] as we have already seen with very long conjugated systems in Section 1.4.3. The square structure will be the transition structure for the interconversion of the one rectangular form into the other, a reaction that can be expected to be fairly easy, but to have a discernible energy barrier. Proper molecular orbital calculations support this conclusion.[36] We must be careful in arguments like this, based only on the $\pi$ system, not to get too carried away. We have not allowed for distortions in the $\sigma$ framework in going from the square to the rectangular structure, and this can have a substantial effect.

### 1.5.3 The Cyclopentadienyl Anion and Cation

A slightly different case is provided by the cyclopentadienyl anion and cation. The device of inscribing the pentagon in a circle sets up the molecular orbitals in Fig. 1.49. The total of $\pi$ bonding energy is $2 \times 3.236\beta = 6.472\beta$ for the anion, in which there are two electrons in $\psi_1$, two electrons in $\psi_2$, and two electrons in $\psi_3$. The anion is clearly aromatic, since the open-chain analogue, the pentadienyl anion has only $2 \times 2.732\beta = 5.464\beta$ worth of $\pi$ bonding (Fig. 1.40), the extra stabilisation being close to $1\beta$, and closely similar to the extent by which benzene is lower in energy than its open-chain analogue, hexatriene. The cyclopentadienyl anion **1.11**, a $4n+2$ system, is well known to be exceptionally stabilised, with the p$K_a$ of cyclopentadiene at 16 being strikingly low for a hydrocarbon. The cation, however, has $\pi$-bonding energy of $2 \times 2.618\beta = 5.236\beta$, whereas its open-chain analogue, the pentadienyl cation, in which there are two electrons in $\psi_1$ and two electrons in $\psi_2$, has more $\pi$ bonding, specifically $2 \times 2.732\beta = 5.464\beta$. The cyclopentadienyl cation **1.18**, a $4n$ system, can be expected to be thermodynamically high in energy overall and therefore difficult to make, and so it is known to be. The cyclopentadienyl cation is not formed from its iodide by solvolysis under conditions where even the unconjugated cyclopentyl iodide ionises easily.[37] In addition, the cyclopentadienyl cation ought to be especially electrophilic for kinetic reasons, since the energy of the LUMO is actually below the $\alpha$ level. It is also known to be a diradical in the ground state.[38] The fluorenyl cation, the dibenz analogue of the cyclopentadienyl cation, however, does not appear to be significantly higher in energy than might be expected of a doubly benzylic cation held coplanar.[39]
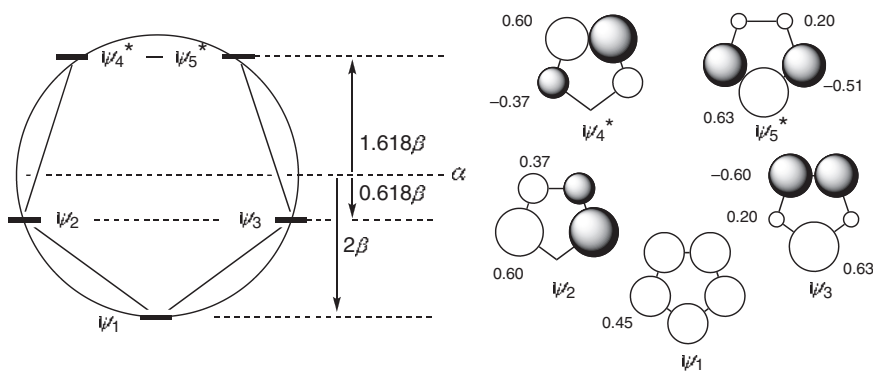


**Fig. 1.49** The energies and coefficients of the $\pi$ molecular orbitals of the cyclopentadienyl system

A striking difference between all the aromatic and all the antiaromatic systems is the energy *difference* between the HOMO and the LUMO. The aromatic systems have a substantial gap between the frontier orbitals, and the antiaromatic systems a zero gap in simple Hückel theory or a small gap if the Jahn-Teller distortion is allowed for. The difference in energy between the HOMO and the LUMO correlates with the hardness of these hydrocarbons as nucleophiles, and with some measures of aromaticity.[40] For example, in antiaromatic rings with $4n$ electrons, there is a paramagnetic ring current, which is a manifestation of orbital effects, just like the diamagnetic ring currents from aromatic rings. The protons at the perimeter of a $4n$ annulene, when it is stable enough for measurements to be made, are at high field, and protons on the inside of the ring are at low field. The slow interconversion of the double and single bonds in antiaromatic systems means that there is no free movement of the electrons round the ring, and so any diamagnetic anisotropy is muted. At the same time, the near degeneracy of the HOMO and the LUMO in the $4n$ annulenes allows a low-energy one-electron transition between them with a magnetic moment perpendicular to the ring, whereas the aromatic systems, with a much larger energy gap between the highest filled and lowest unfilled orbitals do not have this pathway.[41] Single electrons are associated with induced paramagnetic fields, as seen in the ESR spectra of odd electron systems.

### 1.5.4 Homoaromaticity[42]

The concept of aromaticity can be extended to systems in which the conjugated system is interrupted, by a methylene group, or other insulating structural feature, provided that the overlap between the p orbitals of the conjugated systems can still take place through space across the interruption. When such overlap has energy-lowering consequences, evident in the properties of the molecule, the phenomenon is called homoaromaticity. Examples are the homocyclopropenyl cation **1.26**, the trishomocyclopropenyl cation **1.27**, the bishomocyclopentadienyl anion **1.28** and the homocycloheptatrienyl cation **1.29**. Each of these species shows evidence of transannular overlap, illustrated, and emphasised with a bold line on the orbitals, in the drawings **1.26b**, **1.27b**, **1.28b** and **1.29b**. The same species can be drawn without orbitals in localised structures **1.26a**, **1.27a**, **1.28a** and **1.29a** and with the drawings **1.26c**, **1.27c**, **1.28c** and **1.29c** showing the delocalisation. For simplicity, the orbital drawings do not illustrate the whole set of $\pi$ molecular orbitals, which simply resemble in each case the $\pi$ orbitals of the corresponding aromatic system.

However, homoaromaticity appears to be absent in homobenzene (cycloheptatriene) **1.30a** and in trishomobenzene (triquinacene) **1.31a**, even though transannular overlap looks feasible. In both cases, the conventional structures **1.30a** and **1.30c**, and **1.31a** and **1.31c** are lower in energy than the homoaromatic structures **1.30b** and **1.31b**, which appear to be close to the transition structures for the interconversion.



| 1.26a | 1.26b | 1.26c | 1.27a | 1.27b | 1.27c |



| 1.28a | 1.28b | 1.28c | 1.29a | 1.29b | 1.29c |
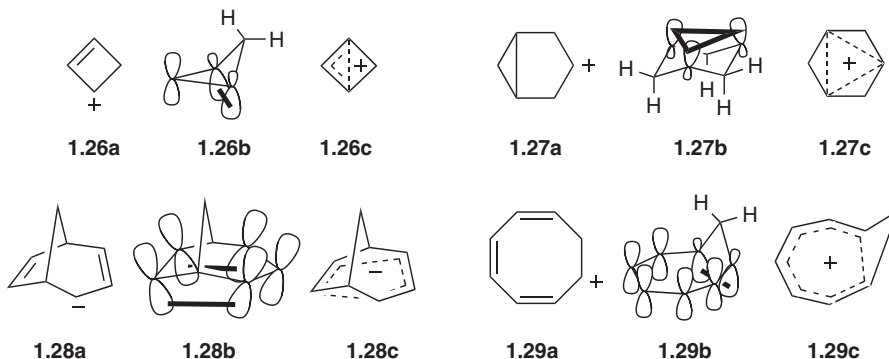
Homoantiaromaticity is even less commonly invoked. Homocyclobutadiene **1.32b** and the homocyclopentadienyl cation **1.33b** are close to the transition structures for the interconversion of cyclopentadiene **1.32a** and bicyclo[2.1.0]pentene **1.32c** and of the cyclohexatrienyl cation **1.33a** and the bicyclo[3.1.0]hexenyl cation **1.33c**. However, homoantiaromaticity does show up in these cases, in the sense that, unlike the interconversions in **1.30** and **1.31**, neither of these interconversions is rapid.
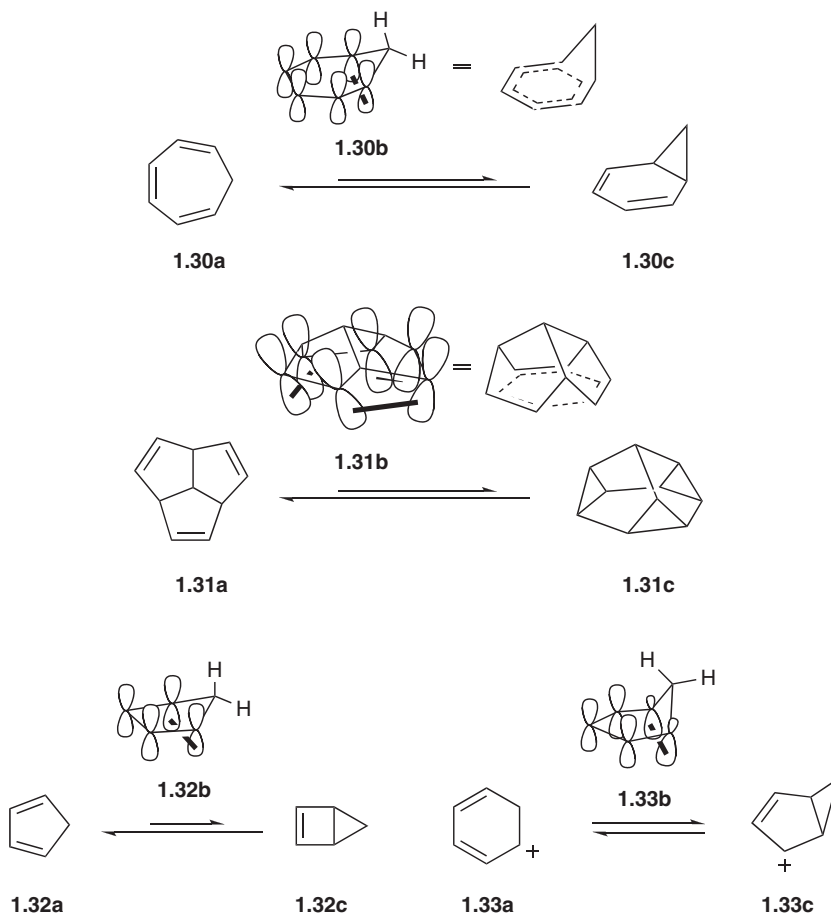


We evidently have three situations, summarised in Fig. 1.50. In Fig. 1.50a, the homoaromatic structures **1.26c–1.29c**, however they may be drawn, are at an energy minimum relative to the hypothetical localised structures **126a–129a**, and there is an energy *E* associated with the cyclic delocalisation. In Fig. 1.50b, we have the localised structures **1.30a** and **c** or **1.31a** and **c** at minima, with the potentially homoaromatic systems **1.30b** or **1.31b** near or at the top of a shallow curve. Finally with the homoantiaromatic systems, the transition structures **1.32b** or **1.33b** are evidently high in energy with a greatly enlarged $\Delta E$, the activation energy for the interconversion of the localised structures. We shall see this again in Chapter 6 with electrocyclic interconversions—those with aromatic transition structures like **1.30b** and **1.31b** are 'allowed', and those with antiaromatic transition structures like **1.32b** and **1.33b** are 'forbidden'.

The *concept* of homoaromaticity and homoantiaromaticity is sound. The nature of the overlap in the aromatic and antiaromatic systems is not dependent upon the atoms being directly bonded by the $\sigma$ framework. The $\sigma$ framework in an aromatic system has the effect of holding the p orbitals close,

(a) Homoaromatic systems    (b) Potentially homoaromatic systems    (c) Homoantiaromatic systems
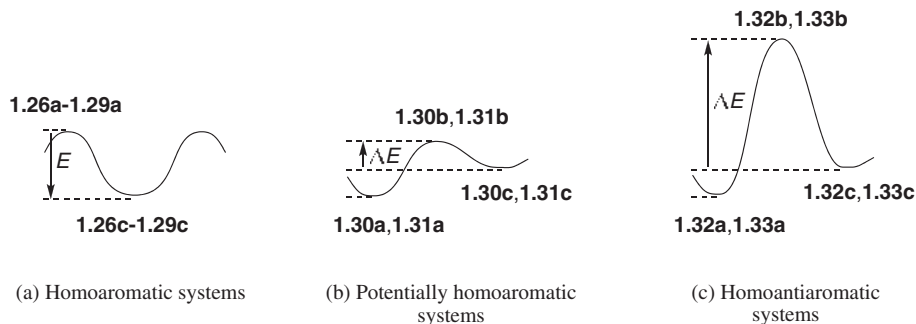
**Fig. 1.50**   Relative energies of some localised, homoaromatic and homoantiaromatic structures

making the $\pi$ overlap strong in consequence. Separating the p orbitals by a methylene group, or any other insulating group, will usually weaken such overlap, and often cause it to be stronger on one surface than the other, but it does not necessarily remove it completely. In favourable cases it can be strong, and lead to noticeable effects. The factors affecting when it is and is not strong have been discussed.[43]

### 1.5.5  Spiro Conjugation

In addition to $\sigma$ and $\pi$ overlap, p orbitals can overlap in another way, even less effective in lowering the energy, but still detectable. If one conjugated system is held at right angles to another in a spiro structure, with the drawing **1.34** representing the general case and hydrocarbons **1.35** and **1.36** two representative examples, the p orbitals of one can overlap with the p orbitals of the other, as symbolised by the bold lines on the front lobes in the drawing **1.34**. The overlap integral will be small, but if the symmetry matches, the interaction of the molecular orbitals can lead to new orbitals, raised or lowered in energy in the usual way. If the symmetry is not appropriate, the overlap will simply have no effect.



**1.34**        **1.35**        **1.36**
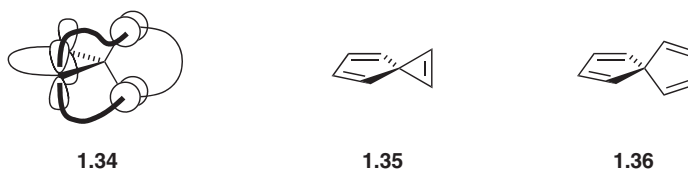
Take spiroheptatriene **1.35**, with the unperturbed orbitals of each component shown on the left and right in Fig. 1.51. The only orbitals that can interact are $\psi_2$ on the left and $\pi^*$ on the right; all the others having the wrong symmetry. For example, the interaction of the top lobes of $\psi_1$ on the left and the upper p orbital of the $\pi$ orbital on the right, one in front and one behind, have one in phase and one out of phase, exactly cancelling each other out; similarly with the front $\pi$ lobes on the right and the upper and lower lobes of the front-right p orbital of $\psi_1$ on the left.

The two orbitals that do interact, $\psi_2$ and $\pi^*$, which have the same symmetry, create the usual pair of new orbitals, one raised and one lowered. Since there are only two electrons to go into the new orbitals, the overall energy of the conjugated system is lowered. The effect, $\Delta E_s$, is small, both because of the poor overlap, and because the two orbitals interacting are far apart in energy, which we shall see later is an important factor. Nevertheless, it is a general conclusion that if the total number of $\pi$ electrons is a $(4n+2)$ number, the spiro system is stabilised, leading to the concept of spiroaromaticity.
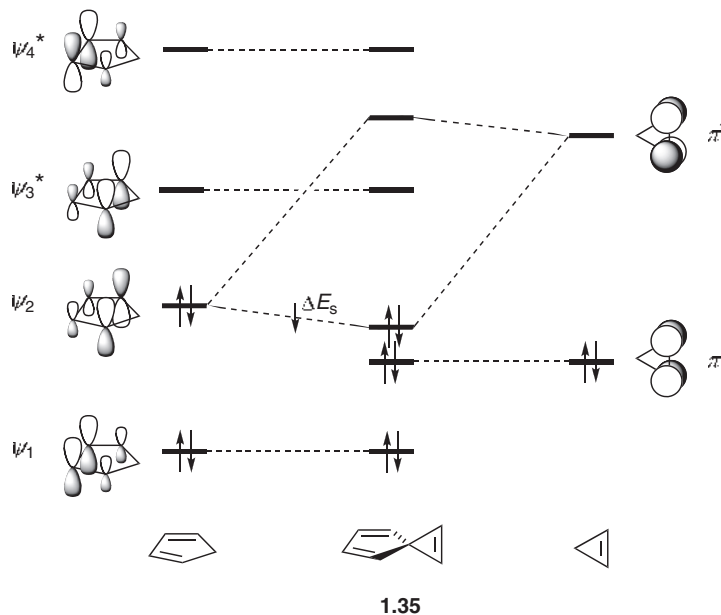
**Fig. 1.51**   $\pi$ Molecular orbitals of the 'aromatic' spiroheptatriene

There is equally a phenomenon of spiroantiaromaticity when the total number of $\pi$ electrons is a $4n$ number, as in spirononatetraene **1.36** (Fig. 1.52). Here the only orbitals with the right symmetry to interact productively are the $\psi_2$ orbitals on each side (ignoring the interaction of the unfilled $\psi_4^*$ orbitals with each other, which has no effect on the energy because there are no electrons in these
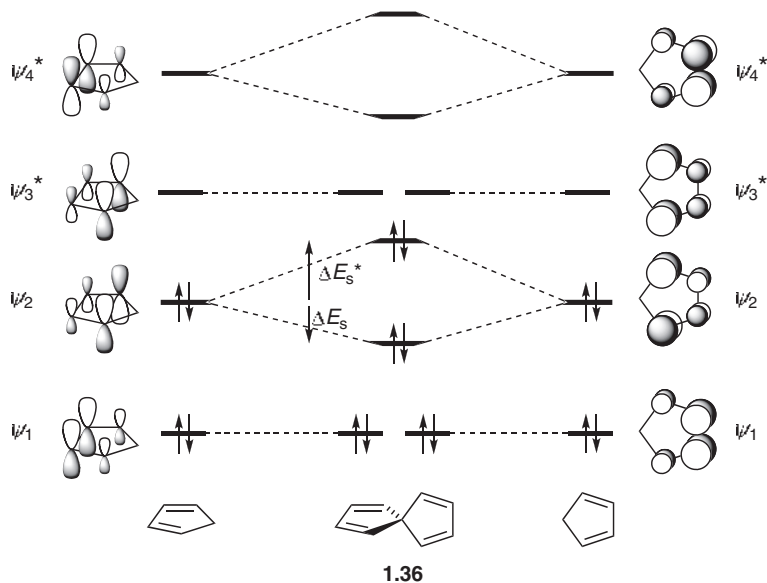


**Fig. 1.52**   $\pi$ Molecular orbitals of the 'antiaromatic' spirononatetraene

orbitals). They lead to the usual two new orbitals, but since there are four electrons to go into them, the net effect is to raise the overall energy, with the bonding combination lowered in energy $\Delta E_s$ less than the antibonding combination is raised $\Delta E_s^*$. The splitting of the energy levels ($\Delta E_s + \Delta E_s^*$) has been measured to be 1.2 eV, and this molecule does show exceptional reactivity, in agreement with the increase in overall energy and the raising of the energy of the HOMO.[44]

## 1.6 Strained σ Bonds—Cyclopropanes and Cyclobutanes

As we have just seen, it is possible to have some bonding even when the overlap is neither strictly head-on nor sideways-on. It is easily possible to retain much more of the bonding when the orbitals are rather better aligned than those in spiro-conjugated systems, as is the case in several strained molecules, epitomised by cyclopropane.
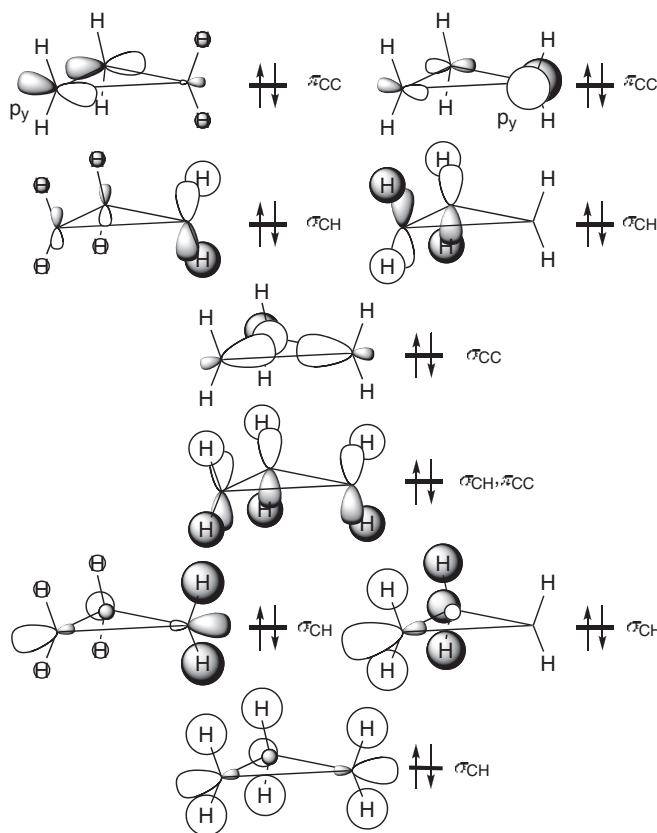
### 1.6.1 Cyclopropanes

There are several ways to describe the σ bonds in cyclopropane. The most simple is to identify the C—H bonds as coming from the straightforward sp$^3$ hybrids on the carbon atoms and the 1s orbitals on the hydrogen atoms **1.37** in the usual way, and the C—C bonds as coming from the remaining sp$^3$ hybrids imperfectly aligned **1.38**. In more detail, these orbitals ought to be mixed in bonding and antibonding combinations to create the full set of molecular orbitals, but even without doing so we can see that C—C bonding is somewhere between σ bonding (head-on overlap) and π bonding (sideways-on overlap). We can expect these bonds to have some of the character of each, which fits in with the general perception that cyclopropanes can be helpfully compared with alkenes in their reactivity and in their power to enter into conjugation. Thus cyclopropane **1.40** is much less reactive than ethylene **1.39** towards electrophiles like bromine, but it is much more reactive than ethane **1.41**. Conjugation of a double bond or an aromatic ring with a cyclopropyl substituent is similar to conjugation with an alkene, but less effective in most cases. However, conjugation between a cyclopropane and an empty p orbital on carbon is more effective in stabilising the cyclopropylmethyl cation than conjugation with a double bond is in the allyl cation (see p. 88).



**1.37**                                          **1.38**



**1.39**   fast          **1.40**   slow          **1.41**
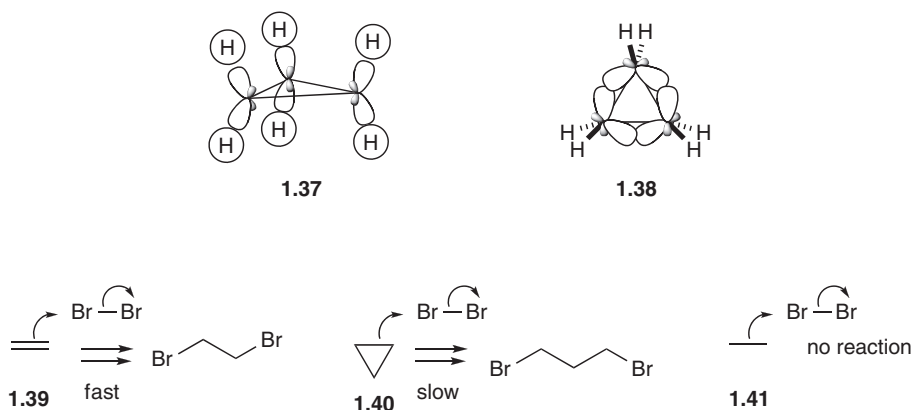
Another way of understanding the C—C bonding, known as the Walsh description, emphasises the capacity of a cyclopropyl substituent to enter into π bonding. In this picture, which is like the picture of the bonding in ethane without using hybridisation (Fig. 1.22), the six C—H bonds are largely made up from the s orbitals on hydrogen and the s, p$_x$ and p$_z$ orbitals on carbon, with the x, y and z axes redefined at each corner to be local x, y and z coordinates. The picture of C—H bonding can be simplified by choosing sp

hybridisation from the combination of the 2s and $2p_x$ orbitals, and using the three sp hybrids with the large lobes pointing outside the ring and the three $p_z$ orbitals to make up the CH bonding orbitals (Fig. 1.53). Some of these orbitals contribute to C—C bonding, notably the $\sigma_{CH},\pi_{CC}$ orbital, but the major contributors are the overlap of the three sp hybrids with the large lobes pointing into the ring, which produce one bonding combination $\sigma_{CC}$, and the three $p_y$ orbitals, which combine to produce a pair of bonding orbitals $\pi_{CC}$, each with one node, and with coefficients to make the overall bonding between each of the C—C bonds equal.



**Fig. 1.53**  A simplified version of the occupied Walsh orbitals of cyclopropane

The advantage of this picture is that it shows directly the high degree of $\pi$ bonding in the C—C bonds, and gives directly a high-energy filled p orbital, the $\pi_{CC}$ orbital at the top right, largely concentrated on C-1, and with the right symmetry for overlap with other conjugated systems, as we shall see in Section 2.2.1.

A remarkable property of cyclopropanes is that they are magnetically anisotropic, rather like benzene—but with the protons coming into resonance in their NMR spectra at unusually *high* field, typically 1 ppm *upfield* of the protons of an open-chain methylene group. For ^{1}H NMR spectroscopy, this is quite a large effect, and it is also strikingly in the opposite direction from that expected by the usual analogy drawn between a cyclopropane and an alkene. The anisotropy[45] is most likely a consequence of the presence of overlap from three sets of orbitals having a total of six electrons in them. These could be seen as the 1s sp[3] orbitals contributing to the C—H bonds **1.37**, which we could have mixed to get a set of orbitals resembling

the $\pi$ orbitals of benzene. Alternatively, turning to Fig. 1.53, the pair of $\sigma_{CH}$ orbitals just below the highest occupied orbitals, together with the $\sigma_{CH},\pi_{CC}$ orbital, clearly have the same nodal pattern as the filled $\pi$ orbitals of benzene (Fig. 1.43), and the pattern is repeated in the three filled orbitals of lowest energy. This pattern of orbitals is associated, as with benzene, with the capacity to support a ring current, but, in contrast to benzene, the derived field places the protons in cyclopropanes in the region experiencing a reduced magnetic field **1.42**.

The same explanation, although we shall not show the molecular orbitals, has been advanced to account for the small difference in chemical shift between the axial and equatorial protons in cyclohexanes, detectable in cyclohexane itself by freezing out at –100 °C the otherwise rapid interconversion of the two chair conformations.[46] The axial protons come into resonance upfield at $\delta 1.1$ and the equatorial protons downfield at $\delta 1.6$. It is possible that the three axial C—H bonds on each side overlap in a $\pi$ sense to create a trishomoaromatic system, with a diamagnetic ring current which places the axial protons in the reduced magnetic field **1.43**, and the equatorial protons in the enhanced magnetic field **1.44**.



**1.42**                          **1.43**                          **1.44**
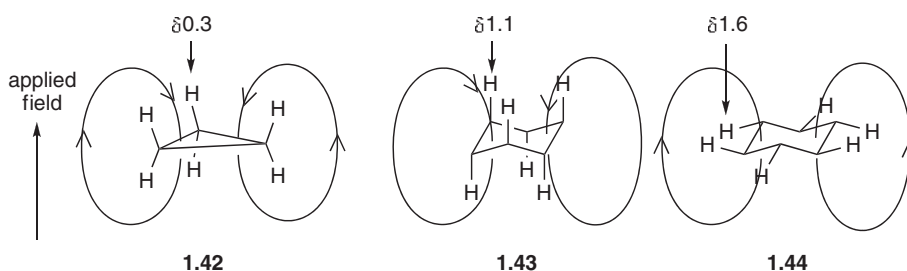
## 1.6.2 Cyclobutanes

It is not necessary to go through the whole exercise of setting up the molecular orbitals of cyclobutanes, which show many of the same features as cyclopropanes, only less so. Cyclobutanes also show enhanced reactivity over simple alkanes, but they are less reactive towards electrophiles, and cyclobutyl groups are less effective as stabilising substituents on electron-deficient centres than cyclopropyl groups.

The most striking difference, however, is that the protons in cyclobutanes come into resonance in their ^{1}H NMR spectra *downfield* of the protons from comparable methylene groups in open-chain compounds.[47] The effect is not large, typically only about 0.5 ppm, with cyclobutane itself, for example, at $\delta 1.96$ in contrast to the average of the cyclohexane signals at $\delta 1.44$. In a cyclobutane, four sets of C—H bonds are conjugated, and the pattern of orbitals will be similar to those of cyclobutadiene (Fig. 1.46). Again there will be two sets, and the top two of each set will be degenerate. The ring current is therefore in the opposite direction, adding to the applied field at the centre of the ring, and the protons experience an enhanced field **1.45**. The effect may be rather less in cyclobutanes than in cyclopropanes, because the cyclobutane ring is flexible, allowing the ring to buckle from the planar structure **1.45**, and the C—H bonds thereby avoid the full eclipsing interactions inevitable in cyclopropanes, and compensated there by the aromaticity they create.



**1.45**
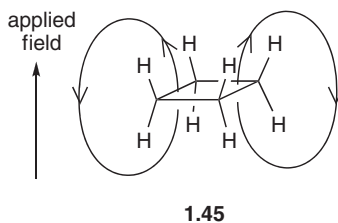
## 1.7 Heteronuclear Bonds, C—M, C—X and C=O

So far, we have been concentrating on symmetrical bonds between identical atoms (homonuclear bonds) and on bonds between carbon and hydrogen. The important interaction diagrams were constructed by combining atomic orbitals of more or less *equal* energy, and the coefficients, $c_1$ and $c_2$, in the molecular orbitals were therefore more or less equal in magnitude. It is true that C—H bonds, both in the picture without hybridisation (Fig. 1.14) and in the picture with hybridisation (Fig. 1.20), involve the overlap of atomic orbitals of different elements, but the difference in electronegativity, and hence in the energy of the atomic orbitals of these two elements, was not significant at the level of discussion used in the earlier part of this chapter. In other cases where we have seen orbitals of different energy interacting, we have either ignored the consequences, because it did not make any significant difference to the discussion at that point, or we have deferred discussion until now. The interaction of orbitals of different energy is inescapable when we come to consider molecules, like methyl chloride and methyllithium, with single bonds to other elements, and molecules with double bonds to electronegative elements like oxygen. As we have mentioned in passing, *atomic orbitals of different energy interact to lower (and raise) the energy of the resultant molecular orbitals less than orbitals of comparable energy.*

### 1.7.1 Atomic Orbital Energies and Electronegativity

There are two standard ways of assessing the relative energies of the orbitals of different elements. One is to use one or another of the empirical scales of electronegativity. Pauling's, which is probably the most commonly used, is empirically derived from the differences in dissociation energy for the molecules XX, YY and XY. Several refinements of Pauling's scale have been made since it first appeared in 1932, and other scales have been suggested too. A good recent one, similar to but improving upon Pauling's, is Allen's,[48] drawn to scale in Fig. 1.54, along with values assigned by Mullay[49] to the carbon atoms in methyl, vinyl and ethynyl groups.

| H and First Row | Hybrids on C | Second Row | Third Row | Fourth Row |
|---|---|---|---|---|
| | | | 0.73 —— K | 0.71 —— Rb |
| 0.91 —— Li | | 0.87 —— Na | 1.03 —— Ca | 0.96 —— Sr |
| | | 1.29 —— Mg | | |
| 1.58 —— Be | | 1.61 —— Al | 1.76 —— Ga | 1.66 —— In |
| | | 1.92 —— Si | 1.99 —— Ge | 1.82 —— Sn |
| 2.05 —— B | | 2.25 —— P | 2.21 —— As | 1.98 —— Sb |
| 2.30 —— H | 2.3 —— sp³ | | 2.42 —— Se | 2.16 —— Te |
| 2.54 ▬▬ C | 2.6 —— sp² | 2.59 —— S | 2.69 —— Br | 2.36 —— I |
| | | 2.87 —— Cl | | |
| 3.07 —— N | 3.1 —— sp | | | |
| 3.61 —— O | | | | |
| 4.19 —— F | | | | |

**Fig. 1.54** Allen electronegativity values and Pauling-based values for carbon hybrids

In spite of the widespread use of electronegativity as a unifying concept in organic chemistry, the electronegativity of an element is almost never included in the periodic table. Redressing this deficiency, Allen strikingly showed his electronegativity scale as the third dimension of the periodic table, and his vivid picture is adapted here as Fig. 1.55.
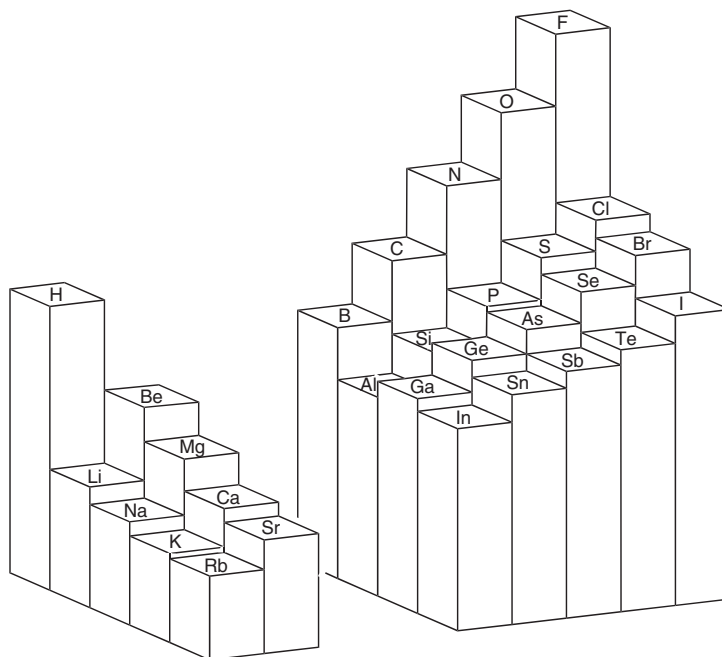
**Fig. 1.55**  Electronegativity as the third dimension of the periodic table (adapted with permission from L. C. Allen, *J. Am. Chem. Soc.*, 1989, **111**, 9003. Copyright 1989 American Chemical Society)
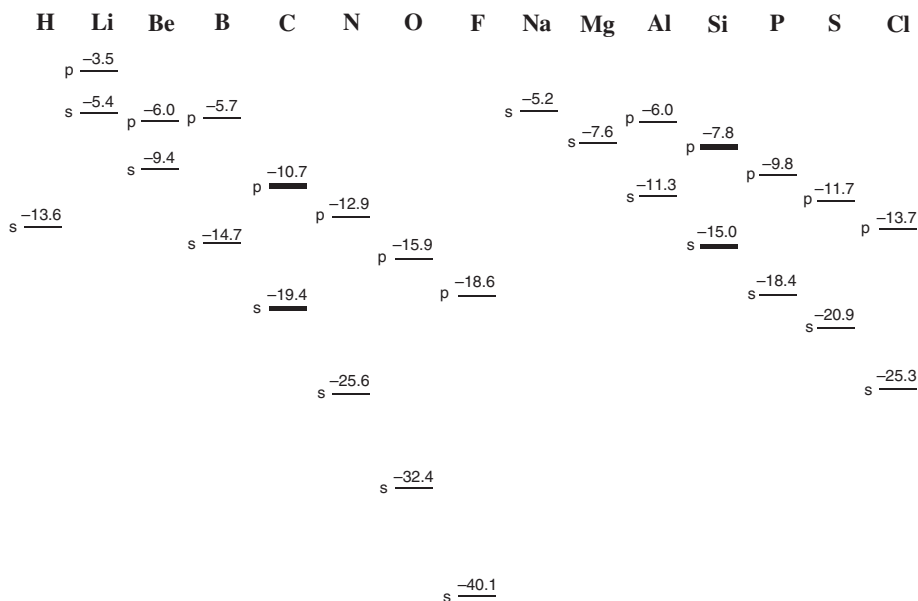
An alternative and more direct way of getting a feel for the relative energies of atomic orbitals is to take them from calculations, reproduced to scale for the first and second row elements in Fig. 1.56.[50] The soundness of these energies is backed up by measurements of the ionisation potentials (IPs), which measure the energy needed to remove an electron from the element. These calculations rank the elements in much the same order, although with a couple of explicable anomalies, which need not concern us here. This figure separates the s and the p orbitals, but we can easily calculate the relative energies of hybrid orbitals on any of the elements from group three to group eighteen. The ranking of the hybrids for carbon, nitrogen, oxygen and fluorine is given in Fig. 1.57 on the same scale and with the s and p orbital energies carried over for comparison.

   The two pictures, the empirical values of Fig. 1.54 and the calculated values of Fig. 1.56, show that the relative positions of the elements on these scales are essentially the same. However, the electronegativity scale shows the methyl, vinyl and ethynyl groups below that for the 1s orbital on hydrogen, whereas the atomic orbital energies place hydrogen in the middle of the range for the different kinds of carbon. This uncertainty provides fuel for debate about which way C—H bonds are polarised, and about whether a C—H bond or a C—C bond is the better electron donor, but the main conclusion is that the energies of the atomic orbitals for C and H are very comparable, and the bond between them is not strongly polarised.

## 1.7.2  C—X σ Bonds

We are now ready to construct an interaction diagram for a bond made by the overlap of atomic orbitals with different energies. Let us take a C—Cl σ bond, in which the chlorine atom is the more electronegative element. Other things being equal, the energy of an electron in an atomic orbital on an electronegative element is lower than that of an electron on a less electronegative element (Fig. 1.56).

   As usual, we can tackle the problem with or without using the concept of hybridisation. The C—X bond in a molecule such as methyl chloride, like the C—C bond in ethane (Fig. 1.22), has several orbitals contributing

**H   Li   Be   B   C   N   O   F   Na   Mg   Al   Si   P   S   Cl**

Li: p −3.5; s −5.4
Be: p −6.0; s −9.4
B: p −5.7; s −14.7
C: p −10.7; s −19.4
N: p −12.9; s −25.6
O: p −15.9; s −32.4
F: p −18.6; s −40.1
H: s −13.6
Na: s −5.2
Mg: p −6.0; s −7.6
Al: p −7.8; s −11.3
Si: p −9.8; s −15.0
P: p −11.7; s −18.4
S: s −20.9; s −25.3
Cl: p −13.7

**Fig. 1.56**   Valence atomic orbital energies in eV (1 eV = 96.5 kJ mol$^{-1}$ = 23 kcal mol$^{-1}$)

**H**        **C**        **N**        **O**        **F**

H: −13.6 1s

C: −10.7 p; −12.9 sp$^3$; −13.6 sp$^2$; −15.1 sp; −19.4 s

N: −12.9 p; −16.1 sp$^3$; −17.1 sp$^2$; −19.3 sp; −25.6 s

O: −15.9 p; −20.0 sp$^3$; −21.4 sp$^2$; −24.2 sp; −32.4 s

F: −18.6 p; −24.4 sp$^3$; −25.8 sp$^2$; −29.4 sp; −40.1 s
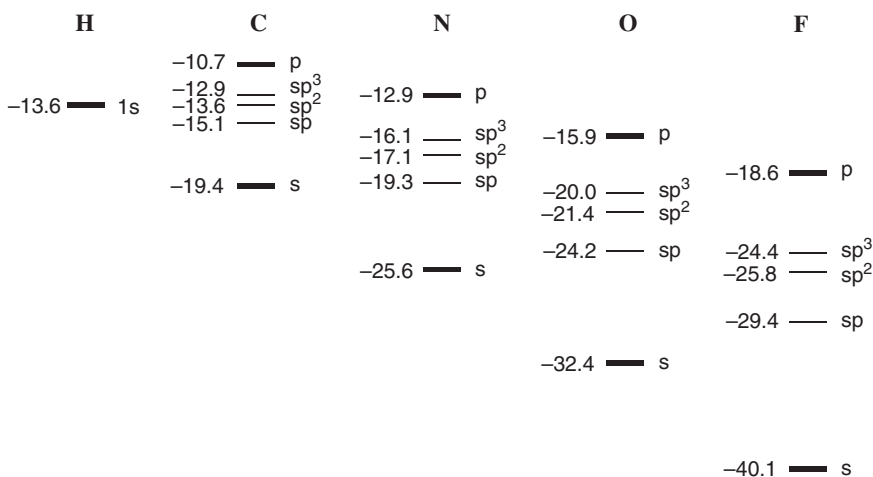
**Fig. 1.57**   Atomic orbital energies for hybrid orbitals in eV

to the force which keeps the two atoms bonded to each other; but, just as we could abstract one of the important pair of atomic orbitals of ethane and make a typical interaction diagram for it (Fig. 1.24), so can we now take the corresponding pair of orbitals from the set making up a C—Cl $\sigma$ bond.

The important thing for the moment is the *comparison* between the C—C orbitals and the corresponding C—Cl orbitals. What we learn about the properties of C—Cl bonds by looking at this one orbital will be the same as we would have learned, at much greater length, from the set as a whole. Alternatively, we can use an interaction diagram for an sp$^3$ hybrid on carbon and an sp$^3$ hybrid on chlorine, and compare the result with

the corresponding interaction of two sp$^3$ hybrids on carbon. Both pictures will be very similar, and we can learn the same lesson from either.

In making a covalent bond between carbon and chlorine from the 2p$_x$ orbital on carbon and the 3p$_x$ orbital on chlorine, we have an interaction (Fig. 1.58) between orbitals of *unequal* energy (–10.7 eV for C and –13.7 eV for Cl, from Fig. 1.56). The interaction diagram in Fig. 1.58 could equally have been drawn using sp$^3$ hybrids on carbon and chlorine in place of the p orbitals. The hybrids have lower energies (–12.9 eV for carbon and –16.6 eV for chlorine), because they have some s character, and the difference in energy between them is greater, but the rest of the story and our conclusions will be unchanged. Alternatively we could use Allen's electronegativities, which effectively take the involvement of s orbitals in hybrids into account.
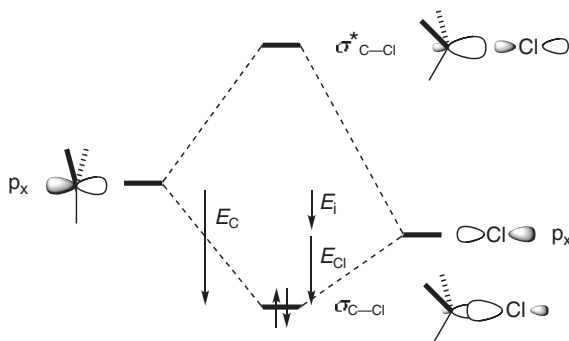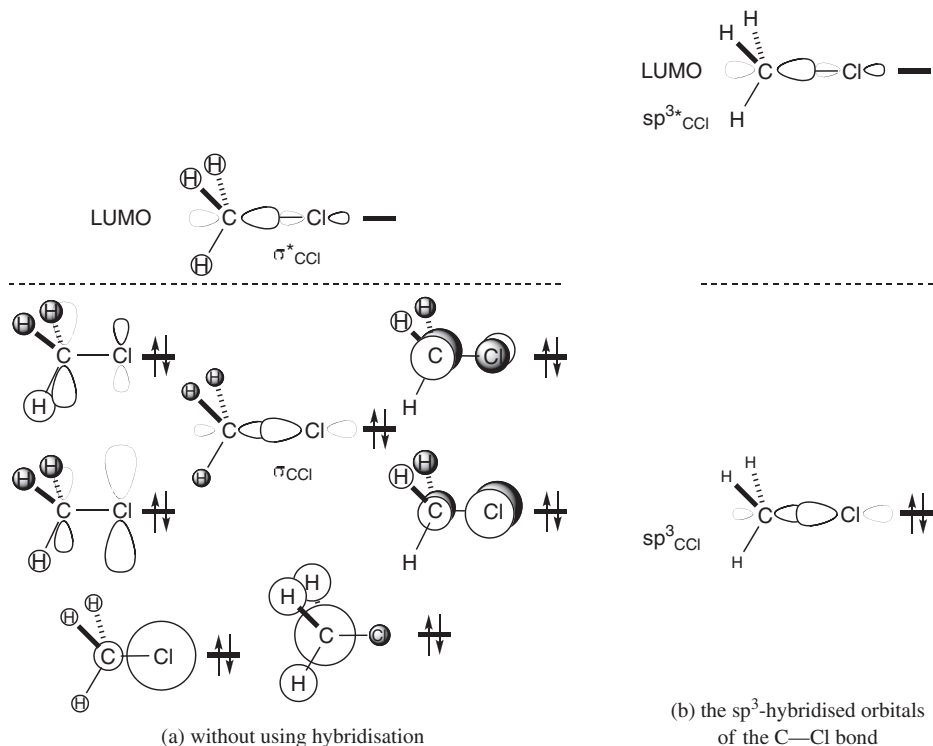


**Fig. 1.58**   A major part of the C—Cl $\sigma$ bond

On account of the loss of symmetry, the chlorine atom has a larger share of the total electron population. In other words, the coefficient on chlorine for the bonding orbital, $\sigma_{CCl}$ is larger than that on carbon. It follows from the requirement that the sum of the squares of all the *c*-values on any one atom in all the molecular orbitals must equal one, that the coefficients in the corresponding antibonding orbital, $\sigma^*_{CCl}$ must reverse this situation: the one on carbon will have to be larger than the one on chlorine.

What we have done in Fig. 1.58 is to take the lower-energy atomic orbital on the right and mix in with it, in a bonding sense, some of the character of the higher-energy orbital on the left. This creates the new bonding molecular orbital, which naturally resembles the atomic orbital nearer to it in energy more than the one further away. We have also taken the higher-energy orbital and mixed in with it, in an antibonding sense, some of the character of the lower-energy orbital. This produces the antibonding molecular orbital, which more resembles the atomic orbital nearer it in energy. When the coefficients are unequal, the overlap of a small lobe with a larger lobe does not lower the energy of the bonding molecular orbital as much as the overlap of two atomic orbitals of more equal size. $E_{Cl}$ in Fig. 1.58, is not as large as $E_\sigma$ in Fig. 1.24.

Using this interaction, and others taking account of the same factors, we can set up a set of filled orbitals for methyl chloride, represented schematically in Fig. 1.59a, along with the lowest of the unoccupied orbitals. As with other multi-atom molecules, several orbitals contribute to C—Cl bonding, with more bonding than antibonding from the overlap of the s orbitals, but probably nearly equal bonding and antibonding from the orbitals having $\pi$ bonding between the carbon and the chlorine. The same degree of bonding can be arrived at by using the hybrid orbitals shown in Fig. 1.59b, where all of the C—Cl bonding comes from the sp$^3$ hybrids.

We might be tempted at this stage to say that we have a weaker bond than we had for a C—C bond, but we must be careful in defining what we mean by a weaker bond in this context. Tables of bond strengths give the C—Cl bond a strength, depending upon the rest of the structure, of something like 352 kJ mol$^{-1}$ (84 kcal mol$^{-1}$), whereas a comparable C—C bond strength is a little lower at 347 kJ mol$^{-1}$ (83 kcal mol$^{-1}$). Only part of the

**Fig. 1.59** The filled molecular orbitals and the lowest unfilled molecular orbital of methyl chloride

(a) without using hybridisation

(b) the sp³-hybridised orbitals of the C—Cl bond

C—Cl bond strength represented by these numbers comes from the purely covalent bonding given by $2E_{Cl}$ in Fig. 1.58. The other part of the strength of the C—Cl bond comes from the electrostatic attraction between the high electron population on the chlorine atom and the relatively exposed carbon nucleus.

We usually say that the bond is polarised, or that it has ionic character. This energy is related to the value $E_i$ in Fig. 1.58, as we can readily see by using an extreme example: suppose that the energies of the interacting orbitals are very far apart (Fig. 1.60, where the isolated orbitals are the 3s orbital on Na and a 2p orbital on F, with energies of –5.2 and –18.6 eV); the overlap will be negligible, and the new molecule will now have almost entirely isolated orbitals in which the higher-energy orbital has given up its electron to the lower-energy orbital. In other words, we shall have a pair of ions. There will be no covalent bonding to speak of, and
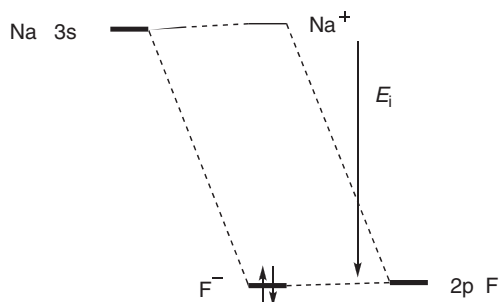


**Fig. 1.60** A much oversimplified ionic bond

the drop in energy in going from the pair of radicals to the cation plus anion is now $E_i$ in Fig. 1.60, which, we can see, is indeed related to $E_i$ in Fig. 1.58.

The C—Cl bond *is* strong, if we try to break it homolytically to get a pair of radicals, and a comparable C—C bond *is* marginally easier to break this way. This is what the numbers 352 and 347 kJ mol$^{-1}$ refer to. In other words, $E_C + E_{Cl}$ in Fig. 1.58 is evidently greater than $2E_\sigma$ in Fig. 1.24. However, it is very much easier to break a C—Cl bond heterolytically to the cation (on carbon) and the anion (on chlorine) than to cleave a C—C bond this way. In other words, $2E_{Cl}$ in Fig. 1.58 is less than $2E_\sigma$ in Fig. 1.24.

The important thing to remember is that *when two orbitals of unequal energy interact, the lowering in energy is less than when two orbitals of very similar energy interact.* Conversely, when it comes to transferring an electron, the ideal situation has the electron in a high-energy orbital being delivered to the 'hole' in a low-energy orbital.

In a little more detail, the extent of the energy lowering $E_{Cl}$ is a function not only of the difference in energy $E_i$ between the interacting orbitals, but also of the overlap integral $S$. The overlap integrals for forming a C—N, a C—O or a C—F bond are essentially, at least in the region for the normal internuclear distances and outwards, parallel to the overlap integral for the formation of a C—C bond (Figs. 1.13b and 1.23b), but displaced successively by about 0.2 Å to shorter internuclear distances for each element. This is because the orbitals of the first-row elements have similar shapes, but the electrons are held more tightly in to the nucleus of the more electronegative elements, and the more electronegative they are the tighter they are held. This simply means that the atoms must be a little closer together to benefit from the overlap. We have already seen that when orbitals of identical energy interact, the energy lowering is roughly proportional to $S$ (see p. 4). When they are significantly different in energy, however, it is roughly proportional to $S^2$. They are also, as we have seen above, inversely proportional to the energy difference $E_i$. The equations for the energies of the lowered and raised orbitals in Fig. 1.58, $E_{\sigma CCl}$ and $E_{\sigma*CCl}$, respectively, take the form shown in Equations 1.13 and 1.14.

$$E_{\sigma CCl} = E_{p_{Cl}} + \frac{(\beta_{CCl} - E_{pCl}S_{CCl})^2}{E_{pCl} \pm E_{\pi C}} \qquad\qquad 1.13$$

$$E_{\sigma*CCl} = E_{p_C} + \frac{(\beta_{CCl} - E_{pC}S_{CCl})^2}{E_{pC} \pm E_{\pi Cl}} \qquad\qquad 1.14$$

Clearly a full expression for the overall electronic energy is a complex one if it is to take account of the changes between these expressions and those in Equations 1.4 and 1.5 for the energies when the interacting orbitals are degenerate.

A picture of the electron distribution in the $\sigma$ orbitals between carbon and chlorine is revealed in the wire-mesh diagrams in Fig. 1.61, which show one contour of the $\sigma_{CCl}$ and $\sigma*_{CCl}$ orbitals of methyl chloride. Comparing these with the schematic version in Fig. 1.58, we can see better how the back lobe on carbon in $\sigma_{CCl}$ overlaps with the s orbitals on the hydrogen atoms, and that the front lobe in $\sigma*_{CCl}$ wraps back behind



$\sigma_{CCl}$                                          $\sigma*_{CCl}$
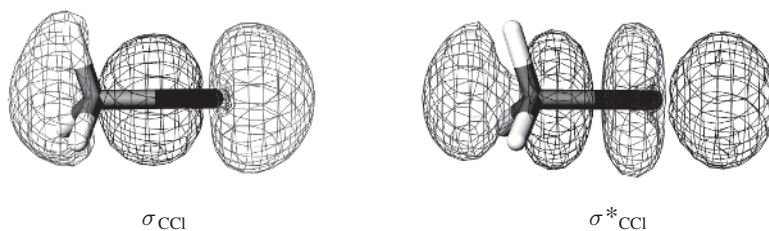
**Fig. 1.61**   The major C—Cl bonding orbital and the LUMO for methyl chloride

the carbon atom to include a little overlap to the s orbitals of the hydrogen atoms. We need to remove an oversimplification and delve a little more into detail in order to see how this comes about.

The pictures in Fig. 1.59a are shown as though the lowest-energy orbitals were made up from the interaction only of s orbitals with each other. Likewise the next higher orbitals are made up only of the interactions of p orbitals on the carbon and chlorine, and necessarily s orbitals on hydrogen. These interactions are certainly the most important, and the simplification works, because the s orbitals on carbon and chlorine are closer in energy to each other than they are to each other's p orbitals, and vice versa, as shown in Fig. 1.62a. However, the direct interactions of s with s and p with p are only a first-order treatment, and a second-order treatment has to consider that the s orbital on carbon can interact quite strongly with the $p_x$ orbital on chlorine, and there will even be a small interaction from the $p_x$ orbital on carbon and the s orbital on chlorine. This complication is similar to something we saw earlier with methylene, with the allyl system and with butadiene (Figs. 1.16. 1.32 and 1.38), where we used the device for constructing molecular orbitals, first looking at the strong interaction of orbitals close in energy, and then modified the result by allowing for the weaker interactions of orbitals further apart in energy. The true mixing of orbitals for methyl chloride would still leave the lowest energy orbital looking largely like the mix of s with s, but there would be a contribution with some p character, in inverse proportion to the energy difference between the s and p orbitals. It is the presence of some p character in the orbitals contributing to the $\sigma^*_{CCl}$ orbital in Fig. 1.61 that allows the outer counters to reach round behind the carbon atom. We saw the same feature earlier in the picture of an $sp^3$ hybrid (Fig. 1.19), where the cause was essentially the same—the mixing of s and p orbitals in optimum proportions for lowering the overall energy.

The problem of identifying sensible mixes of orbitals would have been much more acute had we used methyl fluoride instead of methyl chloride. With methyl fluoride, the 2s orbital on carbon is almost identical in energy with the 2p orbitals on fluorine, as shown in Fig. 1.62b. The $2p_x$ orbital from that element and the 2s orbital on carbon have the right symmetry, and their interaction would provide the single strongest contribution to C—F bonding. Continuing from here to make a full set of the molecular orbitals for methyl fluoride, mixing in a small contribution from the p orbital on carbon, for example, would not have made as tidy and understandable a picture as the one for methyl chloride in Fig. 1.59. Most strikingly, the lowest-energy orbital would be an almost pure, undisturbed s orbital on fluorine, and there would be correspondingly little of this orbital to mix in with the others.



(a) Methyl chloride                  (b) Methyl fluoride                  (c) Methyllithium
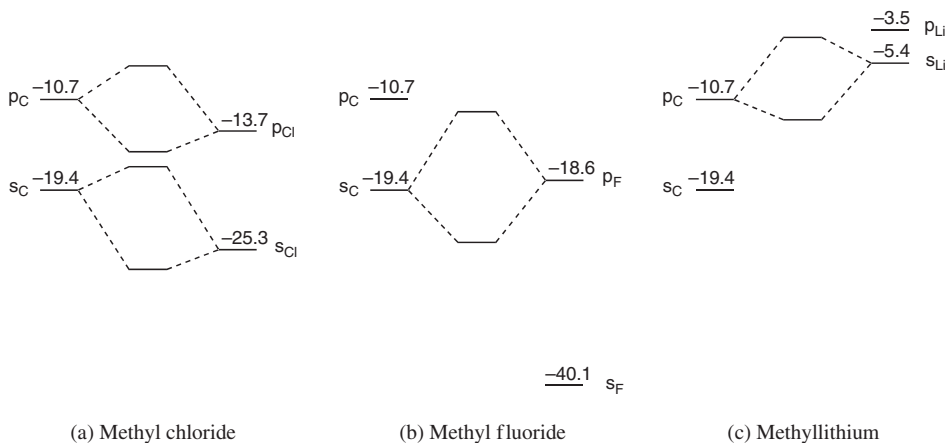
**Fig. 1.62**   Some of the major interactions contributing to C—Cl bonding for MeCl, to C—F bonding for MeF, and to C—Li bonding for MeLi

### 1.7.3 C—M σ Bonds

When the bond from carbon is to a relatively electropositive element like lithium, the same problems can arise—with methyllithium the most strongly interacting orbitals contributing to the C—Li bond (Fig. 1.62c) are the 2s orbital on lithium and the $2p_x$ orbital on carbon. The pictorial set of molecular orbitals therefore is not one in which you can see immediately which atomic orbitals make the major contribution to which molecular orbitals. The interaction between a 2s orbital on lithium and a $2p_x$ orbital on carbon has the form shown in Fig. 1.63. The energy of the lithium 2s orbital is –5.4 eV, making the carbon atom, with a 2p orbital at –10.7 eV, the more electronegative atom. The bonding orbital $\sigma_{LiC}$ is polarised towards carbon, and the antibonding $\sigma^*_{LiC}$ towards lithium. Organic chemists often refer to organolithium compounds as anions. Although there evidently is some justification for this way of thinking, it is as well to bear in mind that they are usually highly polarised covalent molecules. Furthermore, they are rarely monomeric, almost always existing as oligomers, in which the lithium is coordinated to more than one carbon atom, making the molecular orbital description below severely over-simplified
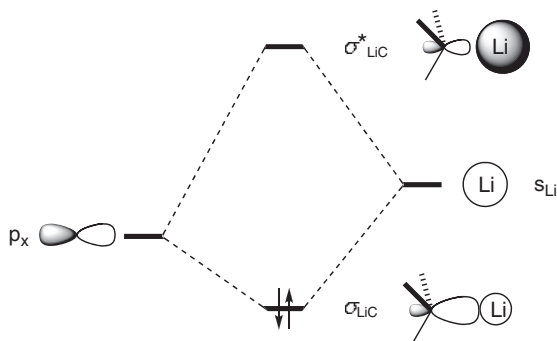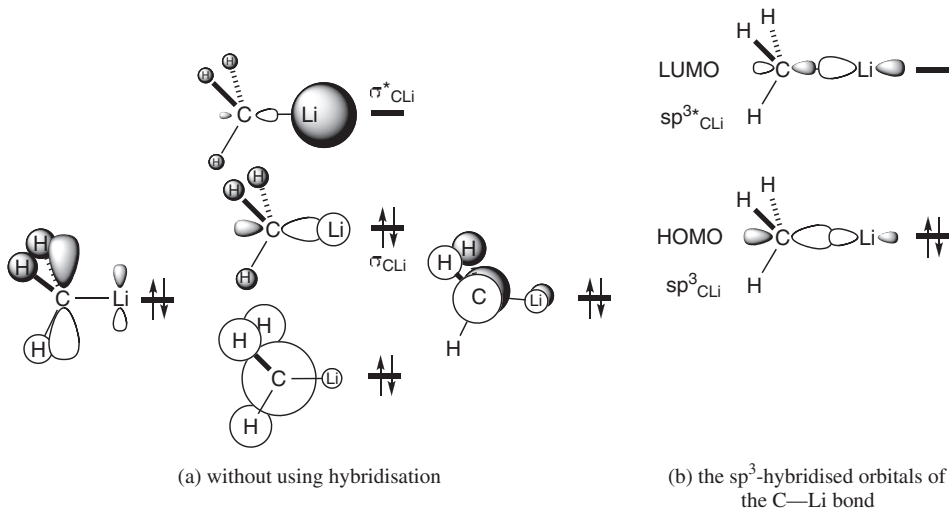


**Fig. 1.63**    A contributory part of the Li—C σ bond

The filled and one of the unfilled orbitals for monomeric methyllithium are shown in Fig. 1.64. The lowest energy orbital is made up largely from the 2s orbital on carbon and the 1s orbitals on hydrogen, with only a little mixing in of the 2s orbital of lithium and even less of the 2p. The next two up in energy are largely $\pi$ mixes of the $2p_z$ and $2p_y$ orbitals on carbon with a little of the $2p_z$ and $2p_y$ on lithium, and, as usual, the 1s orbitals on hydrogen. The $2p_z$ and $2p_y$ orbitals on lithium have a zero overlap integral with the 2s orbital on carbon, and this interaction, although between orbitals close in energy (Fig. 1.62c), makes no contribution. Then come the two orbitals we have seen in Fig. 1.63: the $2p_x$ orbital on carbon interacting productively with the 2s orbital on lithium, giving rise to the highest of the occupied orbitals $\sigma_{CLi}$, which has mixed in with it the usual 1s orbitals on hydrogen and a contribution from the $2p_x$ orbital on lithium, symbolised here by the displacement of the orbital on lithium towards the carbon. The next orbital up in energy, the lowest of the unfilled orbitals, is its counterpart $\sigma^*_{CLi}$, largely a mix of the 2s and the $2p_x$ orbital of lithium, symbolised again by the displacement of the orbital on lithium away from the carbon, with a little of the $2p_x$ orbital of carbon out of phase.

A picture of the electron distribution in the frontier σ orbitals between carbon and lithium is revealed in the wire-mesh diagrams in Fig. 1.65, which show one contour of the $\sigma_{CLi}$ and $\sigma^*_{CLi}$ orbitals of methyllithium, unrealistically monomeric and in the gas phase. Comparing these with the schematic version in Fig. 1.64, we can see better how the s and $p_x$ orbitals on lithium mix to boost the electron population between the nuclei in $\sigma_{CLi}$, and to minimise it in $\sigma^*_{CLi}$. The HOMO, $\sigma_{CLi}$, is used on the cover of this book.

(a) without using hybridisation

(b) the $sp^3$-hybridised orbitals of
the C—Li bond

**Fig. 1.64**    The filled and one of the unfilled molecular orbitals of methyllithium



$\sigma_{CLi}$                                    $\sigma^*_{CLi}$
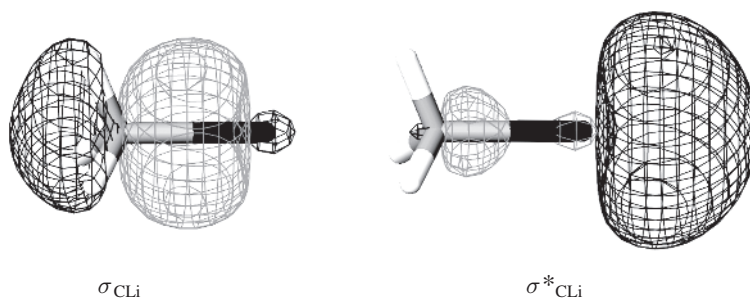
**Fig. 1.65**    The HOMO and LUMO for methyllithium

### 1.7.4  C=O $\pi$ Bonds

Setting up the molecular orbitals of a C=O $\pi$ bond is relatively straightforward, because the p orbitals in the $\pi$ system in Hückel theory are free from the complicating effect of having to mix in contributions from s orbitals. The $p_x$ orbital on oxygen is placed in Fig. 1.66 at a level somewhat more than $1\beta$ below that of the $p_x$ orbital on carbon, although not to scale. The energy of a p orbital on oxygen is $-15.9$ eV and that on carbon $-10.7$ eV (Fig. 1.56). As with $\pi$ bonds in general, the raising of the $\pi^*$ and lowering of the $\pi$ orbitals above and below the atomic p orbitals is less than it was for a C—O $\sigma$ bond, and less than the corresponding $\pi$ bond between two carbon atoms. Both the $\pi_{C=O}$ and the $\pi^*_{C=O}$ orbitals are now lower in energy than the $\pi_{C=C}$ and $\pi^*_{C=C}$ orbitals, respectively, of ethylene, which by definition are $1\beta$ above and $1\beta$ below the $\alpha$ level.

The polarisation of the carbonyl group is away from carbon towards oxygen in the bonding orbital, and in the opposite direction in the antibonding orbital, as usual. The wire-mesh pictures in Fig. 1.67 show more realistically an outer contour of these two orbitals in formaldehyde, and the plots in Fig. 1.68 show the electron distribution in more detail. Note that in these pictures it *appears* that the $\pi$ electron population in the bonding orbital is nearly equal on oxygen and on carbon. This is not the case, as shown by the extra contour around the oxygen atom in the plot in Fig. 1.68. The electron
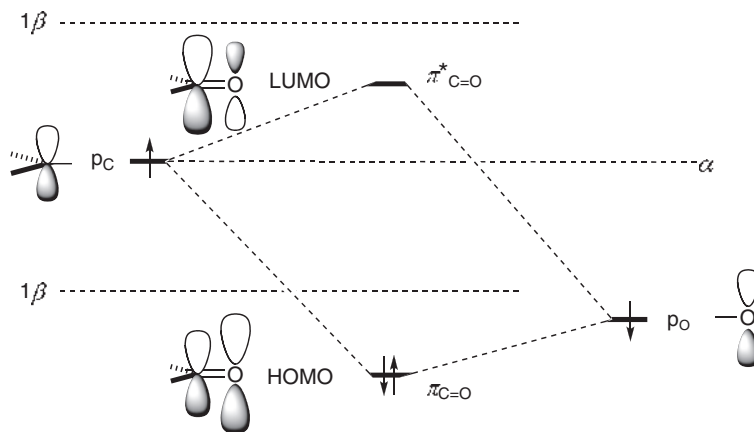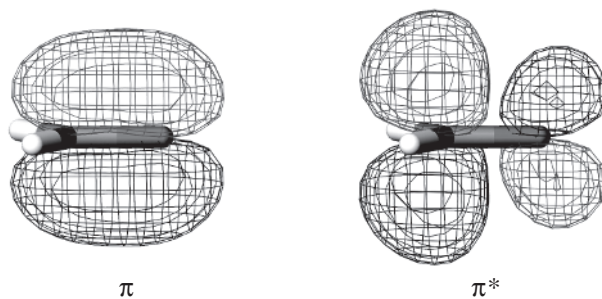
**Fig. 1.66**   A C=O $\pi$ bond



**Fig. 1.67**   Wire-mesh plot of the $\pi$ and $\pi^*$ orbitals of formaldehyde
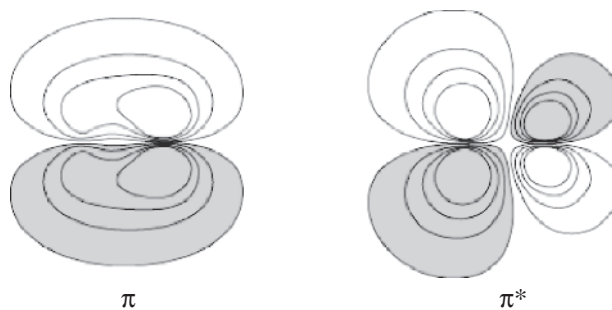


**Fig. 1.68**   Electron population contours for the $\pi$ and $\pi^*$ orbitals of formaldehyde

distribution around the oxygen atom is simply more compact, as a consequence of the higher nuclear charge on that atom. This is another way in which the conventional lobes as drawn in Fig. 1.66 are misleading.

There is no set of fundamentally sound values for $\alpha$ and $\beta$ to use in Hückel calculations with heteroatoms. Everything is relative and approximate. The values for energies and coefficients that come from simple calculations on molecules with heteroatoms must be taken only as a guide and not as gospel. In simple Hückel theory, the value of $\alpha$ to use in a calculation is adjusted for the element in question X from the reference value for carbon $\alpha_0$ by Equation 1.15. Likewise, the $\beta$ value for the C=C bond in ethylene $\beta_0$ is adjusted for C=X by Equation 1.16.

$$\alpha_X = \alpha_0 + h_X \beta_0 \qquad\qquad 1.15$$

$$\beta_{CX} = k_{CX} \beta_0 \qquad\qquad 1.16$$

The adjustment parameters $h$ and $k$ take into account the trends in Figs. 1.54–1.56 and the changes in the overlap integrals for making C—X bonds discussed on p. 54, but are not quantitatively related to those numbers. Instead, values of $h$ for some common elements and of $k$ for the corresponding C=X $\pi$ bonds (Table 1.2) have been recommended for use in Equations 1.15 and 1.16.[51] They are only useful to see trends.

**Table 1.2**   Parameters for simple Hückel calculations for $\pi$ bonds with heteroatoms

| Element | | $h$ | $k$ | Element | | $h$ | $k$ |
|---|---|---|---|---|---|---|---|
| B | | −0.45 | 0.73 | | | | |
| C | C=C | 0 | 1 | Si | =Si | 0 | 0.75 |
| N | N | 0.51 | 1.02 | P | P | 0.19 | 0.77 |
| N | N | 1.37 | 0.89 | P | P | 0.75 | 0.76 |
| O | O | 0.97 | 1.06 | S | S | 0.46 | 0.81 |
| O | O | 2.09 | 0.66 | S | S | 1.11 | 0.69 |
| F | F | 2.71 | 0.52 | Cl | Cl | 1.48 | 0.62 |

As with single bonds to electronegative heteroatoms, it is easier to break a C=O bond heterolytically and a C=C bond homolytically. Some reminders of a common pattern in chemical reactivity may perhaps bring a sense of reality to what must seem, so far, an abstract discussion: nucleophiles readily attack a carbonyl group but not an isolated C=C double bond; however, radicals readily attack C=C double bonds, and, although they can attack carbonyl groups, they do so less readily.

### 1.7.5 Heterocyclic Aromatic Systems

The concept of aromaticity is not restricted to hydrocarbons. Heterocyclic systems, whether of the pyrrole type **1.46** with trigonal nitrogen in place of one of the C=C double bonds, or of the pyridine type **1.47** with a

trigonal nitrogen in place of a carbon atom, are well known. The $\pi$ orbitals of pyrrole are like those of the cyclopentadienyl anion, and those of pyridine like benzene, but skewed by the presence of the electronegative heteroatom. The energies and coefficients of heteroatom-containing systems like these cannot be worked out with the simple devices that work for linear and monocyclic conjugated hydrocarbons. The numbers in Fig. 1.69 are the results of simple Hückel calculations using parameters like those in Table 1.2 for equations like Equations 1.15 and 1.16, and some trends can be seen. The overall $\pi$ energy is lowered by the cyclic conjugation. The lowest-energy orbital $\psi_1$ is always polarised towards the electronegative atom, and the next orbital up in energy $\psi_2$ (and the highest unoccupied orbital) is polarised the other way. This polarisation is more pronounced in the pyridinium cation **1.48**, where the protonated nitrogen is effectively a more electronegative atom. In the pyridine orbitals, the HOMO is actually localised as the nonbonding lone pair of electrons on nitrogen, and the degeneracy of $\psi_2$ and $\psi_3$, and of the corresponding antibonding orbitals, is removed, but not by much. The orbitals with nodes through the heteroatoms are identical in energy and coefficients with those of the corresponding hydrocarbon. The orbitals $\psi_3$ and $\psi_5^*$ in pyrrole, with a node through the nitrogen atom, are identical to $\psi_2$ and $\psi_4^*$ in butadiene, and $\psi_3$ and $\psi_5^*$ in pyridine and its cation are identical to $\psi_3$ and $\psi_5^*$ in benzene.
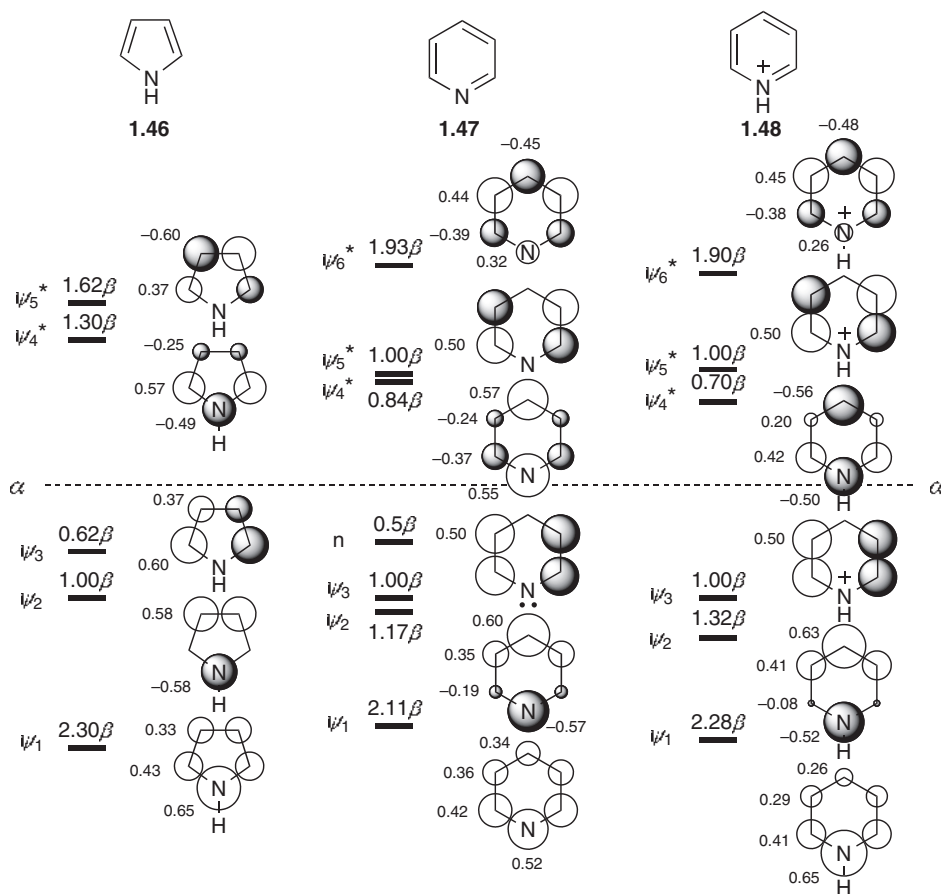


**Fig. 1.69**    $\pi$ Molecular orbitals of pyrrole, pyridine and the pyridinium ion. (Calculated using $h=1$ and $k=1$ for pyrrole, $h=0.5$ and $k=1$ for pyridine, and $h=1$ and $k=1$ for the pyridinium cation)

## 1.8   The Tau Bond Model

The Hückel version of molecular orbital theory, separating the $\sigma$ and $\pi$ systems, is not the only way of accounting for the bonding in alkenes. Pauling showed that it is possible to explain the electron distribution in alkenes and conjugated polyenes using only $sp^3$-hybridised carbon atoms. For ethylene, for example, instead of having $sp^2$-hybridised carbons involved in full $\sigma$ bonding, and p orbitals involved in a pure $\pi$ bond, two $sp^3$ hybrids can overlap in something between $\sigma$ and $\pi$ bonding **1.49**. The overall distribution of electrons in this model is exactly the same as the combination of $\sigma$ and $\pi$ bonding in the conventional Hückel picture (Fig. 1.25). In practice, this model, usually drawn with curved lines called $\tau$ bonds **1.50**,[52] has found few adherents, and the insights it gives have not proved as useful as the Hückel model. For example, the $\tau$ bonds between C-1 and C-2 and between C-3 and C-4 in butadiene **1.51** are not so obviously conjugated as the $\pi$ bonds in the Hückel picture in Fig. 1.37. It is useful, however, to recognise that it is perfectly legitimate, and that on occasion it might have some virtues, not present in the Hückel model, especially in trying to explain some aspects of stereochemistry.



**1.49**                    **1.50**

**1.51**
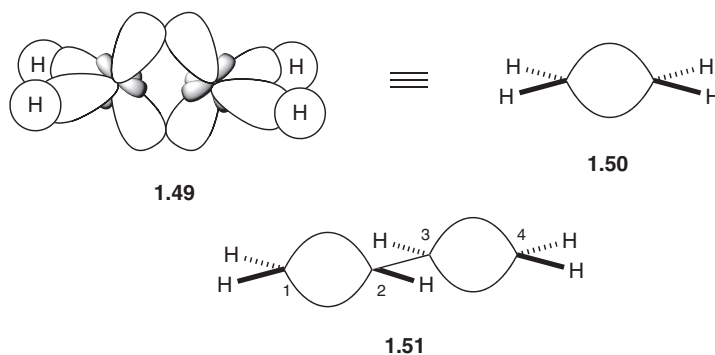
## 1.9   Spectroscopic Methods

A number of physical methods have found support in molecular orbital theory, or have provided evidence that the deductions of molecular orbital theory have some experimental basis. Electron affinities measured typically from polarographic reduction potentials correlate moderately well with the calculated energies of the LUMO of conjugated systems. Ionisation potentials can be measured in a number of ways, and the results correlate moderately well with the calculated energies of the HOMO of conjugated systems.[53] Several other measurements, like the energies of conjugated systems, bond lengths, and energy barriers to rotation, can be explained by molecular orbital theory, and will appear in the normal course of events in the next chapter. A few other techniques, dealt with here, have helped directly in our understanding of molecular orbital theory, and we shall use evidence from them in the analysis of chemical structure and reactivity in later chapters.
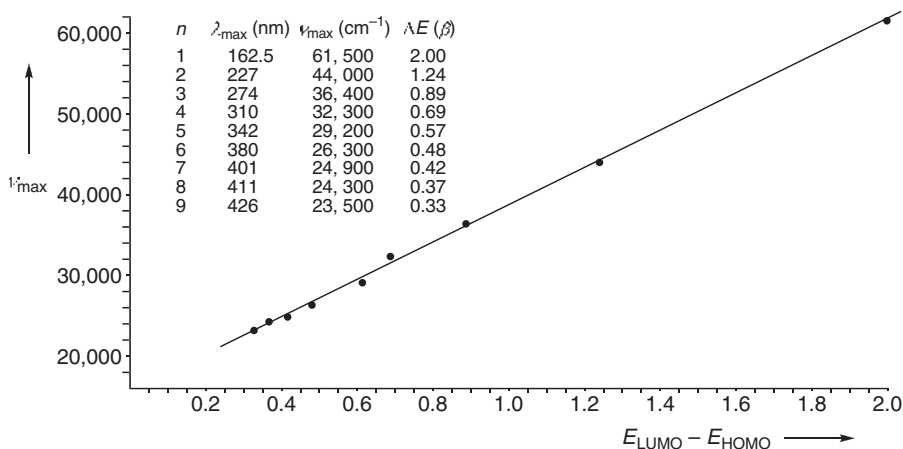
### 1.9.1 Ultraviolet Spectroscopy

When light of an appropriate energy interacts with an organic compound, an electron can be promoted from a low-lying orbital to a higher energy orbital, with the lowest-energy transition being from the HOMO to the LUMO. Selection rules govern which transitions are allowed and which are forbidden. One rule states that electron spin may not change, and another that the orbitals should not be orthogonal. The remaining selection rule is based on the symmetries of the pair of orbitals involved. In most cases, the rules are too complicated to be made simple here.[54] Group theory is exceptionally powerful in identifying which transitions are allowed, and it is one of the first applications of group theory that a chemist pursuing a more thorough understanding comes across. One case, however, is easy—that for molecules which only have a centre of symmetry, like s-*trans* butadiene **1.8**. The

allowed transitions for these molecules are between orbitals that are symmetric and antisymmetric with respect to the centre of symmetry. Thus the HOMO, $\psi_2$, is symmetric with respect to the centre of symmetry half way between C-2 and C-3, and the LUMO, $\psi_3^*$, is antisymmetric (Fig. 1.37). Accordingly, this transition is allowed and is indeed strong, as is the corresponding transition for each of the longer linear polyenes.

Data for this the longest wavelength $\pi \rightarrow \pi^*$ transition are available for ethylene,[55] where the problem is pulling out the true maximum from a broad band in the vacuum UV, and for a long list of the lower polyenes, where the maximum is easy to measure in the UV region when methyl or other alkyl groups are present at the termini to stabilise the polyenes against electrocyclisation and polymerisation. Fig. 1.70 is a plot of the experimentally determined[56] values of $\lambda_{max}$ for the longest wavelength absorption for a range of such polyenes $R(CH{=}CH)_nR$, converted to frequency units, against $(E_{LUMO} - E_{HOMO})$ in $\beta$ units calculated using Equation 1.17:

$$\Delta E = 4\beta \sin \frac{\pi}{2(2n+1)} \qquad\qquad 1.17$$

which is simply derived from the geometry of figures like Figs. 1.31 and 1.39. The correlation is astonishingly good—in view of the simplifications made in Hückel theory, and in view of the fact that most transitions, following the Frank-Condon principle, are not even between states of comparable vibrational energy. Nevertheless, Fig. 1.70 is a reassuring indication that the simple picture we have been using is not without foundation, and that it works quite well for relative energies. Similarly impressive correlations can be made using aromatic systems, and even for $\alpha,\beta$-unsaturated carbonyl systems. It is not however a good measure of absolute energies, and the energy of the $\pi \rightarrow \pi^*$ transition measured by UV cannot be used directly as a measure of the energy difference between the HOMO and the LUMO. This can be seen from that fact that the line in Fig. 1.70 does not go through the origin, as Hückel theory would predict, but intersects the ordinate at $15\,500$ cm$^{-1}$, corresponding to an energy of 185 kJ mol$^{-1}$ (44 kcal mol$^{-1}$).



| $n$ | $\lambda_{max}$ (nm) | $\nu_{max}$ (cm$^{-1}$) | $\Delta E$ ($\beta$) |
|---|---|---|---|
| 1 | 162.5 | 61, 500 | 2.00 |
| 2 | 227 | 44, 000 | 1.24 |
| 3 | 274 | 36, 400 | 0.89 |
| 4 | 310 | 32, 300 | 0.69 |
| 5 | 342 | 29, 200 | 0.57 |
| 6 | 380 | 26, 300 | 0.48 |
| 7 | 401 | 24, 900 | 0.42 |
| 8 | 411 | 24, 300 | 0.37 |
| 9 | 426 | 23, 500 | 0.33 |

**Fig. 1.70**   Frequency of first $\pi \rightarrow \pi^*$ transitions of some representative polyenes $R(CH{=}CH)_nR$ plotted against $(E_{LUMO} - E_{HOMO})$ calculated using Equation 1.17

### 1.9.2 Nuclear Magnetic Resonance Spectroscopy

Chemical shift is substantially determined by the electron population surrounding the nucleus in question and shielding it from the applied field. Chemical shifts, and $^{13}C$ chemical shifts in particular, are therefore used to probe the total electron population. The chemical shift range with protons is so small that aromatic ring currents and other anisotropic influences make such measurements using proton spectra unreliable.

Coupling constants $J$ measure the efficiency with which spin information from one nucleus is transmitted to another. This is not usually mediated through space, but by interaction with the electrons in intervening orbitals. Transmission of information about the magnetic orientation of one nucleus to another is dependent upon how well the orbitals containing those electrons overlap, as well as by the number of intervening orbitals. In a crude approximation, the number of intervening orbital interactions affects both the sign and the magnitude of the coupling constant.

Coupling constants can be either positive or negative. Although this does not affect the appearance of the $^1$H-NMR spectrum, it does change the way in which structural variations affect the magnitude of the coupling constant. To understand why coupling constants can be positive or negative, we need to look into the energetics of coupling. In hydrogen itself, $H_2$, there are three arrangements with different energies: the lowest energy with the nuclear spins of both nuclei H and H′ aligned, the highest with both opposed, and in between two ways equal in energy with the alignments opposite to each other (Fig. 1.71a, where upward-pointing arrows indicate nuclear magnets in their low-energy orientation with respect to the applied magnetic field, downward-pointing arrows indicate nuclear magnets in their high-energy orientation with respect to the magnetic field, and levels of higher energy are indicated by vertical upward displacement). The transitions which the instrument measures are those in which the alignment of one of the nuclei changes from the $N_\beta$ state (the high-energy orientation, aligned with the applied magnetic field) to the $N_\alpha$ state (the low-energy orientation, aligned in opposition to the applied magnetic field). There are four such transitions labelled $W$ in Fig. 1.71a, and all of them equal in magnitude. The receiving coils detect only the one signal, and the spectrum shows one line and hence no apparent coupling.
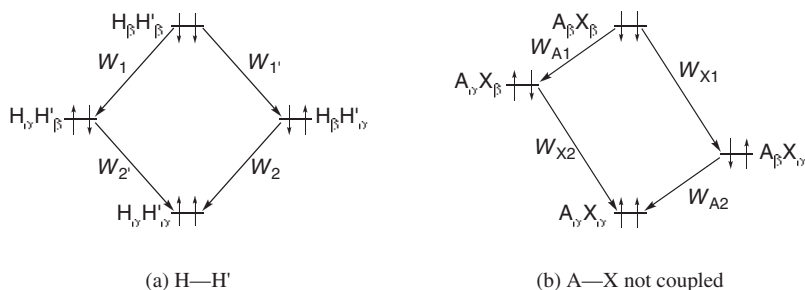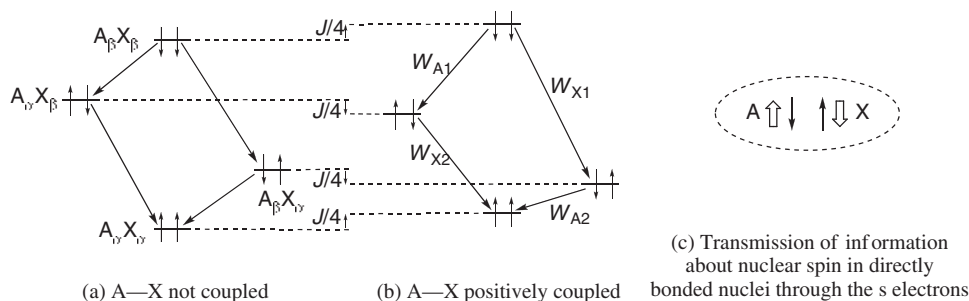


(a) H—H'     (b) A—X not coupled

Fig. 1.71   Energy levels of atomic nuclei showing no coupling

If now we look at two different atoms A and X, we have the same set-up, but this time the two energy levels in the middle are of different energy, one with A aligned and the other with X aligned (Fig. 1.71b). 'A' might be a $^{13}$C, and 'X' a $^1$H atom, but the general picture is the same for all AX systems. If there is no coupling ($J = 0$), as when the nuclei are far apart, the $A_\alpha X_\beta$ energy level will be as much above the mid-point as the energy level for the $A_\beta X_\alpha$ nucleus is below it. There will again be four transitions, two equal for the A nucleus, labelled $W_A$, and two equal for the X nucleus, labelled $W_X$, giving rise to one line from each.
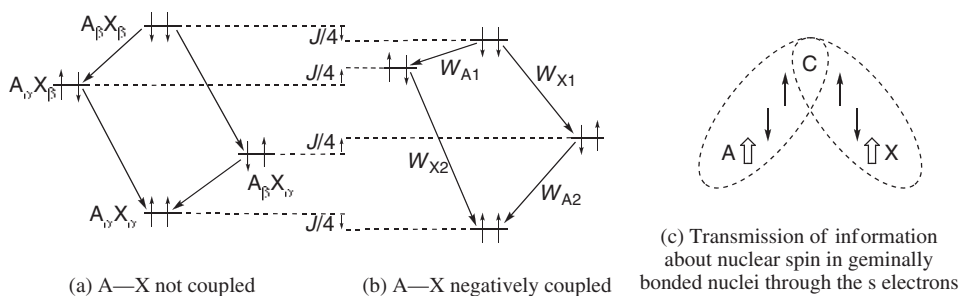
If, however, the two nuclei are directly bonded, they will affect each other. The A spin will be opposed to the spin of one of the intervening electrons in an s orbital (only s orbitals have an electron population at the nucleus); that electron is paired with the other bonding s electron. In the lowest energy arrangement of the system, both the A and X nuclei are spin-paired with the bonding electrons with which they interact most strongly (as in Fig. 1.72c). As a result, the A and the X nuclei will be opposed in the lowest energy arrangement. Conversely, the system will be higher in energy when these spins are aligned. Thus, the two energy levels in which the A and X nuclei have parallel spins will be raised and the two energy levels in which they are opposed will be lowered (Fig. 1.72b). Thus, there are now four new energy levels, four different transitions, $W_{A1}$ and $W_{A2}$, and $W_{X1}$ and $W_{X2}$, and four lines in the AX spectrum. The A signal is a

doublet and the X signal is a doublet, with the same separation between the lines, because $(W_{A1} - W_{A2}) = (W_{X1} - W_{X2}) = J_{AX}$. Thus, the extent of the raising and lowering of each of the energy levels is $J_{AX}/4$. More complicated versions of this kind of diagram, more complicated than can be explained here, are needed to analyse spin interactions for nuclei with values of $I \neq \frac{1}{2}$, for systems more complicated than AX, and even more complicated ones to make sense of those spectra that are not first order.



(a) A—X not coupled          (b) A—X positively coupled

(c) Transmission of information about nuclear spin in directly bonded nuclei through the s electrons

**Fig. 1.72**    Energy levels of atomic nuclei without (a) and with the capacity to show coupling (b)

If instead of being directly bonded, the A and X nuclei are separated by two bonds, the transmission of information through the s electrons leads the two nuclei to be parallel in the *low*-energy arrangement, in contrast to the *high*-energy arrangement of Fig. 1.72. The model that illustrates this point is given in Fig. 1.73c, and implies that the nuclei will be antiparallel in the *high*-energy arrangement. Now the energy levels will have the lowest and highest energy levels lowered by the interaction of the two spins, and the levels in between raised (Fig. 1.73b). If the coupling constant is the same as that in Fig. 1.72, the two transitions for the A nucleus, $W_{A1}$ and $W_{A2}$, are of the same magnitude as before but have changed places, and similarly for $W_{X1}$ and $W_{X2}$. The appearance of the spectrum will not have changed, but the coupling constant $J$ is negative in sign. In general, although not always, one-bond couplings $^1J$ and three-bond couplings $^3J$ are positive in sign, and two- and four-bond couplings $^2J$ and $^4J$ are negative in sign.



(a) A—X not coupled          (b) A—X negatively coupled

(c) Transmission of information about nuclear spin in geminally bonded nuclei through the s electrons

**Fig. 1.73**    Energy levels of atomic nuclei with the capacity to show coupling through two bonds

The connection between spin-spin coupling and orbital involvement can be found in several familiar situations. Thus, the $^1J$ values for $^1H$—$^{13}C$ coupling are correlated with the degree of s character at carbon **1.52–1.54**. More subtly the $^1H$—$^{13}C$ coupling constant is a measure of the C—H bond length, with the axial protons in cyclohexanes having a slightly smaller value (122 Hz) than the equatorial protons (126 Hz),[57] a phenomenon known as the Perlin effect.[58] The explanation is found in the hyperconjugation of the anti-periplanar axial-to-axial C—H bonds on neighbouring atoms (see p. 85). The coupling between geminal

protons is negative but larger in absolute magnitude when both C—H bonds are conjugated to the same $\pi$ bond **1.55** than when they are not **1.56**.
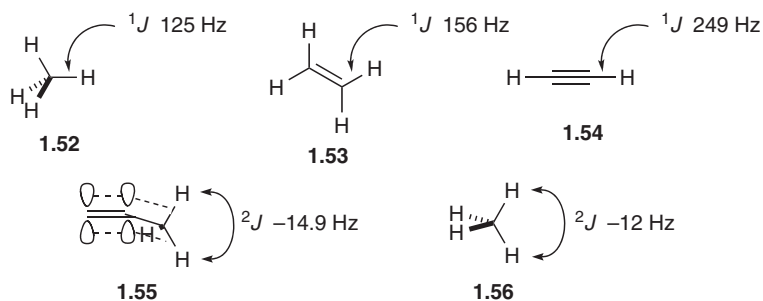


Strong coupling from anti-periplanar and syn-coplanar vicinal hydrogen atoms **1.57** and **1.59**, and virtually zero coupling with orthogonal C—H bonds **1.58** (the Karplus equation), is a consequence of the conjugation of the bonds with each other.[59] Coupling constants are usually larger when the intervening bond is a $\pi$ bond, with the *trans* and *cis* $^3J$ coupling in alkenes typically 15 and 10 Hz for the same 180° and 0° dihedral angles. Longer-range coupling is most noticeable when one or more of the intervening bonds is a $\pi$ bond, most strikingly demonstrated by $^5J$ values as high as 8–10 Hz in 1,4-cyclohexadienes **1.60**. When there are no $\pi$ bonds, the strongest long range coupling is found when the intervening $\sigma$ bonds are oriented and held rigidly for efficient conjugation with $^4J$ W-coupling **1.61** and **1.62**.
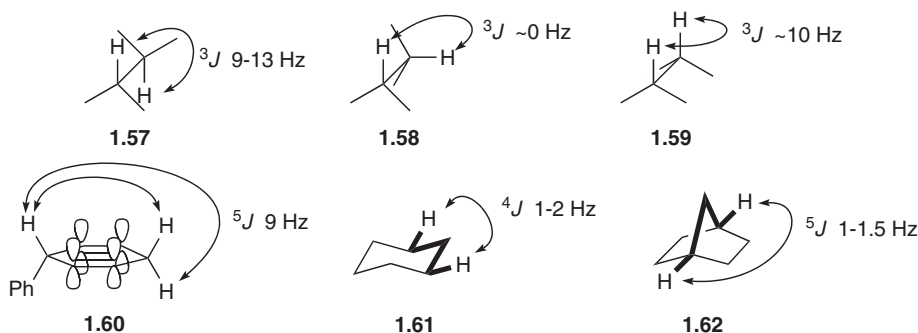


### 1.9.3 Photoelectron Spectroscopy

Photoelectron spectroscopy[60] (PES) measures, in a rather direct way, the energies of filled orbitals, and overcomes the problem that UV spectroscopy does not give good absolute values for the energies of molecular orbitals. The values obtained by this technique for the energies of the HOMO of some simple molecules are collected in Table 1.3. Here we can see how the change from a simple double bond (entry 6) to a conjugated double bond (entry 10) *raises* the energy of the HOMO. Similarly, we can see how the change from a simple carbonyl group (entry 8) to an amide (entry 14) also raises the HOMO energy, just as it ought to, by analogy with the allyl anion (Fig. 1.33), with which an amide is isoelectronic. We can also see that the interaction between a C=C bond ($\pi$ energy –10.5 eV) and a C=O bond ($\pi$ energy –14.1 eV) gives rise to a HOMO of lower energy (–10.9 eV, entry 16) than when two C=C bonds are conjugated (–9.1 eV, entry 10). Finally, we can see that the more electronegative an atom, the lower is the energy of its HOMO (entries 1 to 5). All these observations confirm that the theoretical treatment we have been using, and will be extending in the following chapters, is supported by some experimental evidence.

**Table 1.3**   Energies of HOMOs of some simple molecules from PES (1 eV = 96.5 kJ mol$^{-1}$ = 23 kcal mol$^{-1}$)

| Entry | Molecule | Type of orbital | Energy (eV) |
|:---:|:---:|:---:|:---:|
| 1 | $:PH_3$ | n | –9.9 |
| 2 | $:SH_2$ | n | –10.48 |
| 3 | $:NH_3$ | n | –10.85 |
| 4 | $:OH_2$ | n | –12.6 |
| 5 | $:ClH$ | n | –12.8 |
| 6 | $CH_2=CH_2$ | $\pi$ | –10.51 |
| 7 | $HC{\equiv}CH$ | $\pi$ | –11.4 |
| 8 | $:O=CH_2$ | n | –10.88 |
| 9 | | $\pi$ | –14.09 |
| 10 | $CH_2=CH\text{-}CH=CH_2$ | $\psi_2$ | –9.1 |
| 11 | | $\psi_1$ | –11.4 or –12.2 |
| 12 | $HC{\equiv}C\text{-}C{\equiv}CH$ | $\psi_2$ | –10.17 |
| 13 | $H_2NCH=O:$ | n | –10.13 |
| 14 | | $\pi$ | –10.5 |
| 15 | $CH_2=CH\text{-}CH=O$ | n | –10.1 |
| 16 | | $\pi$ | –10.9 |
| 17 | | $\pi$ | –8.9 |
| 18 | | $\pi$ | –9.25 |
| 19 | | $\pi$ | –9.3 |
| 20 | | n | –10.5 |

### 1.9.4 Electron Spin Resonance Spectroscopy

A final technique which both confirms some of our deductions and provides useful quantitative data for frontier orbital analysis is ESR spectroscopy.[61] This technique detects the odd electron in radicals; the interaction of the spin of the electron with the magnetic nuclei ($^1H$, $^{13}C$, etc.) gives rise to splitting of the resonance signal, and the degree of splitting is proportional to the electron population at the nucleus. Since we already know that the coefficients of the atomic orbitals, $c$, are directly related to the electron population, we can expect there to be a simple relationship between these coefficients and the observed coupling constants. This proves to be quite a good approximation. The nucleus most often used is $^1H$, and the coefficient of the atomic orbital which is measured in this way is that on the carbon atom to which the hydrogen atom in question is bonded.

The McConnell equation (Equation 1.18) expresses the relationship of the observed coupling constant ($a_H$) to the unpaired spin population on the adjacent carbon atom ($\rho_C$) The constant Q is different from one situation to another, but when an electron in a $p_z$ orbital on a trigonal carbon atom couples to an adjacent hydrogen, it is about –24 G. Applied to aromatic hydrocarbons, where it is particularly easy to generate radical cations and anions, there proves to be a good correlation between coupling constants and the calculated coefficients in the HOMO and LUMO, respectively.[62]

$$a_H = Q_{CH}^{H}\rho_C \qquad\qquad 1.18$$

However, the relationship between coupling constant and electron population is not quite as simple as this. Thus, although p orbitals on carbon have zero electron population at the nucleus, coupling is nevertheless observed; similarly, in the allyl radical **1.63**, which ought to have zero odd-electron population at the central carbon atom, coupling to a neighbouring hydrogen nucleus is again observed. This latter coupling turns out to be opposite in sign to the usual coupling, and hence has given rise to the concept of 'negative spin density'. Nevertheless the technique has provided some evidence that our deductions about the coefficients of certain molecular orbitals have some basis in fact as well as in theory: the allyl radical does have most of its odd-electron population at C-l and C-3; and several other examples will come up later in this book. We merely have to remember to be cautious with evidence of this kind; at the very least, the observation of negative spin density should remind us that the Hückel theory of conjugated systems (the theory we have been using) *is* a simplification of the truth.

The standard ways of generating radicals for ESR measurements involve adding an electron to a molecule or taking one away. In the former case the odd electron is fed into what was the LUMO, and in the latter case the odd electron is left in the HOMO. Since these are the orbitals which appear to be the most important in determining chemical reactivity, it is particularly fortunate that ESR spectroscopy should occasionally give us access to their coefficients.

Here is a selection of some of the more important conjugated radicals and radical ions, to some of which we shall refer in later chapters. They all show how the patterns of molecular orbitals deduced in this chapter are supported by ESR measurements. The numbers are the coupling constants $|a_H|$ in gauss.